UC San Diego

UC San Diego Electronic Theses and Dissertations

Title

Novel Roles for Activating Transcription Factor 6 α in the Activation and Differentiation of Cardiac Non-myocytes

Permalink

https://escholarship.org/uc/item/70s7b4p4

Author

Stauffer, Winston Thomas

Publication Date

2020

Peer reviewed|Thesis/dissertation

eScholarship.org Powered by the California Digital Library
University of California

UNIVERSITY OF CALIFORNIA SAN DIEGO

SAN DIEGO STATE UNIVERSITY

Novel Roles for Activating Transcription Factor 6 α in the Activation and Differentiation of Cardiac Non-myocytes

A dissertation submitted in partial satisfaction of the requirements for the degree Doctor of Philosophy

in

Biology

by

Winston Thomas Stauffer

Committee in charge:

San Diego State University

Professor Christopher C. Glembotski, Chair
Professor Sanford I. Bernstein
Professor Ricardo M. Zayas

University of California San Diego

Professor Joan Heller Brown
Professor Maho Niwa

2020

The dissertation of Winston Thomas Stauffer is approved, and it is acceptable in quality and form for publication on microfilm and electronically:

_____

_____

_____

_____

_____

Chair

San Diego State University

University of California San Diego

2020

DEDICATION

This dissertation is dedicated to my mother, Marian Walker Stauffer, for always fighting to provide a loving and stable home in the face of frequently adverse conditions, and to my father, Thomas Michael Stauffer, for consistently encouraging (and sponsoring) my interest in science, history, and how the world works. Their combined love for me and constant care for my well-being and development was essential to my happiness growing up and to my decision to pursue a career as a scientist. Whatever success I have had in life is because of them.

EPIGRAPH

The evidence already discussed stresses the role played by the endoplasmic reticulum and the Golgi complex in the production and processing of secretory proteins. The stress put on secretion leads, however, to an apparent impasse. Since every eukaryotic cell possesses both an endoplasmic reticulum and a Golgi complex, it follows that all eukaryotic cells secrete proteins or that the organs of the secretory pathway have additional, perhaps more general and more important functions than secretion, which have been ignored or are still unknown.

George Emil Palade

Right action is better than knowledge; but in order to do what is right, we must know what is right.

Charlemagne

It’s not the years, honey, it’s the mileage.

Henry Jones Jr.

TABLE OF CONTENTS

LIST OF ABBREVIATIONS

4-PBA	4-phenylbutyrate
AAV9	adeno-associated virus 9
AEBSF	4-(2-aminoethyl)benzenesulfonyl fluoride
AMVFs	adult mouse ventricular fibroblasts
ANOVA	analysis of variance
APR	acute phase response
ATF/CREB	activating transcription factor/cAMP response element binding
ATF	activating transcription factor
ATF3	activating transcription factor 3
ATF4	activating transcription factor 4
ATF6α	activating transcription factor 6 alpha
ATF6β	activating transcription factor 6 beta
BBF2H7	box B-binding factor 2 human homolog on chromosome 7
BCL2	B-cell lymphoma 2
BDM	butanedione monoxime
BFA	brefeldin A
Bim	BCL2-interacting mediator
BiP	binding immunoglobulin protein
bZIP	basic leucine zipper
CHOP	CCAAT-enhancer-binding protein homologous protein
CM	conditioned media
Col1a1	collagen 1a1
COPII	coat protein complex II
CRE	cAMP response element
CREB	cAMP response element binding
CREB3	cAMP response element binding 3
CREB4	cAMP response element binding 4
CREBH	cAMP response element binding H
CRP	C-reactive protein
CSC	cardiac stem cell
cTnT	cardiac troponin T
DC-STAMP	dendritic cell-specific transmembrane protein
Derlin3	degradation in ER protein 3
DHC	dihydroceramide
DHS	dihydrosphingosine
DTT	dithiothreitol
ECM	extracellular matrix
EDEM	ER degradation-enhancing alpha-mannosidase-like 1
eIF2α	eukaryotic initiation factor 2 alpha
ER	endoplasmic reticulum
ERAD	ER-associated degradation
ERp18	endoplasmic reticulum protein 18
ERRγ	estrogen related receptor gamma
ERSE	ER stress response elements

FBS	fetal bovine serum
GADD45A	growth arrest and DNA damage inducible 45 alpha
GAPDH	glyceraldehyde 3-phosphate dehydrogenase
GATA4	GATA-binding protein 4
GLuc	*Gaussia* luciferase
GRP78	Glucose-regulated protein 78
GRP94	Glucose-regulated protein 94
H_2O_2	hydrogen peroxide
HCF1	host cell factor 1
HERP	homocysteine-responsive endoplasmic reticulum-resident ubiquitin-like domain member 1 protein
HIF1α	hypoxia inducible factor 1 alpha
HRD1	HMG-CoA reductase degradation protein 1
iPSC	induced pluripotent stem cells
IRE1	inositol-requiring protein 1
KO	knockout
LAD	left anterior descending artery
LRF	Luman recruitment factor
loxP	locus of X-over P1
MI	myocardial infarction
mTORC1	mammalian target of rapamycin complex 1
MTT	3-(4,5-dimethylthiazol-2yl)-2,5-diphenyltetrazolium
NAC	N-acetyl cysteine
NF-Y	nuclear transcription factor Y
NRF2	nuclear factor erythroid 2-related factor 2
OASIS	old astrocyte specifically induced substance
ORF	open reading frame
PDI	protein disulfide isomerase
PDIA5	protein disulfide isomerase A5
PDIA6	protein disulfide isomerase A6
PF	PF-429242
PERK	protein kinase R-like ER kinase
PGC-1α	peroxisome proliferator-activated receptor gamma coactivator 1 alpha
PMEPA1	prostate membrane protein androgen induced 1
PUMA	p53 upregulated modulator of apoptosis
PVDF	polyvinylidene difluoride
Rheb	Ras homolog enriched in brain
RIP	regulated intramembrane proteolysis
ROS	reactive oxygen species
S1P	site-1 protease
S2P	site-2 protease
SAP	serum amyloid P component
SCF	stem cell factor
SDS-PAGE	sodium dodecyl sulfate–polyacrylamide gel electrophoresis
Smad	small – mothers against decapentaplegic
Smurf	Smad ubiquitination regulatory factor

SRE	serum response elements
SREBP	sterol regulatory element binding protein
SREBP2	sterol regulatory element binding protein 2
SRF	serum response factor
SUG-1	protease regulatory subunit 8 homolog
TAC	trans-aortic constriction
TAD	transcriptional activation domain
TCF21	transcription factor 21
TG	thapsigargin
TGFβ	transforming growth factor beta
TGFβR	transforming growth factor beta receptor
Thbs4	thrombospondin 4
TM	tunicamycin
TTC	2,3,5-triphenyl-2H-tetrazolium chloride
TUDCA	tauroursodeoxycholic acid
UPR	unfolded protein response
UPRE	unfolded protein response element
UTR	untranslated region
VIMP	VCP interacting membrane protein
VWF	von Willebrand factor
WT	wild type
XBP-1	x-box-binding protein 1
XBP-1s	x-box binding protein 1 spliced
YY-1	yin-yang 1
αSMA	alpha smooth muscle actin

LIST OF FIGURES

ACKNOWLEDGEMENTS

I would like to acknowledge and thank my mentor and committee chair, Dr. Chris Glembotski, for his support and guidance throughout my entire graduate school experience, including the preparation of this dissertation. His love for science, research, and teaching is apparent to anyone who spends time in his lab and I am fortunate to have benefited from it. Working with and learning from him has been a true privilege and honor.

I also want to acknowledge and thank my other SDSU committee members, Dr. Sandy Bernstein and Dr. Ricardo Zayas, and my UCSD committee members, Dr. Joan Heller Brown and Dr. Maho Niwa for their advice and guidance, both as part of my committee and during my other interactions with them in class, at PPG meetings, and during seminars. Their contributions to my development as a graduate student were invaluable.

The financial and moral support afforded me by the ARCS Foundation was of great help. Dr. Cathie Atkins was a great supporter and organizer at ARCS and I also especially appreciate Larry and Marti Showley, who chose to sponsor me for the maximum four years.

Likewise, the Rees-Stealy Research Foundation was very supportive for my entire doctorate. Their generous donations allowed me the time I needed to focus on my research. I enjoyed meeting and talking with all of their contributors.

There are many more phenomenal people I wish to thank, who have aided my work through the years and helped me to the finish. Though far too numerous to mention everyone here, I feel compelled to highlight a few: Dr. Shirin Doroudgar was an excellent mentor and friend in my first year in the lab; Khalid Azizi generously took the time to teach me many of the mouse surgery procedures used in this work; Donna Thuerauf, an expert in everything to do with the Glembotski

lab, was a guide for many a student researcher, including myself; my fellow Ph.D. students, soon-to-be Drs. Adrian Arrieta and Erik Blackwood, were great friends and collaborators to have throughout this journey; Erik Blackwood also generated the TAC mouse hearts used in Figure 23 and taught me the procedure for the initial AMVF isolations; Dr. Ingrid Niesman helped teach me tissue sectioning and microscopy; Jenny Waters lent her expertise to the immunofluorescence experiments in Figures 26 and 27 and was a great personal support during the writing of this dissertation amidst the 2020 COVID-19 pandemic. So many more were wonderful supports and friends outside the science world and deserve my thanks. You know who you are.

Section I., Introduction, is, in part, a reprint of the review article "Sledgehammer to Scalpel: Broad Challenges to the Heart and Other Tissues Yield Specific Cellular Responses Via Transcriptional Regulation of the ER Stress Master Regulator ATF6α" as it appears in the International Journal of Molecular Sciences, 2020. Stauffer, Winston T.; Arrieta, Adrian; Blackwood, Erik A.; Glembotski, Christopher C., *Int J Mol Sci*, 2020. The dissertation author was the primary author of this paper.

Section III. C. is, in part, a reprint of the research article "The ER Unfolded Protein Response Effector, ATF6, Reduces Cardiac Fibrosis and Decreases Activation of Cardiac Fibroblasts" as it appears in the International Journal of Molecular Sciences, 2020. Stauffer, Winston T.; Blackwood, Erik A.; Azizi, Khalid; Kaufman, Randal J.; Glembotski, Christopher C., *Int J Mol Sci*, 2020. The dissertation author was the primary author of this paper.

The defense of this dissertation was presented and recorded via YouTube and was available to be viewed, as of July 2020, by searching for "Winston Stauffer Dissertation Defense" on YouTube or by following the link: https://youtu.be/SMactfEOwkI

VITA

EDUCATION

2003-2008 Bachelor of Science, Biology, University of California Santa Cruz
2014-2020 Doctor of Philosophy, Biology, University of California San Diego and San Diego State University

PROFESSIONAL APPOINTMENTS

2008-2013 Production Chemist II, Alere Inc., San Diego, CA
2013-2014 Teaching Assistant, San Diego State University

FELLOWSHIPS

ARCS Foundation (2015-2019)
Rees-Stealy Research Foundation (2014-2020)

PUBLICATIONS

- Stauffer, WT, Blackwood, EA, Azizi, K, Kaufman, RJ, Glembotski, CC. The ER unfolded protein response effector, ATF6, reduces cardiac fibrosis and decreases activation of cardiac fibroblasts. *Int J Mol Sci*, 2020.
- Stauffer, WT, Arrieta, A, Blackwood, EA, Glembotski, CC. Sledgehammer to scalpel: Broad challenges to the heart and other tissues yield specific cellular responses via transcriptional regulation of the ER-stress master regulator ATF6α. *Int J Mol Sci*, 2020.
- Arrieta, A, Blackwood, EA, Stauffer, WT, Santo Domingo, M, Bilal, AS, Thuerauf, DJ, Pentoney, AN, Aivati, C, Sarakki, AV, Doroudgar, S, Glembotski, CC. Mesencephalic astrocyte-derived neurotrophic factor is an ER-resident chaperone that protects against reductive stress in the heart. *J Biol Sci*, 2020.
- Glembotski, CC, Arrieta, A, Blackwood, EA, Stauffer, WT. ATF6 as a nodal regulator of proteostasis in the heart. *Front Physiol*, 2020.
- Blackwood, EA, Bilal, AS, Stauffer, WT, Arrieta, A, Glembotski, CC. Designing novel therapies to mend broken hearts: ATF6 and cardiac proteostasis. *Cells*, 2020.
- Arrieta, A, Blackwood, EA, Stauffer, WT, Glembotski, CC. Integrating ER and mitochondrial proteostasis in the healthy and diseased heart. *Front Cardiovasc Med*, 2020.
- Blackwood, EA, Hofmann, C, Santo Domingo, M, Bilal, AS, Sarakki, A, Stauffer, WT, Arrieta, A, Thuerauf, DJ, Kolkhorst, FW, Muller, OJ, Jakobi, T, Dieterich, C, Katus, HA, Doroudgar, S, Glembotski, CC. ATF6 regulates cardiac hypertrophy by transcriptional induction of the mTORC1 activator, Rheb. *Circ Res,* 2019.

ABSTRACT OF THE DISSERTATION

Novel Roles for Activating Transcription Factor 6 α
in the Activation and Differentiation of Cardiac Non-myocytes

by

Winston Thomas Stauffer

Doctor of Philosophy in Biology

University of California San Diego, 2020
San Diego State University, 2020

Professor Christopher C. Glembotski, Chair

Numerous stresses on the heart, both physiological and pathological, present challenges to ER proteostasis in the heart. Simultaneously, various cardiac cell lineages respond to injury in ways requiring increased protein flux through the ER. While cardiac myocytes react to these stresses largely through hypertrophy or cell death mechanisms, other non-myocyte cells in the heart respond in more dynamic ways, including proliferation and differentiation. Additionally, virtually all cardiac cells secrete signaling cytokines or hormones both at baseline and during injury. Thus, precisely when ER proteostasis is most critical, cells are challenged with conditions which impair ER protein folding. ER unfolded protein response signaling attempts to respond to these challenges through the three main ER stress sensors, PERK, IRE1, and ATF6α. All sense

protein misfolding and induce downstream signaling which, to varying degrees, includes global translational attenuation with concurrent upregulation of chaperones, protein disulfide isomerases, and ER-associated degradation machinery. Of these pathways, ATF6α is the most extensively characterized as adaptive in the heart and other tissues. Additionally, recent studies have identified multiple noncanonical ATF6α gene programs which are only indirectly related to ER proteostasis but are nevertheless critical to the ability of ATF6α to preserve tissue function. Research on the effect of ATF6α in the heart had previously been restricted to ventricular myocytes. Though these cells are the most direct effectors of cardiac function, this ignores critical roles played by other cardiac non-myocyte cells. This work examines the effects of ATF6α gain- and loss-of-function in three model systems designed to uncover previously unknown roles for ATF6α signaling in cardiac non-myocytes. ATF6α global knockout mice were found to progress to heart failure more quickly than wild-type counterparts following permanent-occlusion myocardial infarction, an unexplored disease model in the context of ATF6α signaling. We subsequently explored the role of ATF6α in two murine cardiac non-myocyte cell types. The first, c-Kit$^+$ cardiac stem cells, required ATF6α both for survival and stemness while ATF6α loss-of-function induced multiple lineage markers. Second, we identified roles for ATF6α in limiting fibrosis in a pressure overload injury model and found that ATF6α blunted activation of isolated adult murine ventricular fibroblasts.

I. Introduction

1. Background

The adult heart consists of numerous cell types, including terminally differentiated cardiac myocytes, which are rigidly unable to respond to injury in a dynamic or proliferative sense. Accordingly, many therapeutic strategies focus on limiting damage rather than altering how heart cells change in the face of injury. However, while cardiac myocytes with a limited regenerative capacity contribute the bulk of the mass of the adult myocardium, a majority of the cells in the heart are proliferative and capable of differentiation or trans-differentiation during pathology.[1]

The differentiation of progenitor cells, or the trans-differentiation of somatic cells into new cell types is associated with increases in protein synthesis and folding.[2-6] Of particular importance in responding to injury are secreted proteins, such as cytokines and extracellular matrix (ECM) proteins.[7-9] Many secreted proteins are translated on ribosomes on the rough endoplasmic reticulum (ER), which is the site of the translation and folding of at least 35% of new proteins, most of which move through the ER-Golgi secretory pathway, destined for membrane insertion or secretion.[10] Conditions associated with myocardial injury also pose challenges to the folding environment of the ER by affecting redox status, calcium handling, and adenosine triphosphate (ATP) production.[11-13] These and other insults perturb ER proteostasis, which is defined as the balance between the translation, folding, and degradation of ER proteins. The misfolded ER proteins that result from these challenges are detected by three ER-transmembrane proteins: protein kinase R-like ER kinase (PERK)[14], inositol-requiring protein-1 (IRE1)[15], and activating transcription factor-6 α (ATF6α)[16, 17]. Together, these sensors constitute the three major branches of the ER unfolded protein response (UPR), sometimes called the ER stress response, which is

associated with a gene program that functions initially to preserve proteostasis in the ER, while at later times to guide the cell toward apoptosis, if protein misfolding is not resolved.[11, 18]

ER stress response pathways are important during the development and differentiation of certain cell types, especially professional secretory cells.[2, 4] For example, in stimulated B lymphocytes, which differentiate into antibody-secreting plasma cells, activation of IRE1 and its downstream effector, x-box-binding protein 1 (XBP1), are necessary to accommodate the required expansion of ER membranes and increased production of secreted antibodies made in the ER.[5] Members of the old astrocyte specifically induced substance (OASIS) family, which are related to ATF6α, are associated with differentiation in chondrocytes and osteoblasts.[19] Further, ATF6α itself was recently shown to drive induced pluripotent stem cells (iPSCs) toward mesenchymal lineages, while suppressing differentiation toward endo- and ectodermal lineages.[6] Lastly, ER stress signaling was shown to promote fibroblast-to-myofibroblast trans-differentiation in a manner similar to transforming growth factor β (TGFβ) signaling.[20, 21]

ER stress effectors, particularly ATF6α, are critical for the mitigation of myocardial tissue damage and the preservation of heart function during heart disease.[11] Additionally, ATF6α and ER stress are important factors in the development of multiple tissue types.[6, 22, 23] The activation, proliferation, and differentiation of cardiac non-myocytes is a known feature of heart disease, including long-term heart failure,[7-9, 24] however the role of ATF6α or the ER stress response in this process is not known.

2. ER Stress Overview

The ER UPR responds to stresses that perturb ER protein folding capacity, i.e., ER stresses that result in the accumulation of misfolded proteins in the ER lumen. ATF6α is a master regulator

of one of the three main branches of the ER UPR, each of which is initiated by the ER-transmembrane proteins, PERK, IRE1, and ATF6α **(Figure 1A)**.[17]

a. PERK:

In response to misfolded proteins, PERK dimerization results in the activation of its cytosolic kinase function, leading to autophosphorylation and the phosphorylation of numerous proteins outside the ER, including eukaryotic initiation factor 2α (eIF2α) **(Figure 1B)**.[3, 14] eIF2α promotes the initiation of ribosomal translation of mRNA transcripts in a GTP dependent manner. eIF2α phosphorylation by PERK confers a global arrest of translation by reducing the available pool of GTP-bound eIF2α, thus decreasing the protein-folding load on the ER machinery.[25, 26] This arrest does not affect translation of mRNAs for genes that aid in protein folding and the degradation of misfolded proteins, or which otherwise address the problem of ER protein misfolding. One example of escape from PERK-mediated translational arrest is ATF4, the primary effector transcription factor downstream of PERK. While ATF4 mRNA is continually transcribed, it contains two 5' open reading frames (ORFs) upstream of its coding region, the second of which is inhibitory and prevents further translation of the ATF4 transcript. eIF2α phosphorylation causes the ribosomes to skip the translation of the second inhibitory ORF and to reinitiate downstream at the ATF4 coding region, thus resulting in the synthesis of the ATF4 protein.[27, 28] ATF4 target genes vary, but are frequently associated with pro-apoptotic pathways, especially when ATF4 is chronically active. For example, ATF4 target gene CAAT enhancer-binding protein-homologous protein (CHOP) is a transcription factor which mediates apoptotic cell death.[29] CHOP down-regulates anti-apoptotic factors like the BCL2 family[30] and up-regulates pro-apoptotic factors like Bim[31] and PUMA[32]. PERK and ATF4 are thus important when protein misfolding continues, unresolved, and ER stress signaling becomes maladaptive.

b. IRE1:

Upon ER stress, IRE1 also dimerizes and becomes autophosphorylated on its cytosolic domain, which activates it as an RNA splicing enzyme that, with the aid of tRNA ligase, converts x-box binding protein 1 (XBP-1) mRNA to a so-called spliced form that encodes an active transcription factor, XBP-1s **(Figure 1C)**.[15] The XBP-1s gene program is commonly understood to be an adaptive pathway and, among other things, results in the upregulation of chaperones, like glucose binding protein 78 (GRP78, also known as BiP), which aid in ER protein folding.[33] In mammals, unspliced XBP-1 mRNA is also translated and, while not transcriptionally active, it binds to XBP-1s mRNA and increases its degradation.[34] IRE1 and XBP-1, analogous to HAC-1 in yeast, together represent evolutionarily the oldest and most highly conserved ER stress pathway.[35-37] Additionally, IRE1 functions independently of XBP-1 in two ways. First, IRE1 can also become pro-apoptotic when active, by binding the adaptor protein TRAF2, which leads to the activation of the pro-apoptotic JNK pathway.[38] Second, the same endonuclease function of active IRE1 which cleaves XBP-1 also increases the degradation of mRNAs that are in close proximity to the cytosolic face of the ER. By degrading mRNAs on, or about to be engaged with ER-bound ribosomes, this process, called regulated IRE1-dependent decay (RIDD), further reduces the trafficking of nascent proteins through the ER.[39, 40]

c. ATF6α:

In contrast to PERK and IRE1, when ATF6α senses misfolded proteins in the ER, it translocates to the Golgi, where it is proteolytically clipped **(Figure 1D)**.[16] The resulting N-terminal fragment is a basic leucine zipper (bZIP) transcription factor related to others in the activating transcription factor/cAMP response element binding (ATF/CREB) family.[41, 42] ATF6α was the first of its subgroup of the ATF/CREB family to be identified, and since then a related

isoform, ATF6β, which has significant homology to ATF6α, has been assigned to the ATF/CREB family. ATF6β can bind to, and transcriptionally induce many of the same genes as ATF6α, but ATF6β is a much weaker transcriptional activator, perhaps serving as an endogenous modulator of ATF6α, as described below.[43, 44]

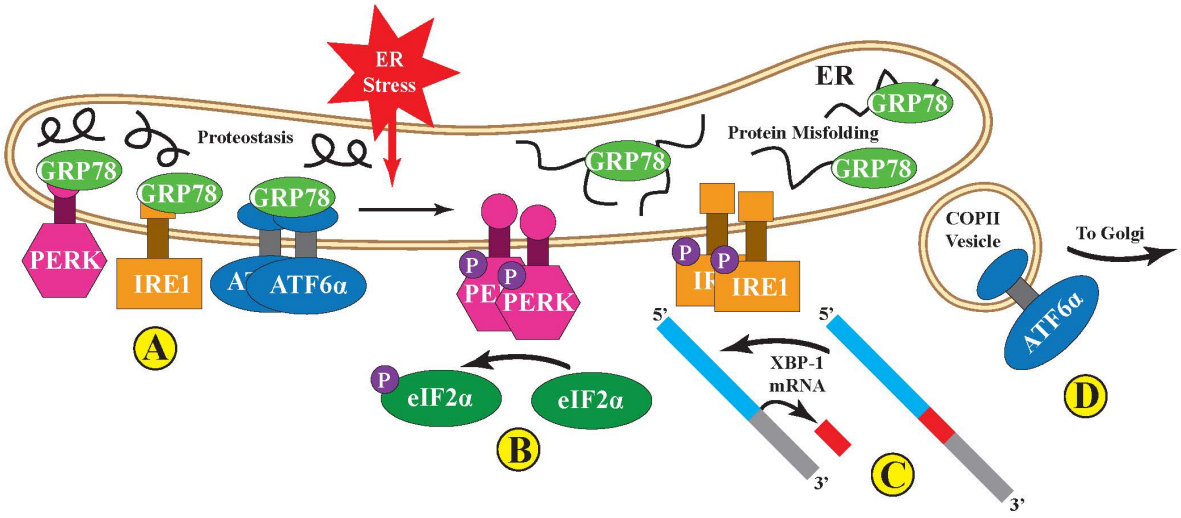

Figure 1. Overview of the activation of the three branches of the ER UPR.
(A) PERK, IRE1, and ATF6α are all ER transmembrane proteins with cytosolic and luminal domains that act as sensors to detect the build-up of misfolded proteins characteristic of ER stress. When the capacity of the ER to translate and fold nascent proteins is sufficient to meet demand, protein misfolding is minimal and the ER is in proteostasis. During such periods, canonical ER chaperone GRP78 (also known as BiP) binds the luminal domains of all three UPR sensors and helps hold them in an inactive state. PERK and IRE1 are held in monomeric form, while inactive ATF6α is an oligomer. Upon induction of ER stress, by challenges such as ischemia, oxidative stress, or increases in ER protein flux, nascent ER proteins begin to misfold and can build up in the ER lumen. GRP78 then actively unbinds the ER sensors to bind the misfolded proteins and promote their proper folding. Simultaneously, the three sensor branches become active; **(B)** PERK, which has cytoplasmic kinase domains, dimerizes with itself and becomes autophosphorylated. It then phosphorylates its substrate, eIF2α, in the cytoplasm which acts to slow translation of all non-UPR-related proteins; **(C)** IRE1, which has cytoplasmic kinase and endonuclease domains, also dimerizes and is autophosphorylated. This activates its endonuclease function to splice out a section of XBP-1 mRNA to create a new, spliced transcript, XBP-1s, which codes for a transcription factor that upregulates some UPR-related transcripts; **(D)** ATF6α, which is both a sensor of ER stress and a UPR-effector transcription factor, becomes monomeric upon induction of ER stress, whereupon it exits the ER via COPII vesicles and transits to the Golgi, where the active transcription factor is liberated from the transmembrane domain by Golgi proteases.

3. ATF6α Activation

In its transcriptionally inactive state, ATF6α is anchored in the ER partly by binding to the well-characterized ER chaperone, GRP78.[45] Under these conditions, ATF6α forms oligomers via intermolecular disulfide bonds between conserved cysteine residues in its luminal domain **(Figure 2A)**.[46, 47] During periods of ER stress, brought on by pathophysiological conditions including ischemia[13], GRP78 is actively diverted to the misfolded proteins that accumulate in the ER lumen, thus releasing its hold on ATF6α.[48] This mechanism of activation involving the release of ATF6α by GRP78 may be shared with PERK and IRE-1, thus fostering the activation of all three branches of the ER stress response.[49, 50] Subsequently, the disulfide bonds in ATF6α become reduced, which decreases ATF6α oligomerization **(Figure 2B)**, leading to the translocation of ATF6α to the Golgi **(Figure 2C)**. In the Golgi ATF6α is proteolytically cleaved by regulated intramembrane proteolysis (RIP) by the Golgi resident proteases, site 1 protease (S1P) and site 2 protease (S2P) **(Figure 2D)**.[51]

More recently, other paradigms of ATF6α activation have emerged. For example, thrombospondin 4 (Thbs4), a secreted calcium-binding protein, was shown to interact with ATF6α during stress and to promote its shuttling to the Golgi. In that study, it was found that without Thbs4, ATF6α activation was blunted, as were the other ER stress branches, suggesting a broader role for Thbs4 in the ER UPR.[52] Recently, multiple protein oxidoreductases have been shown to associate with, and reduce ATF6α during ER stress; this reduction, which also causes the dissociation of ATF6α oligomers, is thought to facilitate the movement of ATF6α out of the ER to the Golgi.[46, 47] In particular, the ER-resident protein disulfide isomerase (PDI), PDIA5, was shown to be necessary for the proper reduction of ATF6α before packaging into Golgi-bound vesicles in cancer cells.[53] Another PDI, termed ER protein 18 (ERp18), was found to associate with, and

reduce ATF6α during ER stress. In the absence of ERp18, ATF6α was improperly processed by the S1P/S2P proteases, impairing the release of the soluble nuclear form of ATF6α.[54]

Small molecule compounds have been discovered which take advantage of this reduction/activation dynamic and in so doing, they are effective and specific inhibitors or activators of ATF6α. A class of pyrazole amides, dubbed Ceapins, have been discovered[55], which inactivate ATF6α by inhibiting its transport from the ER to the Golgi. Furthermore, ATF6α that has been retained in the ER by Ceapins is still able to be processed by the Golgi proteases, if those proteases are experimentally relocated from the Golgi to the ER. Indeed, the fact that Ceapins have no effect on S1P/S2P forms the likely basis for why Ceapins are so specific for ATF6α.[56] Other compounds, such as AEBSF[57] or PF429242[58], also inhibit the formation of activated ATF6α, but do so by inactivating serine proteases, including S1P. Thus, a caveat to these compounds is that they impact other proteins that are activated by RIP, such as the transcription factor, sterol regulatory element binding protein (SREBP), as well as some other members of the ATF6 subgroup, including ATF6β (see below).[55, 56] Another chemical recently discovered in a high-throughput screen, is a selective ATF6α activator.[59] This chemical, called compound 147, promotes the formation of ATF6α monomers and thus enhances the transit of ATF6α from the ER to the Golgi, promoting subsequent proteolytic cleavage of ATF6α to its active form.[60] Compound 147 is specific for ATF6α and does not activate other members of the ATF6 subfamily.[59] Likewise, the naturally occurring sphingolipids dihydrosphingosine (DHS) and dihydroceramide (DHC) have also been shown to specifically activate ATF6α[61], though the resulting upregulation of ATF6α target transcripts can vary significantly depending on the activation stimulus (see below). These reagents are very useful for studies requiring selective pharmacologic manipulation of

ATF6α activity and, as will be discussed below, may also be of future utility in disease treatment, where ATF6α is a therapeutic target **(Figure 2)**.

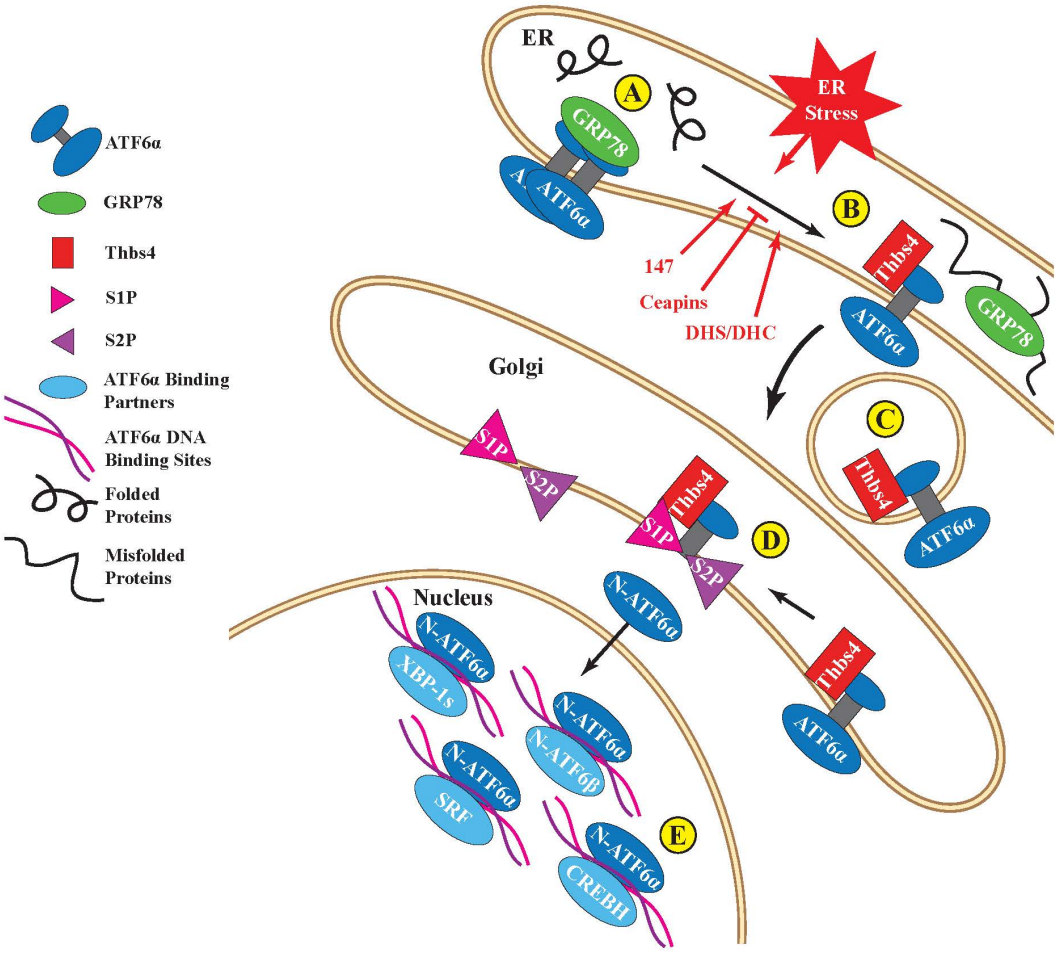

Figure 2. Focus on ATF6α activation.
(A) In the absence of ER stress, ATF6α exists in an oligomeric state and its luminal domain associates with GRP78; **(B)** During ER stress, GRP78 relocates from ATF6α to misfolded proteins; ATF6α is then reduced to a monomeric state. Chemicals, such as compound 147, or certain sphingolipids, can promote ATF6α relocation out of the ER in the absence of overt ER stress. Other chemicals, called Ceapins, inhibit this process, even during ER stress; **(C)** ATF6α and binding partners, such as Thbs4, are packaged into COPII vesicles and transit to the Golgi; **(D)** Golgi resident proteases, S1P and S2P, cleave the N-terminal cytosolic region of ATF6α from the transmembrane domain. The soluble N-terminal fragment (N-ATF6α) is then free to enter the nucleus where it binds to target genes and influences transcription; **(E)** N-ATF6α binds DNA as a homodimer but is also known to form heterodimers with a number of other nuclear proteins, including N-ATF6β, XBP-1s, SRF, and CREBH. Binding different partners can alter which gene programs N-ATF6α induces.

4. ATF6α Transcriptional Activity and Degradation

Once cleaved, the N-terminal fragment of ATF6α is liberated from the ER and, via a nuclear localization sequence, it translocates to the nucleus where it homodimerizes, or forms a heterodimer by binding a myriad of other potential partners[62], and activates transcription of select genes **(Figure 2E)**. The transactivation domain (TAD) of ATF6α was found to contain an eight amino acid sequence with homology to the Herpes simplex virus transcription factor, VP16.[63] This sequence, referred to as VN8 in that same study, has been shown to confer both high transcriptional potency and a high rate of degradation to ATF6α **(Figure 3A, B)**. Amongst the ATF6α subfamily, only ATF6α possesses a VN8 sequence in its TAD. Indeed, while other unrelated transcription factors are also known to be quickly degraded when active[64], ATF6α is the only such mammalian transcription factor known to have a VN8 sequence[63]. Mutating specific residues in the VN8 region of ATF6α in ways known to inactivate VP16 were found to be sufficient to significantly reduce its transcriptional potency and significantly increase its stability, analogous to the effects of these mutations on VP16.[43] It is interesting to note that while ATF6β is relatively similar to ATF6α, it does not have a VN8 domain; consistent with this, ATF6β is a comparatively poor transcription factor and it is degraded very slowly **(Figure 3C, D)**.[65] Moreover, mutation studies demonstrated that transferring the VN8 domain of ATF6α onto ATF6β transformed ATF6β from a long-lived, weak transcription factor into a short-lived, strong transcription factor, resembling the characteristics of ATF6α.[43]

The exact mechanism by which activated ATF6α is rapidly degraded remains unknown. While ATF6α has been reported to be ubiquitylated[66, 67], and while it is known to be degraded by proteasomes[63, 68], less is known about the timing, location, and importance of these events. In so far as the VN8 sequence of VP16 is shared with ATF6α, it is interesting to note that the ubiquitin-

proteasome system has been shown to be required for the activity of VP16.[69] In that study, a specific subunit of the 19S proteasome, 26S proteasome regulatory subunit 8 (SUG-1), was required to ubiquitylate and degrade VP16. Interestingly, this subunit was also required for the transcriptional activity of VP16, suggesting that, at least for VP16, ubiquitylation is a requirement for its transcriptional activity, rather than a consequence of its transcriptional activation.[69] Thus, it is possible that SUG-1 may also be required for ATF6α ubiquitylation and the associated transcriptional activation and degradation. ATF6α has also been shown to be post-translationally modified in other ways, such as glycosylation[70] and SUMOylation[71], and it is certainly true that many post-translational modifications, including ubiquitylation, have been reported to be essential regulators of other transcription factors[72]. Meanwhile, there are varying reports concerning whether nuclear proteasomes are functional and whether ubiquitylated nuclear proteins, potentially including ATF6α, are degraded in the nucleus, or whether they are first transported back to proteasomes in the cytosol for degradation.[73-75]

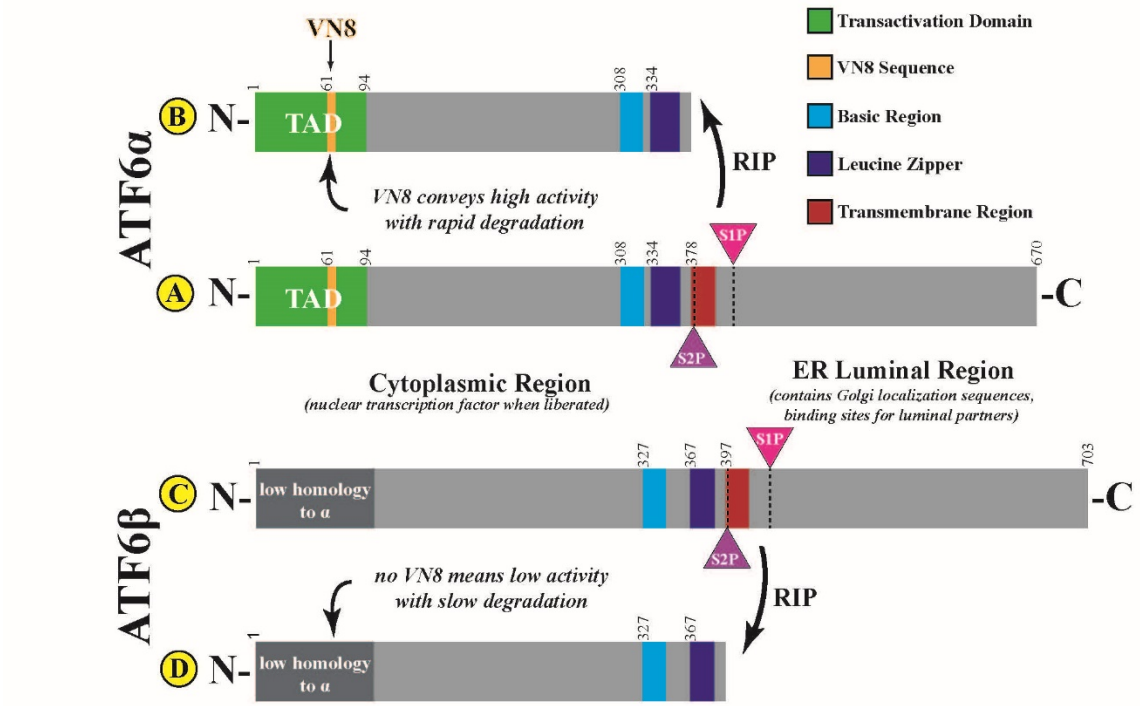

Figure 3. Structural comparison between ATF6 α and β.
(A) Full length ATF6α has an N-terminal cytosolic region with a transcriptional activation domain (TAD), a central basic leucine zipper domain (bZIP), and a transmembrane domain followed by a C-terminal luminal region; **(B)** The cytosolic region is liberated from the ER membrane by S1P and S2P Golgi proteases in a process called regulated intramembrane proteolysis (RIP). The TAD of the N-terminal ATF6α fragment contains an eight-amino acid sequence, from amino acids 61 to 68, called the VN8, which confers high transcriptional activity and rapid degradation; **(C)** Full length ATF6β has a similar structure to ATF6α and its cytosolic region is also liberated from the ER membrane by S1P and S2P mediated RIP; **(D)** The N-terminal region of the soluble portion of ATF6β has low homology to ATF6α and, in particular, lacks the VN8 domain. N-ATF6β is thus a weak transcriptional activator with a long half-life.

5. ATF6α Dimerization and Nuclear Binding Partners

ATF6α, like other bZIP transcription factors, forms homodimers, as well as heterodimers with other transcription factors, not all of which are members of the ATF/CREB family; presumably, it is through selective dimerization that the transcriptional programs regulated by ATF6α can be fine-tuned.[76] ATF6α was first discovered as a dimerization partner of serum response factor (SRF), a MADS-box transcription factor that upregulates a variety of genes through serum response elements (SRE).[77] SRF binding to ATF6α was shown to enhance the activation of SRF-responsive transcript expression.[78] ATF6α binding to its target DNA sequences is also dependent on interactions with other proteins, such as NF-Y, which also binds these gene targets.[79] Other binding partners that synergistically enhance the activity of ATF6α include YY-1[80], fellow ER stress response effector XBP-1s[33], PGC-1α[81], ERRγ[82], and CREBH (see below)[83]. Additionally, binding partners have the potential to negatively regulate the transcriptional activity of ATF6α, as is the case with ATF6β (see below)[65].

The mechanisms that determine the selectivity by which ATF6α partners with other transcription factors remain obscure. It seems unlikely that ATF6α homo- or heterodimerization could begin in the ER because only monomeric ATF6α is packaged into COPII vesicles for exit from the ER.[47] Dimerization could take place in the Golgi, though when cleavage of ATF6α is experimentally forced to take place in the ER, using mutant forms of S1P/S2P proteases engineered with C-terminal K-D-E-L amino-acid ER retention sequences, ATF6α is processed normally and is functional.[84] Lastly, ATF6α may find its binding partners during or even after translocation to the nucleus, perhaps in the process of binding DNA sequences. Indeed, in the case of bZIP-bZIP dimers, the dimer structure of the combined transcription factors is required for proper binding to the major groove of the DNA.[85]

6. ATF6α Promoter Elements

The specific promoter sequences to which ATF6α binds were first reported by Kazutori Mori's group and were named ER stress response elements (ERSEs).[86] In that study, it was shown that the consensus sequence of ERSEs is CCAAT-N_9-CCACG, which includes the binding sites for both NF-Y (CCAAT) and the ATF6α dimer, itself (CCACG), with a nine-nucleotide spacer in between.[86] Subsequent studies identified variations of this sequence, as well as an entirely new ERSE, called ERSE-II, the sequence of which, AATTG-N-CCACG, was also found to be important for the ATF6α transcriptional program.[87]

7. ATF6α Transcriptional Programs

In the heart, ATF6α induces at least 400 gene transcripts *in vivo*; many of these genes have ERSE or ERSE-like elements.[88] RNA-seq performed on mouse hearts expressing a tamoxifen-activatable form of ATF6α revealed a wide range of upregulated transcripts involved in many critical processes.[12] As one would expect, many of these gene products are directly involved in the adaptive ER stress response and act to enhance ER protein folding capacity under adverse conditions. These gene products include those that encode ER luminal chaperones like GRP78 and GRP94[86, 89] and PDIs, like PDIA6[90] which, in addition to roles in the activation of ER stress sensors, bind nascent proteins in the ER and promote their correct folding into secondary and tertiary structures by facilitating disulfide bond formation.[90]

Another subset of ATF6α-regulated genes is involved in ER-associated degradation (ERAD) pathways. Terminally misfolded proteins cannot be repaired and must therefore be degraded before they accumulate in the ER lumen and become potentially toxic. Because there are no proteasomes in the ER lumen, these proteins must be transported out of the ER lumen to the cytosol for degradation.[91, 92] Intimately involved in this process is the ATF6α-inducible gene

product, HMG-CoA reductase degradation protein 1 (Hrd1), an ER transmembrane E3 ubiquitin ligase that both transports misfolded proteins out of the ER and ubiquitylates them, after which they are degraded by proteasomes on the cytosolic face of the ER.[93, 94] Interestingly, Hrd1 is the only transmembrane E3 ubiquitin ligase induced by ATF6α in the heart.[88, 95] Other ERAD components that are induced by ATF6α include degradation in ER protein 3 (Derlin3)[96] and VCP-interacting membrane protein (VIMP)[11]. Through their roles as ERAD components, these proteins preserve ER proteostasis and enhance cell survival[97, 98] and thus, ATF6α is commonly associated with the adaptive ER stress response.[99, 100]

However, persistent ER stress and ATF6α activation can activate maladaptive pathways, which guide the cell towards apoptosis.[29, 101] Amongst these maladaptive ATF6α transcriptional targets is CHOP, which induces apoptotic signaling, showing that ATF6α is not always adaptive in a cellular sense.[30, 102, 103]

Other candidates revealed in RNA-seq datasets as ATF6α-regulated genes in the heart, and which have been confirmed in recent discoveries, are several non-canonical ATF6α transcriptional targets that are not directly involved in ER protein homeostasis. For example, the well-known antioxidant enzyme catalase, which is found in peroxisomes and not in the ER, is induced by ATF6α in the heart.[11] Therefore, by inducing catalase, ATF6α can reduce the levels of reactive oxygen species (ROS), which has functional implications far beyond ER proteostasis. Another example of a non-canonical ATF6-regulated gene product is the small GTPase Ras homolog enriched in brain (Rheb), which, when induced by ATF6α in the heart, activates mammalian target of rapamycin complex 1 (mTORC1) and thus drives protein synthesis and hypertrophic cardiac myocyte growth.[12] Again, this indirectly affects ER protein folding but further shows how ATF6α can be a master regulator of global cellular responses.

8. Stimulus-Specific ATF6α Transcriptional Programs

Recently, it has been found that a wide range of cellular stresses can activate ATF6α; intriguingly, the transcriptional programs regulated by active ATF6α appear to be stress specific.[12] For example, the canonical ATF6α-target gene product, GRP78, which is directly involved in protein folding in the ER, is induced by conditions that acutely increase ER protein misfolding **(Figure 4A)**. However, the more recently identified ATF6α-regulated gene product, catalase, a peroxisomal antioxidant enzyme, is induced mainly by ATF6α when it is activated by oxidative stress, but not when ATF6α is activated by ER protein misfolding **(Figure 4B)**. Finally, Rheb, which is not induced by ATF6α when it is activated by oxidative stress, is induced by ATF6α when it is activated by growth signals **(Figure 4C)**; under these conditions, which were studied in the heart, ATF6α was required for cardiac myocyte growth in response to growth factor treatment.

Another recent study by Tam et. al. revealed that ATF6α is selectively activated by the sphingolipids dihydrosphingosine (DHS) and dihydroceramide (DHC).[61] Like treatment with compound 147, activation by either DHS or DHC is not associated with ER protein misfolding and it is limited to ATF6α, without activating the other arms of the ER stress response. Uniquely, however, this mode of activation causes ATF6α to induce a previously unknown ATF6α-regulated transcriptional program involved in enhancing lipid production for membrane expansion.[61] Given that ATF6α activation in all these scenarios still appears to involve the canonical ER-Golgi-nucleus pathway, it is unclear how each stimulus directs ATF6α to a specific subset of genes. It is likely that there are critical roles being played by thus far unknown post-translational modifications, binding partners, and epigenetic regulators which are induced by each stimulus and guide ATF6α to the appropriate gene set.

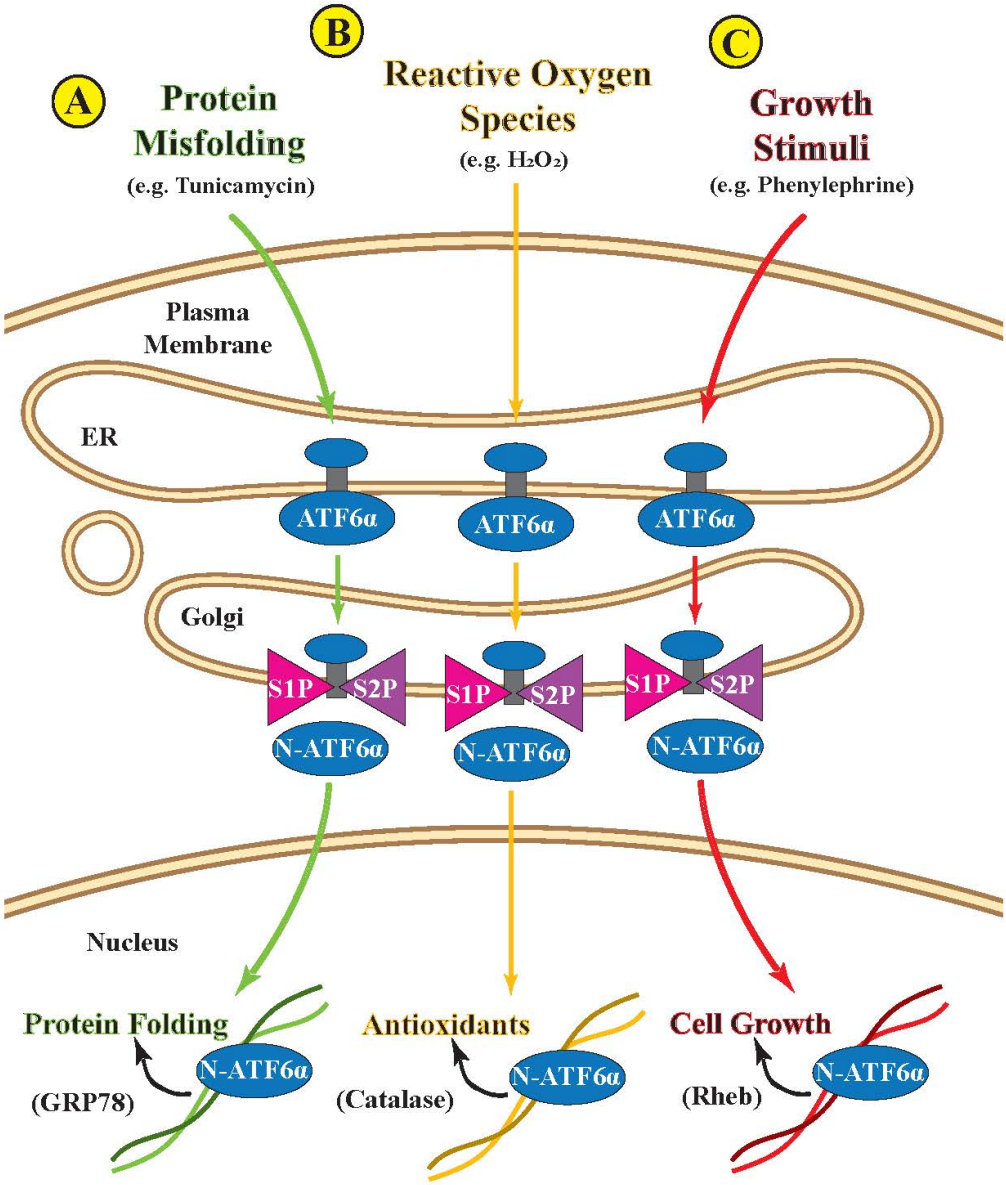

Figure 4. Stimulus-specific transcriptional programs for ATF6α.
Different stimuli cause ATF6α to induce different transcriptional targets, in a stimulus dependent manner, despite activating ATF6α with the same proteolytic machinery. **(A)** N-ATF6α induces canonical ER chaperone GRP78 in response to protein misfolding; **(B)** N-ATF6α upregulates antioxidant catalase, but only in response to oxidative stress; **(C)** N-ATF6α upregulates cell growth inducer Rheb, but only in response to growth signals.

9. ATF6α in Disease

Transcriptional regulation of a transcription program as extensive as that mediated by ATF6α naturally has profound consequences in a variety of disease states. For example, protein aggregation is a common feature of numerous forms of cardiac pathology. In numerous studies of ATF6α in the heart, it has been consistently found to play protective roles in multiple forms of cardiac injury.[11-13, 21, 52, 104, 105]

For example, Martindale et. al. overexpressed a tamoxifen inducible form of ATF6α in mouse hearts and then performed *ex vivo* global ischemia/reperfusion injury on the isolated mouse hearts. Hearts with activated ATF6α exhibited significantly smaller infarcts and had preserved cardiac function compared to hearts from mice that were not treated with tamoxifen.[21]

In a later study, Lynch et. al. investigated Thbs4 in hearts from mutant mice that constitutively develop a buildup of cardiac misfolded protein aggregates. They found that Thbs4 was protective against accumulation of such aggregates because of its role in the activation of ATF6α.[52]

More recently, Jin et. al. performed ischemia/reperfusion surgeries in mice, where damage to the heart is due in part to the generation of ROS upon reperfusion. Endogenous ATF6α was found to be activated by ischemia/reperfusion and was shown to be protective because it induces the antioxidant, catalase.[11]

Blackwood et. al. discovered that ATF6α was necessary for compensatory cardiac growth in response to pressure overload induced by transaortic constriction (TAC) surgeries, which mimic chronic high blood pressure, due to its induction of the mTORC1 activator Rheb.[12] In a subsequent study exploring the use of compound 147 as a drug candidate, Blackwood et al. found 147 to be globally protective against ischemia/reperfusion models in the heart, kidney, and brain.[105]

ATF6α and the ER stress response are generally found to be highly activated in professional secretory cells, due to increased protein flux through the ER. Sharma and colleagues accordingly found that ATF6α contributes to the proliferation of insulin-producing beta cells in the pancreas, with implications for diabetes.[106]

The ER stress response is also highly active in cancer cells, which, in addition to rapid proliferation, must also survive in the hypoxic environment inside tumors, both of which can place high demands on protein synthesis and folding machinery. Indeed, ATF6α confers chemoresistance in leukemia cells.[53]

Lastly, naturally occurring ATF6α mutations have been found in humans that can alter its activation in response to ER stress. Certain single nucleotide polymorphisms that increase the amount of ATF6α signaling have been associated with increases in blood cholesterol in patients at risk of cardiovascular disease, potentially because ATF6α may interact with the SREBP2 lipid biosynthesis pathway.[104] Other mutations that lead to the truncation and degradation of ATF6α transcript have been shown to cause the autosomal recessive eye disorder achromatopsia, which is characterized by non-functional cone cells, resulting in color-blindness, photophobia, and other maladies.[107]

10. ATF6α Relatives

While the importance of the varied and complex outcomes of ATF6α signaling is apparent in multiple tissues and disease states, it should be noted that ATF6α is related to other transcription factors, many of which are included in the large ATF/CREB family.[41, 42] Like ATF6α, all members of the ATF/CREB family are bZIP transcription factors consisting of a basic DNA binding region next to an alpha-helical coiled coil region for dimerization. They can all recognize cAMP response element (CRE) or CRE-like promoter elements in their target genes, though some, as in ATF6α,

show preference to other specific sequences like ERSE. All form dimers in order to properly bind DNA and activate transcription. These dimers can be in the form of homodimers or heterodimers, often with other ATF/CREB family members. ATF/CREB members include CREB, CREM, ATF1, ATF2, ATF3, ATF4, ATF5, ATF6α, ATF6β, ATF7, and BATF as well as the old astrocyte specifically induced substance (OASIS) subfamily[41, 42, 108] members described below. While other members of the ATF/CREB family are involved in other stress responses in addition to ER stress, like ATF3[109], ATF4[28], or ATF5[110], only the OASIS and ATF6 subfamilies are type II ER-transmembrane transcription factors that, like ATF6α, are activated by proteolytic cleavage by Golgi-resident S1P/S2P proteases.

In all cases the liberated cytosolic N-terminal fragment is a bZIP transcription factor with a high degree of structural homology to the activated form of ATF6α, including an N-terminally located TAD and a C-terminal bZIP DNA binding/dimerization domain.[41, 111, 112] However, none have a TAD sequence that is homologous to that of ATF6α.[63] Additionally, the luminal regions of the rest of the OASIS subfamily (except for ATF6β) do not resemble ATF6α **(Figure 5)**. In particular, some lack GRP78-binding domains and do not have apparent Golgi localization sequences.[112] Thus, the specific mechanism of activation for some family members is obscure.

Many OASIS members exhibit tissue specificity in terms of their expression, while ATF6α is broadly expressed in all tissues.[112, 113] OASIS members also bind to differing promoter sequences. Some are known to bind to ERSE, unfolded protein response elements (UPRE), or otherwise ATF6-like sequences, while others show preference to CRE or CRE-like promoter elements.[111, 112] It is unclear to what degree OASIS members are involved in ER stress. Some are activated by ER stress while some respond to other stimuli.[111, 112, 114] Like the rest of the

ATF/CREB family, they form homodimers in order to bind DNA and activate transcription and have the potential to heterodimerize with similar transcription factors, including ATF6α.[19, 111, 112]

a. Luman/CREB3:

Luman protein is present exclusively in ganglionic neurons, monocytes, and dendritic cells. Luman has been shown to be cleaved and activated by S1P but this cleavage does not take place in response to chemical ER stressors. However, in the nucleus, Luman binds to ERSE-II and UPRE-like promoter elements, and it upregulates ER-associated degradation (ERAD) genes, specifically HERP and EDEM, suggesting some involvement in the ER stress response. Luman interacts with binding partners which control its activation in the Golgi, like DC-STAMP, or regulate its transcriptional activity in the nucleus like HCF-1 or LRF.[115]

b. OASIS/CREB3L1:

OASIS is expressed primarily in osteoblasts and in astrocytes. As with ATF6α, during ER stress OASIS translocates to the Golgi where it is cleaved and activated by S1P/S2P, though how this happens, given that its luminal domain structure diverges from that of ATF6α, is unclear. In osteoblasts OASIS increases Col1a1 production by directly binding a CRE element in the Col1a1 promoter as a part of driving differentiation and bone formation.[113, 116]

c. BBF2H7/CREB3L2:

BBF2H7 is structurally very similar to OASIS but has different patterns of expression. It is primarily known for its high expression in chondrocytes and cartilage. Just like OASIS, it is activated by ER stress and is clipped at the Golgi after which the N-terminal fragment travels to the nucleus where it activates genes with CRE-like promoter elements. BBF2H7 directly upregulates Sec23a, which is responsible for COPII vesicle formation and is thus critical for the secretion of extra cellular matrix (ECM) proteins involved in cartilage development.[108, 113]

d. CREBH/CREB3L3:

CREBH is primarily expressed in hepatocytes in the liver where it is activated by ER stress and is clipped at the Golgi. CREBH primarily binds CRE- and ATF6-like promoter elements but has also been reported to bind ERES and UPRE elements. Proinflammatory signaling activates ER stress and CREBH, which is responsible for the expression of acute phase response (APR) proteins CRP and SAP. Importantly, CREBH heterodimerizes with ATF6α, which enhances the induction of APR proteins.[83]

e. CREB4/CREB3L4:

CREB4 is expressed in the prostate in humans and in testis in mice, as well as in the intestines. It has two isoforms, α and β. CREB4β is a strong transcriptional activator while α is weak or inactive. CREB4 is cleaved at the Golgi but the steps involved in its activation remain unknown because it is insensitive to experimental maneuvers which should cause it to encounter the Golgi S1P and S2P proteases. For example, BFA treatment, which causes the merging of ER and Golgi membranes does not result in its activation nor does expression of ER targeted versions of the Golgi proteases.[117] CREB4 activation may thus have additional requirements that are thus far unknown. However, CREB4 has some involvement in the ER stress response because it binds to UPRE sequences and induces ERAD components, like EDEM.[112]

f. ATF6β/CREBL1:

In terms of amino acid sequence, ATF6β is the most closely related OASIS subfamily member to ATF6α and the two together are sometimes considered to form their own subfamily.[41, 44] Like ATF6α, ATF6β is an ER transmembrane protein with an N-terminal bZIP domain that is liberated by Golgi proteases upon ER stress.[45] ATF6β has significant sequence homology to ATF6α, not only in its bZIP and transmembrane domains, which it shares with the OASIS

subfamily members, but also in other areas of its cytosolic and luminal domains.[44, 45] Again, however, one area of noted difference is in its TAD, which lacks the critical eight amino acid VN8 sequence found in ATF6α.[43] When activated, ATF6β is a relatively weak transcriptional activator with a long half-life. Because ATF6β can both bind the same ERSE regions and form heterodimers with ATF6α, it can thus slow the activity of α and function as a transcriptional repressor.[43, 65, 118] However, it has more recently been shown to upregulate at least some of the same transcripts as ATF6α. Given its greater stability it thus may be able to compensate in model systems in which ATF6α has been deleted, a hypothesis that agrees with the fact that while either ATF6α or β knockout mice survive to adulthood, double-knockouts are embryonic lethal.[119]

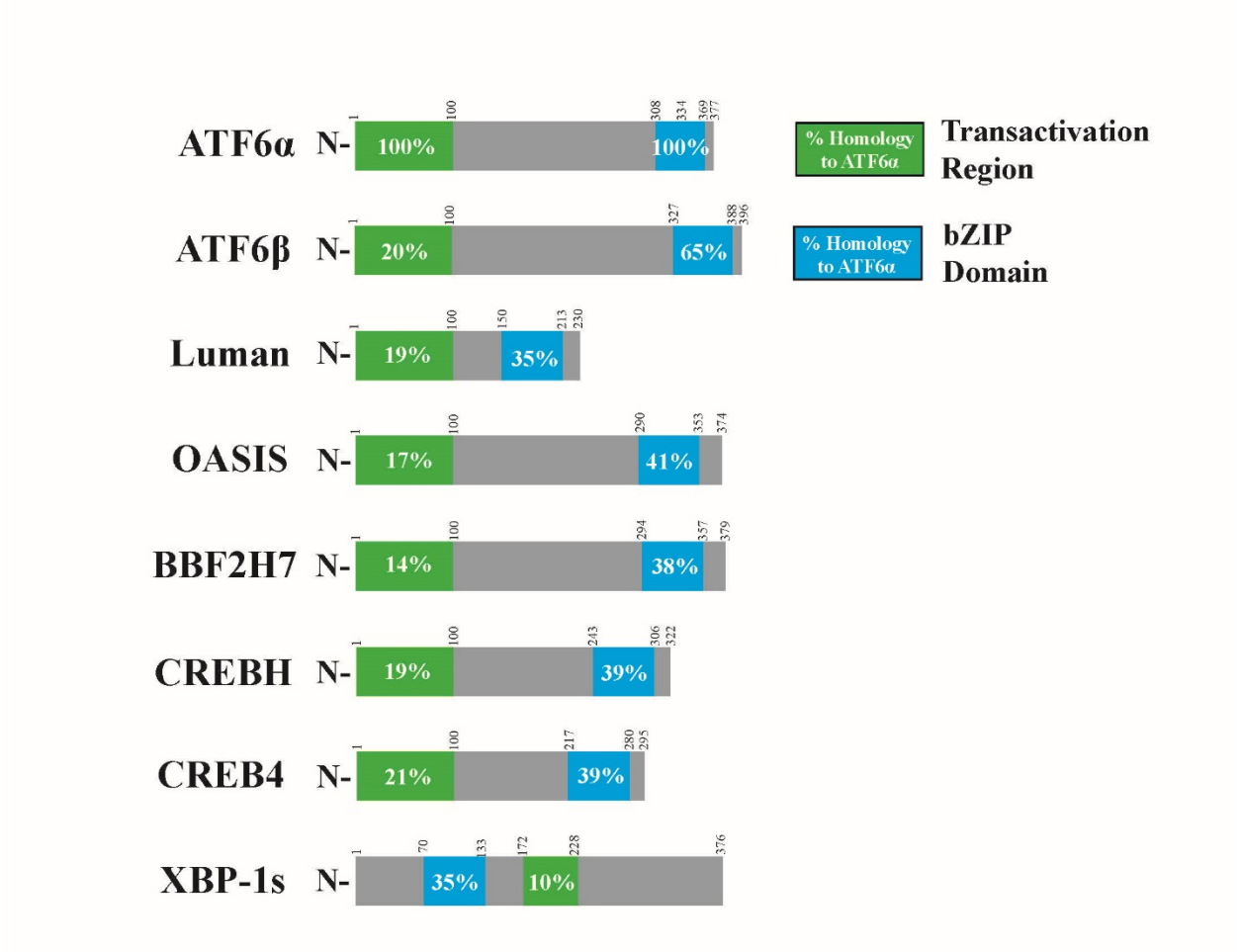

Figure 5. Sequence homologies to soluble N-terminal ATF6α amongst OASIS family members.
While all OASIS members have similar structure in their N-terminal fragments, they have low sequence homology to ATF6α in their TADs. There is greater homology, however, in their bZIP domains, especially for the member most closely related to ATF6α, ATF6β. Fellow ER stress effector XBP-1s, which is a bZIP transcription factor but is not in the OASIS subfamily, is included here for comparison.

11. Aims

The main objective of this dissertation is to elucidate the roles of ATF6α in cardiac non-myocytes during long-term cardiac injury. To address this objective, research reported in this dissertation will utilize a loss-of-function approach involving ATF6α global knockout mice in a long-term MI-induced heart failure model. Research reported here will also examine ATF6α gain- and loss-of-function approaches in two isolated primary multi-potent cardiac non-myocyte cell lines known to respond to injury by activation, proliferation, and/or differentiation into somatic cell types.

a. The Role of ATF6α in a Murine Model of Long-Term MI-Induced Heart Failure

To review, the Glembotski lab previously showed that, in the heart, ischemia activates ATF6α.[13] Furthermore, transgenic mouse hearts expressing a conditionally-activated form of ATF6α, and subjected to *ex vivo* ischemia/reperfusion, exhibited preserved heart function and smaller infarcts.[21] The Glembotski lab also showed that by serving as a novel inducer of a global antioxidant gene program, endogenous ATF6α limits cardiac damage caused by reactive oxygen species during reperfusion.[11] More recently, the Glembotski lab showed that ATF6α in cardiac myocytes is necessary for compensatory cardiac growth, following trans-aortic constriction surgery-induced pressure-overload, due to its non-canonical induction of the mTORC1 activator Rheb.[12] Lastly, pharmacological activation of ATF6α was shown to be protective in ischemia/reperfusion models in multiple tissues, including the heart.[105] However, less is known about the effect of endogenous ATF6α long-term in an MI-induced failing heart. Since ATF6α limits infarct size and preserves heart function following I/R injury, we hypothesized these benefits would have measurable effects on heart function long-term. Potentially deleterious cardiac remodeling, fibrosis, and heart failure, all of which can be long-term consequences of MI[120-122],

might be exacerbated in the absence of ATF6α. Furthermore, for the research done here, a permanent-occlusion model of MI[123] was employed, which results in the complete infarction of all tissue downstream of the occlusion. This serves to emphasize the effect of ATF6α on the regions of the heart remote from the infarct, likely including cardiac non-myocytes which respond to injury. We found that in the weeks following infarction, compared to wild type (WT) mice, ATF6α global KO mouse hearts exhibited decreased function and faster progression to heart failure, as measured by change in ejection fraction, the fraction of the total volume of blood held in the left ventricle that is ejected during each contraction. While control and ATF6α KO mouse hearts hypertrophied to a similar degree, KO mice showed greater cardiac dilation. Lastly, induction of the fetal gene program, which is characteristic of heart failure, was significantly higher in ATF6α KO hearts compared to WT.

b. ATF6α in the Proliferation and Differentiation of c-Kit$^+$ Cardiac Stem Cells

c-Kit$^+$ cardiac stem cells isolated from the adult mouse heart (CSCs, also known as cardiac progenitor cells) are a controversial cell type, primarily because previous claims of differentiation into mature cardiac myocytes[124-126] have been questioned on a functional level[127-129]. Additionally, clinical trials testing the use of autologous CSC therapy met with promising but ambiguous results.[130, 131] These trials involved CSCs grown in culture and then reinjected into the failing heart to promote a reduction in infarct size and a restoration of cardiac function. However, it became apparent that reinjected CSCs were quickly washed out and did not remain in the heart long enough to implant.[132] Investigators in the field subsequently struggled to explain any observed beneficial results, theorizing that exogenous CSCs release adaptive cytokines or exosomes, with positive effects on cardiac myocytes, before they are washed away.[133-135] However, lineage tracing experiments have shown that endogenous CSCs do indeed activate, proliferate, and differentiate

in response to injury.[127] They have been shown to primarily differentiate into endothelial cells or mast cells, which may indicate importance for vascularization or inflammation respectively.[127] Preliminary unpublished work from the Glembotski lab showed that initiating differentiation by stimulation with dexamethasone (Dex) treatment activates ER stress markers in isolated CSCs. Likewise, ER stress induces expression of multiple differentiation markers. Surprisingly however, in this dissertation, it was found that ATF6α plays a moderating role in the induction of differentiation markers of these cells, despite being a primary responder to ER stress stimulus. This may be due to the observed hyperactivation of the ER stress response (measured by XBP-1 splicing) when ATF6α cannot be activated. This effect is especially apparent when observing induction of the important smooth muscle and myofibroblast marker αSMA. Additionally, this lab has shown that ATF6α governs an antioxidant gene program which reduces the accumulation of ROS and contributes to its cardioprotective effect during ischemia-reperfusion.[11] ROS are known to play important roles during development and during the differentiation of various cell types.[136-138] N-acetyl cysteine, a glutathione precursor, is a potent chemical inhibitor of ROS.[139] If ATF6α loss of function in CSCs enhances the induction of differentiation markers with Dex stimulus due to the loss of its antioxidant gene program, NAC co-treatment may blunt this effect. Here we show that NAC rescues decreased viability with ATF6α inhibition and blunts the hyper-induction of differentiation markers with Dex stimulus in CSCs with ATF6α loss of function.

c. ATF6α in the Activation and Differentiation of Adult Murine Ventricular Fibroblasts

Upon myocardial injury, fibroblasts in the heart infiltrate the affected area and differentiate into new cell types called myofibroblasts. These cells are characterized both by the induction of contractile proteins and the secretion of extracellular matrix proteins, which form fibrotic scar

tissue.[7-9, 24] Investigating the factors governing fibroblast activation is key to understanding how these cells function in the heart and may be key to identifying novel therapeutic strategies. ATF6α plays critical roles in development[140], as well as in the differentiation of certain cell types[6, 141], yet ATF6α has not been studied in cardiac fibroblasts and its effect on fibrosis in the heart is unknown. Here, we hypothesized that ATF6α is an important regulator of fibroblast function. We found that fibroblast activation markers, including αSMA, were increased in infarcted hearts with global ATF6α deletion. Additionally, hearts with TAC-induced pressure overload showed increased fibrosis staining in global ATF6α-null mice relative to WT hearts. In isolated adult murine ventricular fibroblasts (AMVF), loss of ATF6α induced myofibroblast markers with and without the activation stimulus TGFβ. ATF6α loss of function also enhanced the effect of TGFβ on fibroblast contraction. These effects were associated with an increase in Smad phosphorylation, a crucial step in the TGFβ pathway. Interestingly, the effect of ATF6α loss of function in AMVF was erased when treated with the TGFβ receptor inhibitor SB431542. Additionally, when ATF6α was overexpressed or when endogenous ATF6α was pharmacologically activated, myofibroblast markers were reduced and activation by TGFβ was blunted. ATF6α activation also prevented the formation of αSMA contractile fibers, also known as stress fibers. In a PCR array of fibrosis genes, ATF6α activation downregulated the majority of genes interrogated, while ATF6α silencing resulted in the opposite. Among the most upregulated genes with ATF6α gain-of-function were several TGFβ/Smad pathway[142] negative regulators including Smurf1[143], Smurf2[144], and PMEPA1[145, 146], though none of these are known to be ATF6α target genes. Among the genes downregulated by ATF6α were the TGFβ receptors and two TGFβ isoforms. These data suggest that ATF6α decreases fibroblast activation.

Section I., Introduction, is, in part, a reprint of the review article "Sledgehammer to Scalpel: Broad Challenges to the Heart and Other Tissues Yield Specific Cellular Responses Via Transcriptional Regulation of the ER Stress Master Regulator ATF6α" as it appears in the International Journal of Molecular Sciences, 2020. Stauffer, Winston T.; Arrieta, Adrian; Blackwood, Erik A.; Glembotski, Christopher C., *Int J Mol Sci*, 2020. The dissertation author was the primary author of this paper.

II. Materials and Methods

A. Laboratory Animal Use

The research reported here has been reviewed in animal protocol 19-09-010G and approved November 25, 2019 by the San Diego State University Institutional Animal Care and Use Committee (IACUC) and conforms to the Guide for the Care and Use of Laboratory Animals published by the National Research Council.

B. c-Kit$^+$ Cardiac Stem Cell Isolation

Adult mouse c-Kit$^+$ cardiac stem cells (CSCs) were isolated as previously described.[147] Accordingly, the ascending aorta of each WT mouse heart was cannulated and retrograde perfused at 3 mL/min for 5 min at 37 °C with basic buffer (Joklik Modified Minimum Essential Medium (cat# M-0518, Sigma-Aldrich, St. Louis, MO, USA) supplemented with 2 g/L sodium bicarbonate (cat# S-8875, Sigma-Aldrich), 10 mM HEPES (cat# 15630-080, Gibco, ThermoFisher, Waltham, MA, USA), 30 mM taurine (cat# T8691, Sigma-Aldrich), and 2 mM glutamine (cat# G8540, Sigma-Aldrich), pH 7.3). Hearts were then digested by perfusing for 8-15 min with basic buffer that contained type 2 collagenase (50–60 mg; ~320 U/mL, cat# LS004176, Worthington, Lakewood, NJ, USA) until the tissue became pale and compliant. To stop digestion, the heart was then perfused with 5 mL BSA solution (the above basic buffer with 5 mg/mL BSA (cat#A6003, Sigma-Aldrich) added). The heart was then placed in BSA solution on ice and, if necessary, additional hearts were prepared. Once all hearts were fully perfused, they were collected and transferred to a 15 ml beaker then further dissociated with fine-tip scissors into ~1 mm chunks. The suspension was then aspirated up and down using transfer pipets until it became cloudy. The suspension was then centrifuged at 300 g, low brake, for 1 minute at room temperature (20–22°C) to separate into myocyte and non-myocyte fractions. The supernatant containing the non-myocytes

was brought up to 30 mL with BSA solution and then passed through a 40 μm mesh filter before centrifuging again at 600 g (medium high brake) for 10 minutes at room temperature to collect the non-myocytes. A 25 mL aliquot of the supernatant was removed and the pellet was resuspended in the remaining 5 mL. The suspension was then passed through a 30 μm pre-separation filter (cat#130041407, Miltenyi, Bergisch Gladbach, Germany) and centrifuged again at 600 g for 10 minutes. The supernatant was removed, and the pellet was resuspended in 80 uL of washing buffer (D-PBS (cat# 14190144, Gibco, ThermoFisher) with 0.5% BSA). The suspension was incubated with 20-40 uL of anti-CD117 (c-Kit) microbeads (cat#130091224, Miltenyi) per every two hearts, depending on the size of the pellet, rocking for 20 minutes at 4 °C in the dark. An aliquot of 1 mL of washing buffer was added before centrifuging for 10 minutes at 600 g at 4 °C. The pellet was resuspended in 500-1000 μL of washing buffer, depending on the pellet size. The cell solution was passed through MS columns (cat# 130042201, Miltenyi) held by a magnet stand to retain the beads and the attached cells in the column. The column was then flushed with additional washing buffer. Once removed from the magnet, the column was flushed once more with 1 mL of washing buffer and the cells expelled from the column using a plunger. The cells were centrifuged once more for 10 minutes at 600 g at room temperature. The pellet was resuspended in CSC media (DMEM:F12 (cat# 11330-032 Gibco, ThermoFisher) with 10% embryonic stem cell qualified fetal bovine serum (esFBS, cat# 10439024, Gibco, ThermoFisher), 20 ng/mL epidermal growth factor (cat# E9644, Sigma-Aldrich), 20 ng/mL fibroblast growth factor (cat# 100-18, Peprotech, Cranbury, NJ, USA), and 10 ng/mL leukemia inhibitory factor (cat#ESG1107, Sigma-Aldrich) and plated on 1% gelatin (cat# S25335, ThermoFisher) coated plates. Once passaged 3 times, cells were frozen back in liquid nitrogen in a media containing 45% CSC media, 45% esFBS, and 10% DMSO (cat#317275, MilliporeSigma, Burlington, MA, USA), 50,000 cells per vial, and were thawed as needed for all

experiments. Cells were passaged using a 1:1 solution of TrypLE (cat# 12605-010, Gibco, ThermoFisher) and Cell Stripper (cat# 25-056-CL, Corning, NY, USA).

C. Cardiac Non-Myocyte Isolation

Adult mouse ventricular fibroblasts (AMVFs) were isolated as previously described for adult ventricular myocytes[11] with the non-myocyte fraction cultured to select for a culture dominated by fibroblasts. Accordingly, the ascending aorta of each mouse heart was cannulated and retrograde perfused at 3 mL/min for 4 min at 37 °C with heart medium (Joklik Modified Minimum Essential Medium (cat# M-0518, Sigma-Aldrich, St. Louis, MO, USA) supplemented with 10 mM HEPES (cat# 15630-080, Gibco, ThermoFisher), 30 mM taurine (cat# T8691, Sigma-Aldrich), 2 mM D-L-carnitine (cat#C9500, Sigma-Aldrich), 20 mM creatine (cat#C0780, Sigma-Aldrich), 5 mM inosine (cat# I4125, Sigma-Aldrich), 5 mM adenosine (cat# A9351, Sigma-Aldrich), and 10 mM butanedione monoxime (BDM) (cat# B0753, Sigma-Aldrich), pH 7.36). Hearts were then digested by perfusing for 13 minutes with heart medium that contained type 2 collagenase (50–60 mg; ~320 U/mL, cat# LS004176, Worthington, Lakewood, NJ, USA) and 12.5 μM $CaCl_2$ (cat# 449709, Sigma-Aldrich). Beginning 5 minutes into the digestion, effluent dripping from the heart was collected. The cannula was then removed, and the heart was submerged in a dish with 2.5 mL of the accumulated effluent where the aorta and atria were excised. The remaining ventricles were then dissociated with forceps. The collagenase was neutralized with 2.5 mL of heart medium supplemented with 10% fetal bovine serum (FBS, cat# FB-12, lot# 206018, Omega Scientific, Tarzana, CA, USA), and the final concentration of $CaCl_2$ was adjusted to 12.5 μM. The now digested heart slurry was further dissociated into a cell suspension by gently and repeatedly pipetting up and down with a transfer pipette for 4 minutes. The cell suspension was then gravity-filtered through a 100 μm mesh filter into a 50 mL conical tube. Following filtration, myocytes

were sedimented by gravity. After 6 minutes, the supernatant containing non-myocytes was carefully removed. The remaining sedimented myocytes were resuspended and used for other unrelated experiments. The non-myocyte fraction was centrifuged and resuspended in 10% FBS with penicillin/streptomycin/glutamine (PSG) (cat# 10378016, Gibco, ThermoFisher) and plated on 12 well (0.5 mL per well) or 10 cm tissue culture dishes (Falcon Brand, Corning) (10 mL per well). Following 16 hours of incubation at 37 °C, the media were changed to remove non-viable cells and associated debris. The culture was then maintained for approximately 7 days, with further media changes every 2 days, until the cells were morphologically flat and spindle shaped and sufficiently dense to be used for experiments. Culturing the non-myocyte fraction for this period significantly increased the fibroblast marker *Tcf21*[127] and abolished any remaining cardiac myocyte markers **(Figure 6)**. All AMVF used in these experiments were primary cell cultures and were not frozen back for later use.

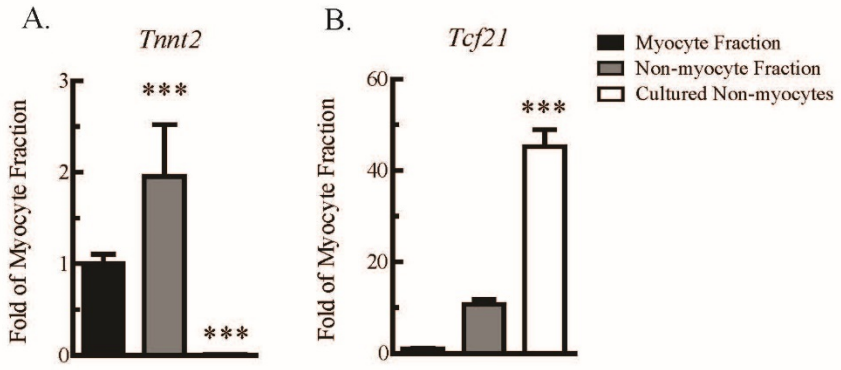

Figure 6. qRT-PCR of different fractions isolated from a WT adult mouse heart.
Fractions are separated by gravity sedimentation as described. The pellet contains the adult myocytes (black bars) and the supernatant contains the non-myocyte fraction (gray bars). Culturing the non-myocyte fraction for one week (white bars), with regular media changes, allows for the removal of debris and dead myocytes and the enrichment of cardiac fibroblasts (AMVF). **(A)** Immediately post-isolation both the myocyte fraction and non-myocyte fractions are positive for the cardiac myocyte marker *Tnnt2*. However, after one week of culture, *Tnnt2* signal is almost completely gone, reflecting the death and removal of any remaining myocytes. **(B)** Immediately post-isolation the myocyte fraction is negligible for the common fibroblast marker *Tcf21* while the non-myocyte fraction is higher. After one week of culture, the non-myocytes are significantly higher in *Tcf21*, reflecting fibroblast enrichment over time. ****p≤0.001 by one-way ANOVA*.

D. NIH 3T3 Cell Culture

NIH 3T3 immortalized fibroblast cells were thawed from previously frozen stocks for experimental use. 3T3s were maintained in 10% FBS DMEM:F12 media with PSG and passaged with TrypLE.

E. Cell Proliferation Assay

For experiments where cell number was determined, cells were plated in 6-well culture dishes. After the prescribed waiting period, the cultures were washed with D-PBS and then trypsinized with 250 μL TrypLE for 5-15 min, until cells were floating. The TrypLE was neutralized with 750 μL 10% FBS growth media and the cell suspension was transferred to Eppendorf tubes, one per well, and spun down at 300 rpm, low brake, for 15 min. Supernatant was carefully removed and the pellet resuspended in 100 μL-1000 μL of serum-free 1:1 DMEM:F12, depending on the size of the pellet. An aliquote of 10 μL of the cell suspension was transferred to each side of a hemacytometer (cat# 1475, Hausser Scientific, Horsham, PA, USA) with cover glass and three 1 mm squares were counted per side and averaged. The average count per square was multiplied by 10^4 to get the total cell number per well.

F. Immunoblotting

Cells were lysed in buffer comprising 50 mM Tris (cat# 02-004-508, J.T.Baker, ThermoFisher) -HCl (cat# 9535-03, J.T.Baker, ThermoFisher) (pH 7.5), 150 mM NaCl (cat# 215700, Beantown Chemical, Hudson, NH, USA), 0.1% SDS (cat# 4095-02, J.T.Baker, ThermoFisher), 1% Triton X-100 (cat# T9284, Sigma-Aldrich), protease inhibitor cocktail (cat# 05892791001, Roche Diagnostics, Indianapolis, IN, USA) and phosphatase inhibitor cocktail (cat# 4906837001, Roche Diagnostics). Lysates were subjected to centrifugation at 15,000 × g for 15 minutes at 4 °C to sediment any cell debris, and the protein concentration was determined using

the DC™ protein assay (cat# 5000111, Bio-Rad, Hercules, CA, USA). Samples, typically comprising 10–30 μg of protein, were mixed with 6X concentrated Laemmli sample buffer including 2-mercaptoethanol (cat# M7154, Sigma-Aldrich), heated at 95 °C for 5 min, then subjected to SDS-PAGE followed by transferring onto PVDF membrane (cat# NEF1002001PK, ThermoFisher) for immunoblotting analysis. Antibodies were purchased that were raised against ATF6α (cat# 24169-1-AP, Proteintech, Rosemont, IL, USA, 1:1000), KDEL proteins (cat# ADI-SPA-827-F, Enzo, Farmingdale, NY, USA, 1:8000), Smad 2/3 (cat# 3102, Cell Signaling, Danvers, MA, USA, 1:1000), phosphorylated Smad 2 (Ser456/467) (cat# 3108, Cell Signaling, 1:1000), or GAPDH (cat# RDI-TRK5G4-6C5, Fitzgerald Industries International, Concord, MA, USA, 1:150 × 20,000).

G. RNA Extraction

RNA was extracted from CSCs, AMVFs, or NIH 3T3 cultures using Quick-RNA MiniPrep Kit, according to the manufacturer's instructions (cat# R1055, Zymo Research, Irvine, CA, USA). RNA was extracted from mouse heart tissue using RNeasy Mini Kit, according to the manufacturer's instructions (cat# 74106, Qiagen, Germantown, MD, USA).

H. Quantitative Real-Time PCR (qRT-PCR)

cDNA was generated using Superscript III, according to the manufacturer's instructions (cat# 18080-300, Life Technologies, Carlsbad, CA, USA). qRT-PCR was performed on an Applied Biosystems StepOnePlus™ Real-Time PCR System using the Maxima SYBR Green/ROX 2× qPCR Master mix (cat# K0223, Thermo Scientific, Waltham, MA, USA) and the mouse primers for *Acta2*, *Atf6*, *Col1a1*, *Hspa5*, *Myh6*, *Myh7*, *Nppa*, *Nppb*, *Pmepa1*, *Smurf1*, *Smurf2*, *Tcf21*, *Tnnt2*, and *Gapdh*. Sequences listed below:

Acta2—Fwd 5'-GTTCAGTGGTGCCTCTGTCA-3'

Acta2—Rev	5’-ACTGGGACGACATGGAAAAG-3’
Atf6—Fwd	5’-CTTCCTCCAGTTGCTCCATC-3’
Atf6—Fwd	5’-CTTCCTCCAGTTGCTCCATC-3’
Col1a1—Fwd	5’-AAGACGGGACGGCGAGTGCT-3’
Col1a1—Rev	5’-TCTCACCGGGCAGACCTCGG-3’
Gapdh—Fwd	5’-ATGTTCCAGTATGACTCCACT-3’
Gapdh—Rev	5’-GAAGACACCAGTAGACTCCAC-3’
Hspa5—Fwd	5’-GATACTGGCCGAGACAACAC-3’
Hspa5—Rev	5’-AGGAGGAGACACGAAGCA-3’
Nppa—Fwd	5’-GAGAGAGAGAAAGAAACCAGAGTG-3’
Nppa—Rev	5’-CTCATCTTCTACCGGCATCTTC-3’
Nppb—Fwd	5’-GTCAGTCGTTTGGGCTGTAA-3’
Nppb—Rev	5’-GCAAGTTTGTGCTCCAAGATAAG-3’
Myh6—Fwd	5’-CGGAAAGACGGTGACCATAAA-3’
Myh6—Rev	5’CTGATAGGCGTTGTCAGAGATG-3’
Myh7—Fwd	5’-TGCCCGATGACAAAGAAGAG-3’
Myh7—Rev	5’-AAGAGGCCCGAGTAGGTATAG-3’
Pmepa1—Fwd	5’-TGTCCTCGGAAGGATGCCTCTGG-3’
Pmepa1—Rev	5’-CAGCGAGTCGGTCAGTGGGC-3’
Smurf1—Fwd	5’-AGGCTCTGCAAGGCTCTACAG-3’
Smurf1—Rev	5’-GGTGGTTGTGAGCAAGACTCTG-3’
Smurf2—Fwd	5’-AAGAACTACACAGTGGGAACGC-3’
Smurf2—Rev	5’-CACGTTGCACCATTTGTTCC-3’

Tcf21—Fwd 5’-CATTCACCCAGTCAACCTGA-3’

Tcf21—Rev 5’-CCACTTCCTTCAGGTCATTCTC-3’

Tnnt2—Fwd 5’-GGAAGAGACAGACAGAGAGAGA-3’

Tnnt2—Rev 5’-GGTTTCGCAGAACGTTGATTT-3’

I. PCR Arrays

PCR arrays were performed on cDNA generated using Qiagen RT^2 First Strand Kit (cat# 330401, Qiagen, Germantown, MD, USA) from isolated RNA (described above) using RT^2 Profiler PCR Arrays for Mouse Cell Cycle (cat# PAMM-020Z, Qiagen, Germantown, MD, USA), Oxidative Stress (cat# PAMM-065Z), and Fibrosis (cat# PAMM-120Z) according to the manufacturer’s instructions.

J. XBP-1 Splicing Assay

This assay utilized the same cDNA generated for qPCR as above. An aliquot of 4 µL of sample cDNA was combined in a PCR tube with 45 µL of Platinum Blue PCR Supermix (cat# 12580, ThermoFisher) and 0.5 µL of the *Xbp1* primers listed below:

Xbp1—Fwd 5’-TTACGGGAGAAAACTCACGG-3’

Xbp1—Rev 5’-ACAGGGTCCAACTTGTCCAG-3’

The reaction mix was then run on a thermocycler with the following settings:

1. 94°C for 2 minutes
2. 36 cycles of: 94°C for 30 seconds → 60°C for 30 seconds → 72°C for 60 seconds
3. 72°C for 10 minutes

The reaction products were then separated on a 2-3% agarose gel at 100 volts for 60 minutes with 1:100000 ethidium bromide. The resulting bands were viewed under UV light and

were inferred to be spliced or unspliced, based on size relative to a GeneRuler 100 bp DNA ladder (cat# SM0241, Thermo Fisher).

K. siRNA Transfection

Targeted gene knockdown was achieved with siRNA designed using Thermo Fisher Block-IT RNAi designer software (Thermo Fisher Scientific, Waltham, MA, USA). Transfection was achieved with HiPerFect transfection reagent (cat# 301704, Qiagen, Germantown, MD, USA), as follows: Cell cultures were switched to 0.5%, antibiotic-free media that had been incubated at room temp for 15 minutes with HiPerFect and siRNA. Six microliters of 20 nM siRNA and 6 µL of HiPerFect were added per 1 mL of media and vortexed briefly prior to the 15-minute incubation. siRNA was targeted to murine ATF6α (cat#10620312, Thermo Fisher Scientific, Waltham, MA, USA) and a non-targeting sequence (cat# 12935300, Thermo Fisher) was used as a control.

L. 3-(4,5-dimethylthiazol-2-yl)-2,5-diphenyltetrazolium (MTT) Assay

Cells were plated and treated in a 12-well dish. Following, treatment media was removed and replaced with 500 µL growth media with 18 µL MTT reagent (cat# 11465007001, Roche Diagnostics) and incubated at 37 °C for 4 hours. Afterwards, cells were examined under the microscope to verify the appearance of purple formazan crystals in viable cultures. Cells were then solubilized by adding 500 µL DMSO to the media already in the well and aspirating to mix. Optical density of samples from each well was then read on a plate reader at a wavelength of 540 nm.

M. *Gaussia* Luciferase Secretion Assay

Expression of *Gaussia* Luciferase (GLuc) in cultured CSCs was achieved by transfection of pCMV-GLuc 2 Control Plasmid (cat# N8081, New England Biolabs, Ipswich, MA, USA). The GLuc plasmid or GFP plasmid (as a control) was transfected into CSCs cultured on 6-well dishes using Fugene Transfection Reagent (cat# E2311, Promega, Madison, WI, USA). 2 µg of plasmid

was combined with 6 µL Fugene Reagent and then the solution was brought up to 100 µL with CSC growth media and incubated for 15 minutes at room temperature. 10 µL of the solution was then added to each well and allowed to incubate at 37 °C for 24 hours. The media was then refreshed and incubation continued for another 24 hours at 37 °C before any treatments were added. The activity of GLuc was assessed using the BioLux *Gaussia* Luciferase Assay Kit (cat# E3300L, New England Biolabs) as per the manufacturer's instructions using the Stabilized Assay Protocol II for injector-equipped luminometers. Secreted GLuc was assessed in media samples, while intracellular GLuc was assessed in cell lysates prepared using Luciferase Cell Lysis Buffer (cat# B3321, New England Biolabs). Samples were loaded into and read by an injector equipped luminometer and the injector primed using assay solution.

N. Collagen Gel Contraction Assay

NIH 3T3 cells were resuspended in chilled serum-free culture media at a concentration of 150,000 cells/mL. For each gel, 400 µL of the cell suspension was combined with 200 µL of chilled 3 mg/mL Cultrex Rat Collagen I (R&D Systems, Minneapolis, MN, USA) and 12 µL of filtered 1 M NaOH (cat#72068, Sigma-Aldrich) as well as any experimental treatment. 500 µL of this solution were quickly transferred to each well of a 24-well dish and incubated at 37 °C for 20 minutes. 1 mL of 10% FBS culture media, including any treatments, was then added to each well, and the polymerized gel disk was freed from the bottom of the disk using an autoclaved 200 µL pipette tip. The gels were verified to be freely floating before returning to the incubator. Contraction was then monitored at regular intervals up to 48 hours.

O. Immunocytofluorescence

AMVFs or NIH 3T3s were plated and maintained as described above on four chamber glass slides (Falcon Brand, Corning). After cells had reached approximately 70% confluency, the

medium was changed to medium containing ±10 μM compound 147 and/or 10 ng/mL TGFβ for 48 hours. After each treatment, AMVFs were washed with D-PBS, fixed for 15 min with 4% paraformaldehyde, and then permeabilized for 10 min with 0.5% Triton X-100 + 3 mM EDTA (cat# E5134, Sigma-Aldrich). Slides were blocked for 1 hour with SuperBlock (cat# 37515, Sigma-Aldrich), and subsequently incubated with a primary antibody to αSMA (cat# A2547, MilliporeSigma, St. Louis, MO, USA, 1:500) for 16 hours at 4 °C. Slides were incubated with Cy3 fluorophore-conjugated secondary antibodies for 1 hour, followed by a Hoechst nuclear counter stain (1:1000) for 10 min.

P. Myocardial Infarction

Permanent occlusion myocardial infarction (MI) was performed in vivo by ligating the left anterior descending artery (LAD), as previously described.[123] Briefly, adult male mice were anesthetized using a 2% isoflurane (cat# NDC66794-013-25, Piramal, Mumbai, India)/O_2 mixture. Using aseptic technique, an incision was made to expose the trachea and the animal was intubated. Mice were then treated with buprenorphine HCl (0.1 mg/kg IP, cat# NDC 12496-0757-5, Reckitt Benckiser Healthcare Ltd., Hull, England, UK) before an approximately 2 cm skin incision was made, lateral to the sternum and extending towards the axillary region. The left pectoralis muscle was retracted with an elastic retractor and the chest cavity penetrated with forceps in between the third and fourth ribs. Additional retractors were used to expose the anterior side of the left ventricle of the heart and the LAD. Using a 7–0 silk suture, the LAD was permanently ligated at a point just proximal to its downstream bifurcation and adjacent to the left atrium. Sham surgery mice were given the same procedure, except that the LAD was not ligated. The thoracic cavity and all skin incisions were then closed with surgical glue and the mice were transferred to individual cages to recover. Animals were again injected with buprenorphine HCl (0.1 mg/kg IP) 12 h after surgery

to aid in recovery and were continually monitored for signs of pain or distress thereafter. If such signs became apparent, additional doses of buprenorphine were administered. For the acute MI model, seven days after surgery, animals were anesthetized, sacrificed, and the hearts removed. Hearts were dissected to separate atria and the right and left ventricle. The left ventricle was further separated into infarct, peri-infarct, and distal regions and then frozen in liquid nitrogen before transfer to a −80 °C freezer for storage. For the long-term, MI-induced heart failure model, animals were maintained post-surgery for 11 weeks. Heart function and physical parameters were monitored biweekly, starting on week 1 post-surgery, via echocardiography (see below). Following the week 11 echo, mice were sacrificed as before. Additionally, heart weights and tibia lengths were also recorded.

Q. 2,3,5-triphenyl-2H-tetrazolium chloride (TTC) Staining

Immediately before sacrifice, TTC powder (cat# T8877, Sigma-Aldrich) was reconstituted at 0.5 g in 50 mL of D-PBS to make a working stock, which was covered in foil and kept on ice until used. Mice were sacrificed using pentobarbitol intraperitoneal injection and their hearts removed. Hearts were washed in three chilled D-PBS washes and the blood vessels, atria, and right ventricle were removed. Hearts were then briefly frozen (~5 minutes at -80° C) and then divided into 1 mm sections using seven razor blades in a tissue matrix. Sections were then transferred to a scintillation vial with 5 mL of the TTC solution, which was then covered in foil and incubated in a 37 °C waterbath for 15 minutes. Sections were then removed from the TTC and suspended in 10% formalin (cat# SF100-4, ThermoFisher) and stored at 4 °C overnight. The next day, sections were imaged on an ordinary scanner set to highest resolution. To obtain the area of infarct, the area of the red (viable) area was subtracted from the total area of the entire section, areas which were

then added together with all the other sections for each heart. Areas were measured using ImageJ software.

R. Transthoracic Echocardiography

Transthoracic echocardiography of WT and ATF6α KO mice was performed using a high-resolution echocardiograph system (Vevo 2100 System, Fujifilm VisualSonics, Toronto, Ontario, Canada). Mice were anesthetized using an induction box with 2% isoflurane flow. The chest fur of the mice had previously been removed using Nair. The unconscious mice were transferred to a heated platform with electrodes to detect heart rate. A nose cone also connected to isoflurane flow kept the mice unconscious. All measurements, whenever possible, were taken when the mice had a heart rate between 450-500 bpm. Isoflurane flow was adjusted as necessary to maintain this window. The mice were laid supine and the exposed chest skin coated in warmed ultrasound gel (cat# 01-50, Parker Laboratories, Fairfield, NJ, USA). All four paws were taped over the electrodes with added electrode conductive cream (cat# 17-05, Parker Laboratories). The probe was then moved into place and both long-axis (B-mode) and short-axis (B- and M-mode) images were captured. The short axis plane was determined by locating the apex of the heart and then moving anterior until the papillary muscles first appeared. The M-mode line was placed just alongside the papillary muscle landmarks to ensure consistency between mice. B-mode images were purely for visual reference while all measurements were made using the short-axis M-mode images. Data analysis was conducted using the onboard Vevo 2100 software suite.

S. Transverse Aortic Constriction Surgery

Transverse aortic constriction (TAC) was performed in vivo by using a 6-0 silk suture to partially ligate the aorta as previously described.[12] Briefly, adult male mice were first anesthetized in an induction chamber using a 2% isoflurane/O2 mixture. Using aseptic technique, an incision

was made to expose the trachea and the animal was intubated. Mice were then treated with buprenorphine (0.1 mg/kg IP) before an approximately 1.5 cm vertical skin incision was made, lateral to the sternum and extending towards the axillary region. The left pectoralis muscle was retracted with an elastic retractor and the chest cavity punctured with forceps in the fourth intercostal space. Additional retractors were used on adjacent ribs to expose the heart and aortic arch. The aorta was isolated from the surrounding tissue, and partially ligated between the innominate and left common carotid arteries with a 6-0 silk suture. Partial ligation of the aorta was performed by placing a dull 27-gauge needle to the side of the artery and tying the ligature firmly to both the needle and the artery, before the needle was removed leaving a calibrated stenosis of the aorta. Sham operated mice were given the same procedure, except that the aorta was not constricted. The thoracic cavity and all skin incisions were then closed with surgical glue and the mice were transferred to individual cages to recover. Animals were again injected with buprenorphine (0.1 mg/kg IP) 12 h after surgery to aid in recovery and were continually monitored for signs of pain or distress thereafter. If such signs became apparent, additional doses of buprenorphine were administered. Seven days after surgery, animals were anesthetized, sacrificed, and the hearts removed. Immediately prior to sacrifice, alterations in Doppler velocities of the innominate and left carotid arteries seven days post-TAC were quantified, as previously described.

T. Picro-Sirius Red Staining

Mouse hearts embedded in paraffin wax blocks were sectioned using a manual microtome into 5 μM sections across the long-axis of the left ventricle. Sections were bonded to charged glass slides (cat# 1158B91, Denville, Thomas Scientific, Swedesboro, NJ, USA) for long-term storage. Prior to staining, sections were deparaffinized in xylene and graded alcohol solutions by sequential submersion as follows:

Xylene – 5 min. → Xylene – 5 min. → Xylene – 5 min. → Alcohol 100% – 3 min. → Alcohol 100% – 3 min. → Alcohol 100% – 3 min. → Alcohol 95% – 3 min. → Alcohol 95% – 3 min. → Alcohol 70% – 3 min. → DDI Water – 5 min. → DDI Water – 5 min. → DDI Water – 5 min.

Slides were then placed in a Coplin jar and submerged in Picro-Sirius Red solution (cat# 26357-02, Electron Microscopy Services, Hatfield, PA, USA) for 60 minutes. Following this, slides were rinsed twice with Acetic Acid Solution (cat# V193-46, Mallinckrodt, Staines-Upon-Thames, Surrey, UK) and then dehydrated by sequential submersion in graded alcohol solutions and xylene as follows:

Alcohol 70% – 5 min. → Alcohol 95% – 3 min. → Alcohol 100% – 3 min. → Xylene – 3 min. → Xylene – 3min.

Slides were then mounted using Permount mounting medium (cat# 17986-01, Electron Microscopy Services) and a glass slide. Staining was imaged using a slide scanner and epifluorescence microscope.

U. WT and ATF6α Knockout Mice

The ATF6α global knockout (KO) mice used in this study were 10-week-old male C57/Bl6 generated so that both ATF6α alleles had exons 5 and 6 globally deleted in all tissues and cell types, leading to a complete absence of any ATF6α protein but without affecting the other ATF6 isoform, ATF6β. ATF6α global knockout mice were a gift of Dr. Randall Kaufman and have been previously described.[100] ATF6α-floxed mice were a gift from Gokhan S. Hotamisligil. Briefly, ATF6α-floxed mice were generated with a targeting-construct, flanking exons 8 and 9 of ATF6α with locus of X-over P1 (LoxP) sequences on a C57B/6J background, as previously described.[148] The plasmid encoding the human cardiac troponin T promoter driving Cre-recombinase was a gift

from Dr. Oliver Müller.[149] Adeno-associated virus 9 (AAV9) preparation and injection were carried out as previously described.[11, 100] Eight-week-old ATF6α-floxed mice were injected via the lateral tail vein with 100 μL of AAV9-control or AAV9-cTnT-Cre containing 1×10^{11} viral particles and housed for 2 weeks before either sacrifice or experimental initiation, as previously described.

V. Dexmethasone, PF429242, TGFβ, SB431542, and Compound 147 Treatment

All treatments applied to cell cultures were added in 10% FBS culture medium. Dexamethasone-water soluble (cat# D2915) was purchased from Sigma-Aldrich and resuspended in water at 10 mg/mL to create a stock solution. Porcine, platelet-derived TGFβ1 (cat# 101-B1) was purchased from R&D Systems (Minneapolis, MN, USA). TGFβ1 stock solution was created by resuspending in 4 mM HCl with 0.1% BSA at 10 μg/mL. TGFβR1 inhibitor compound SB431542 (cat# 1614) was purchased from Tocris (Minneapolis, MN, USA). SB431542 stock solution was created by resuspending in DMSO at 10 mM. ATF6α activator compound 147 was a gift of Dr. Luke Wiseman and Dr. Jeffrey Kelly and has been previously described.[59, 60] 147 stock solution was created by resuspending in DMSO at 10 mg/mL.

W. Statistics

All error bars shown are ±SEM and statistical treatments are Student's t-test when comparing two values or one-way analysis of variance (ANOVA) with Newman–Keuls post hoc analysis when comparing more than two values.

III. Results

A. Effect of Global ATF6α Loss-of-Function in an MI-Induced Model of Heart Failure

1. Introduction

Common conditions, such as hypertension, hyperlipidemia, diabetes, and obesity are risk factors for the development of atherosclerosis, defined as the build-up of atheromatous plaques inside coronary arteries.[150, 151] Narrowing and eventual occlusion of these arteries causes the cessation of blood-flow to downstream tissue. Frequently this cessation is quite sudden, as when the plaque ruptures and triggers an immune response, creating a blood clot which can completely block the artery. The reduction or cessation of blood-flow creates ischemic conditions in all tissue downstream of the blockage.[152] This causes numerous stresses on each affected cell, including hypoxia, hypoglycemia, and the buildup of metabolic wastes.[13, 153] If ischemia continues, the downstream tissue will eventually become infarcted, or dead, and in the heart the damaged myocardium, which cannot regenerate, needs to be replaced with a fibrotic scar to avoid cardiac rupture.[121] Clinical interventions typically include reopening the artery and reperfusing the tissue, before total infarction occurs, by administering anticoagulants, or by catheterization.[154] However, sudden resumption of blood flow causes its own reperfusion damage, characterized by the generation of reactive oxygen species (ROS).[155] ROS are normally produced during cellular metabolism but sudden, excessive increases in ROS, as occurs in reperfusion, cause mitochondrial dysfunction, damage to DNA and lipid membranes, and altered enzymatic function.[156] In the ER, ROS-induced oxidative stress impairs the folding of nascent proteins in the ER lumen.[11, 21, 105] All of these stresses can result in cell death. Thus, reperfusion therapy adds to the total area of infarction, while still preserving some of the tissue in the total area at risk and, overall, reducing mortality.[155, 156] It should also be noted that not all myocardial infarctions (MI) are treated, such as

those that are too minor to be noticed. These can lead to the permanent infarction of all affected tissue.[157] Infarction of an area of the myocardium, if not immediately fatal, decreases the ability of the heart to adequately pump blood because the infarct is covered by a stiff, fibrotic scar that is both noncontractile and disruptive to the propagation of electrical signaling to the rest of the heart. Over time, this leads to compensatory hypertrophy of the still-viable cardiac tissue, followed by myocyte dropout and decompensatory dilation of the affected ventricle, usually the left, ultimately leading to heart failure.[120-122]

In the ER, ischemia results in a reduction of ATP and an imbalance in ER calcium, both of which impair ER protein folding. Ischemia thus causes ER stress and activation of the ER stress response. Unresolved ischemic ER stress causes apoptosis and contributes to overall myocardial cell death. ATF6α is activated during simulated ischemia in cultured cardiac myocytes.[13] Furthermore, ATF6α activation has a beneficial preconditioning effect when employed at or prior to initiation of ischemia, providing some protection upon further ischemia and reperfusion. In cardiac myocytes, ATF6α has been shown to reduce infarct size and preserve cardiac function following cardiac ischemia/reperfusion injury.[11, 21, 105] This, is in part due to the ability of ATF6α to improve cardiac myocyte viability by preserving ER protein folding capacity, thereby reducing cell death during adverse conditions.[13] Since cardiac myocytes have little to no proliferative potential, preservation of preexisting myocytes is key to preservation of cardiac function.[158] Additionally, cardiac non-myocytes, which are activated during injury and contribute to the formation of scar tissue and other aspects of cardiac remodeling, also influence cardiac function, though the role of ATF6α in those cell types was previously unknown.[1, 7-9, 24, 109, 127, 129]

In this dissertation research the model selected for study was a mouse model of permanent occlusion MI and MI-induced heart failure[24, 159, 160]. This model was chosen to isolate the effects

of ATF6α loss-of-function on the ischemic phase, which has not been explored before *in vivo*, and which is clinically relevant to patients with untreated MIs[157]. Additionally, permanent occlusion results in the largest possible infarcted area, which was predicted to cause maximal progression to post-MI heart failure, mimicking clinical patients most in need of novel therapeutic intervention. ATF6α global KO mice were chosen in order to model ATF6α loss-of-function beyond cardiac myocytes, since cardiac non-myocytes also play significant roles during ischemia and subsequent cardiac remodeling. In the absence of any cardiac stress maneuvers, ATF6α KO mice develop normally and are morphologically and physiologically similar to their WT counterparts.[100]

2. Short-term (One week) MI

C57/Bl6 mice were subjected to short-term permanent occlusion MI surgery. Accordingly, WT and ATF6α KO mice were sacrificed one week after surgery and the hearts sectioned and stained with TTC immediately after sacrifice to determine the area of infarct. White-colored TTC stain (2,3,5-triphenyl-2H-tetrazolium chloride) is reduced to red-colored 1,3,5-triphenylformazan only in living tissue. Thus, in infarcted hearts stained with TTC, the dead infarct area appears pale or white while the still viable tissue is stained red. One week was chosen to be sufficient time to allow for complete infarction of the entire tissue area at risk.[24] These mice were also subjected to echocardiography before surgery and again immediately before sacrifice to obtain data on heart function, pre- and post-MI. Though the area of infarct in the KO hearts appeared larger, there was no significant difference between the two groups. Likewise, while MI generally caused a significant reduction in cardiac function, as measured by ejection fraction, there was no difference in heart function between WT and ATF6α KO groups **(Figure 7)**.

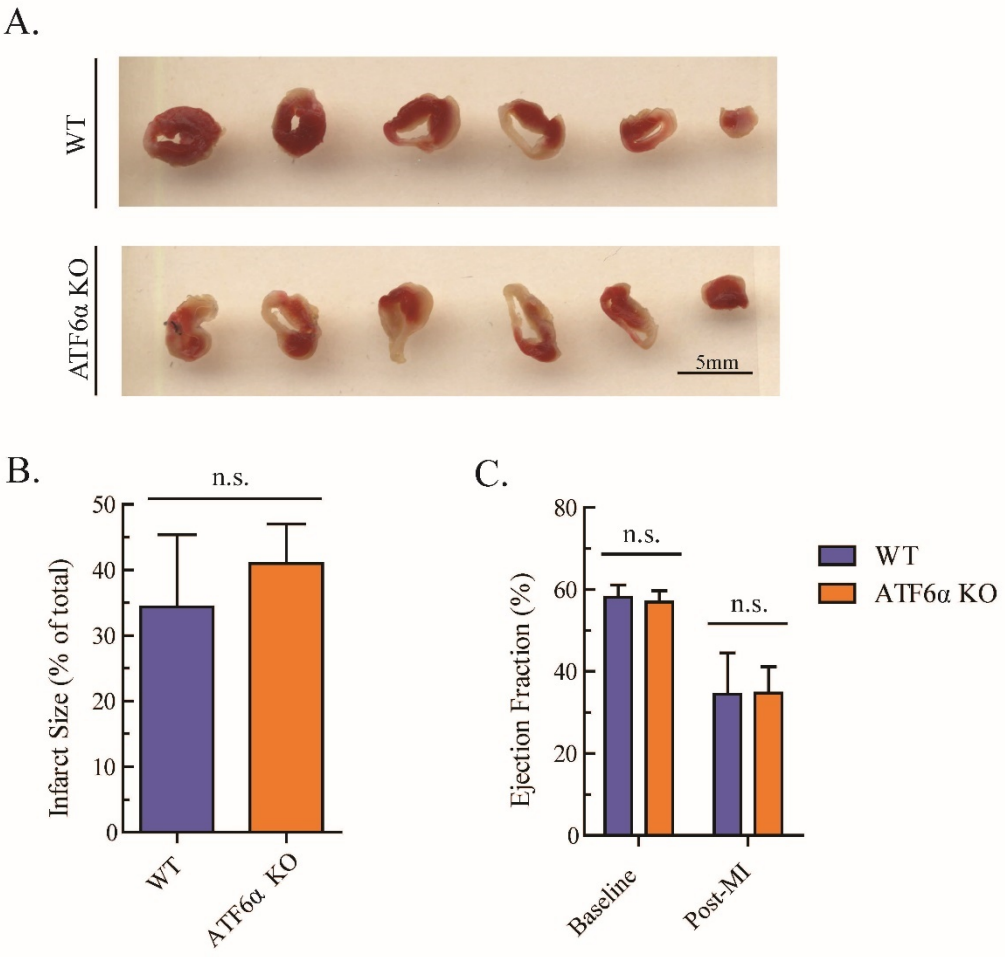

Figure 7. Analysis of infarct size and heart function of WT and ATF6α KO mouse hearts one week following MI surgery.

Following MI, WT and ATF6α KO ventricles were sectioned and stained with TTC to distinguish viable tissue (red) from dead, infarcted tissue, (pale). Representative images are seen in **(A)**. Infarct size as a % of total area is quantified in **(B)**. No significant difference was found between WT and ATF6α KO hearts. The same mice were subjected to echocardiography before surgery and again immediately before takedown. Heart function, as measured by ejection fraction, is quantified in **(C)**. Ejection fraction decreased post-MI in both groups, but no significant difference was found between groups at either timepoint. *n.s. indicates no statistical significance as determined by student's t-test.*

3. Long-term (11 week) MI Progression to Heart Failure

Since the absence of ATF6α in the heart had no significant effect on infarct size and cardiac function one week post-MI, an experiment was undertaken to determine the effect of ATF6α in a more chronic model of heart disease in mice, i.e. long-term progression to heart failure.[24, 159, 160] Accordingly, WT and ATF6α KO mice were subjected to identical MI surgeries as before, and then allowed to recover with continual monitoring for 11 weeks. Though infarct size might be similar, we reasoned that the remote areas of the heart, including relevant non-myocytes, might respond differently in an ATF6α-dependent manner over the course of time and that this might be reflected in changes in the structure, function, and genetic regulation of the heart. In this iteration of the experiment, sham surgery groups were included for both the WT and ATF6α KO conditions. These sham groups were treated identically in every respect, except the LAD artery was not occluded. We show here, via qPCR, that ATF6α KO post-MI mice upregulate transcripts for fetal isoforms of contractile proteins to a significantly greater degree compared to WT **(Figure 8A-C)**. *Myh6*, the gene name for αMHC, is the primary isoform of myosin heavy chain expressed in the adult mouse ventricle whereas *Myh7*, or βMHC, is expressed perinatally. The upregulation of the fetal isoform, and the downregulation of the adult isoform of MHC are hallmarks of cardiac disease and a leading indicator of heart failure.[161] The altered ratio of βMHC to αMHC is shown in **Figure 8D**. Ventricular expression of natriuretic gene transcripts *Nppa* and *Nppb* (ANP and BNP, respectively), another feature of the fetal gene program, was also significantly increased post-MI in ATF6α KO mice compared to WT **(Figure 8E-F)**. In the adult mouse, as in humans, ANP and BNP are primarily expressed in the atria where they act as the primary natriuretic hormones fulfilling the atria's endocrine function. ANP and BNP are exclusively expressed in the fetal ventricle or in adults during cardiac disease.[161]

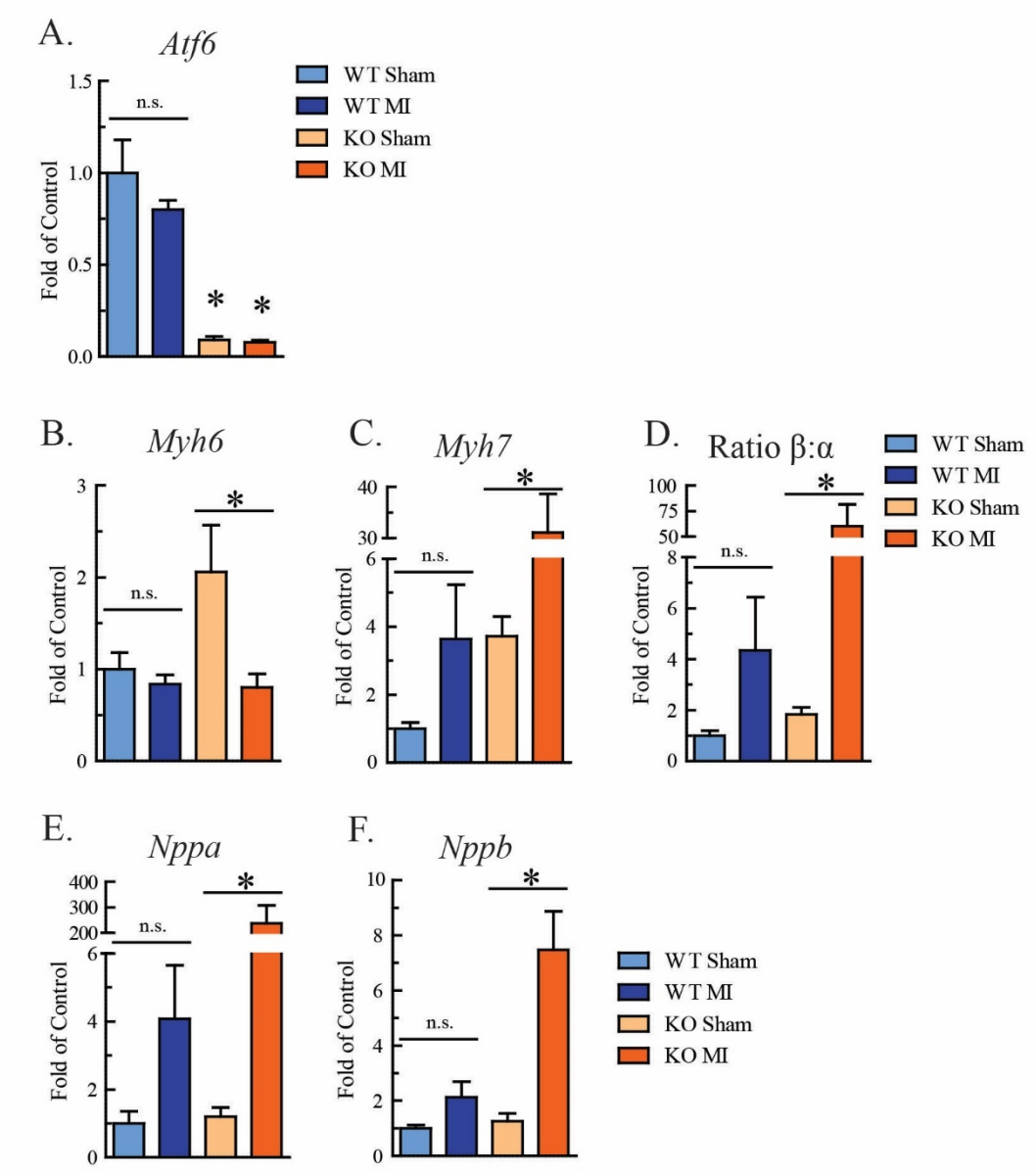

Figure 8. qPCR of RNA isolated from mouse left ventricles following the conclusion of the 11-week MI study.

ATF6α knockout was confirmed in the ventricles **(A)**. Following MI, ventricles show a significant decrease in the adult murine α-myosin heavy chain (MHC) contractile protein **(B)** and a significant increase in the fetal β isoform **(C)**. An increase in the β-MHC to α-MHC ratio **(D)** is an indicator of failing heart muscle in mice. While the WT MI ventricles had a non-significant increase in β to α ratio, the increase seen in ATF6α KO ventricles was highly significant. ATF6α KO ventricles show significant increases in transcript levels of natriuretic proteins ANP **(E)** and BNP **(F)** post-MI, further evidence of a switch to fetal gene expression characteristic of heart failure. WT ventricles show non-significant increases in both ANP and BNP transcript following MI. * *indicates $p \leq 0.05$ significant difference between the compared groups as determined by one-way ANOVA. n.s. indicates no statistical significance.*

Additionally, ATF6α KO mice subjected to MI surgery progress to heart failure faster, specifically by week 3, as measured by decreased ejection fraction observed via echocardiography. Heart function was overall lowest in ATF6α KO post-MI hearts throughout the study, though it was only significantly different at week 3. Echo analysis also showed that ATF6α KO hearts exhibit increased dilation at later timepoints, as measured by increased systolic left ventricular interior diameter **(Figure 9)**. This is despite no observed difference in heart weight relative to tibia length measured immediately following sacrifice. This disparity may be explained in multiple ways. It is possible ATF6α deletion causes increased cell death in the remote region of the heart, leading to faster myocyte dropout and dilation of the ventricle. It is perhaps also indicative of a lack of a compensatory hypertrophy phase, as is discussed below.

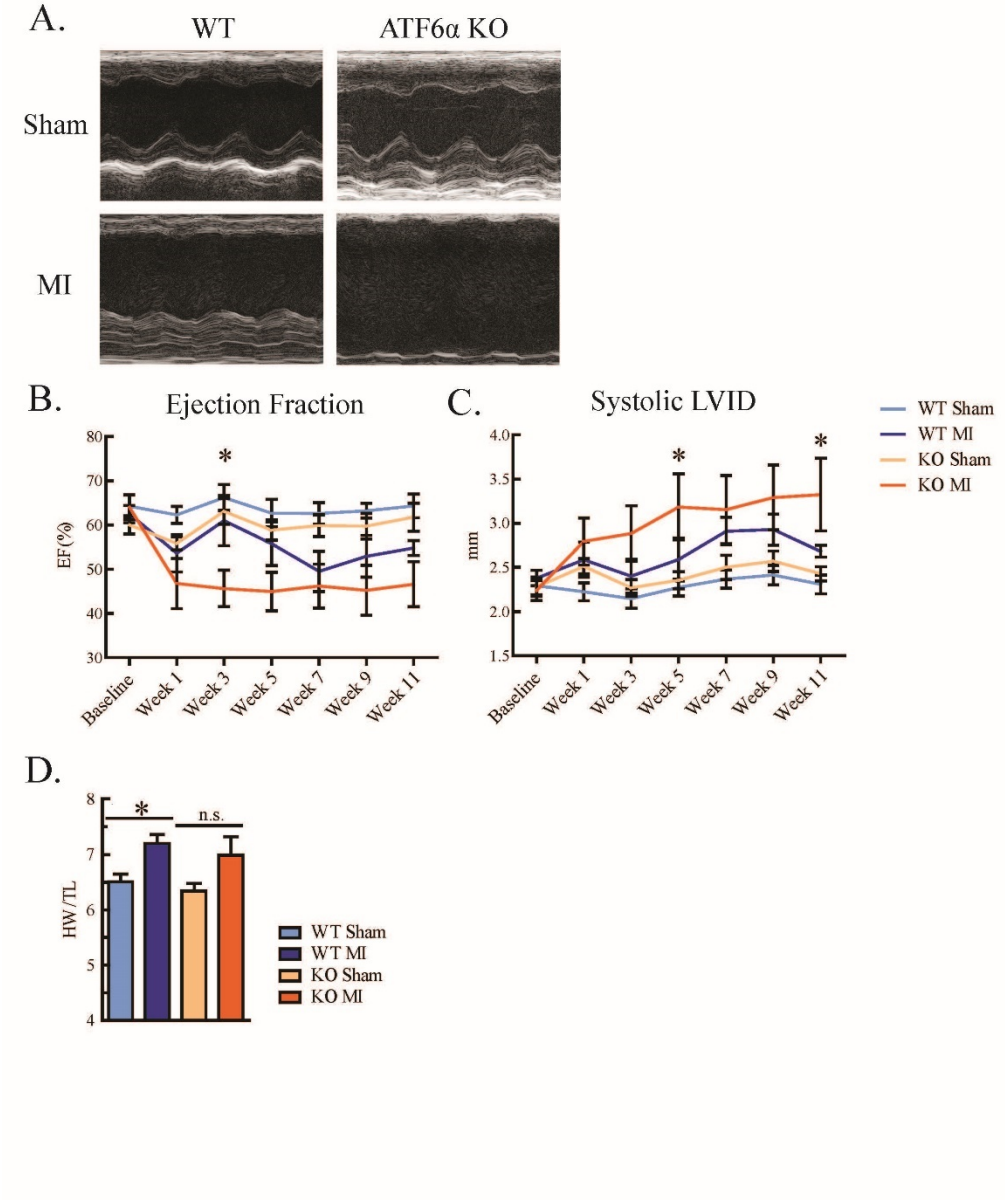

Figure 9. Effect of ATF6α KO on heart function following the conclusion of the 11-week MI study. Echocardiogram images of short-axis M-mode line-scans **(A)** from WT and ATF6α KO mice 11 weeks post-sham or MI surgeries. KO-MI hearts became dilated to a greater degree than WT-MI mice as measured by systolic left ventricular internal diameter (LVID) **(B)**. Heart function measured by ejection fraction (EF) **(C)** also decreased sooner for KO-MI mice compared to WT-MI mice. WT and ATF6α KO MI hearts increased in weight (HW) per tibia length (TL) **(D)**. The increase for KO hearts was not significant. * *indicates p≤0.05 significant difference for KO-MI mice relative to all other groups at each indicated timepoint as determined by one-way ANOVA. * over a line comparing two bars indicates p≤0.05 significant difference between compared groups as determined by student's t-test. n.s.indicates not significant.*

4. Conclusions

The observed lack of difference between WT and ATF6α KO hearts in infarct size, or cardiac function after one week of MI, was surprising given there are repeated publications demonstrating the role of ATF6α in reducing infarct size following ischemia/reperfusion.[11, 21, 105] This result may be due to the nature of permanent occlusion causing maximal infarction, thereby hiding any beneficial effect ATF6α might have had during the ischemic phase. Alternatively, it may be that the effects of ATF6α are primarily exerted during the reperfusion phase, *in vivo*, perhaps via its recently discovered antioxidant gene program centered around catalase.[11] Here, it was only by observing the post-MI mice long-term that differences between WT and ATF6α became more apparent. From these results it is reasonable to hypothesize that while the cells in the infarct zone may be lost to the same extent regardless of ATF6α activity, due to the permanent loss of blood flow, cells in the remote regions require ATF6α for their function and survival. These cells may include cardiac myocytes or cells which migrate to the infarct region over time like fibroblasts, endothelial cells, or stem cells. If so, these effects likely result in the observed long-term differences.

Despite a faster progression to heart failure in the ATF6α KO post-MI hearts relative to WT, there was no observed difference in heart weight. Additionally, the significant increase in heart weight seen in the WT post-MI hearts relative to its own sham was not seen in the ATF6α KO hearts. While this result initially seemed at odds with the available literature, subsequent research in the Glembotski lab found that ATF6α was required for compensatory cardiac hypertrophy via its upregulation of the mTORC1 activator, Rheb.[12] Though the injury model used in that study was pressure overload-induced by transaortic constriction, it is possible that Rheb, and thus ATF6α, are also required for cardiac hypertrophy in this injury model.

Lastly, while the use of the ATF6α global knockout model is useful for examining the role of ATF6α in all the cell types of the heart, it should also be remembered that ATF6α is deleted in all the other cell types and tissues in the body as well. Therefore, it is formally possible that lack of ATF6α in non-cardiac tissues influences the progression of cardiac disease in this model. The following chapters deal with isolated cardiac cells to examine the effects of ATF6α gain- or loss-of-function without the influence of other cell types.

B. Effect of ATF6α Gain- and Loss-of-Function in c-Kit Derived Cardiac Stem Cells

1. Introduction

The c-Kit gene encodes a type-III receptor tyrosine-kinase which is frequently used as a surface marker for a variety of proliferative cell types with multipotent differentiative potential.[162] These can include embryonic stem cells[163], hematopoietic stem cells[164], bone marrow cells[165], and cardiac stem cells found in the adult heart[162]. Stem cell factor (SCF) is known to bind to c-Kit, which induces proliferative downstream signaling in many cell types.[166] However, it remains unclear what role c-Kit plays in cardiac cells.

Initial animal research posited that c-Kit$^+$ cells from the heart could be isolated, expanded, and reimplanted, and would subsequently contribute to the creation of new cardiac myocytes. It was posited that these reimplanted cells could significantly repair tissue-wide ischemic damage, replacing infarcted zones with new contractile cardiac muscle.[124-126] Following these studies, human clinical trials were conducted, such as the SCIPIO (Cardiac Stem Cell Infusion in Patients with Ischemic Cardiomyopathy)[130] or CADEUCES (Cardiosphere-Derived Autologous Stem Cells to Reverse Ventricular Dysfunction)[131] trials, which showed some beneficial, albeit ambiguous, effects of this autologous cardiac stem cell therapy. In the case of the SCIPIO trials, c-Kit$^+$ cardiac cells were harvested from cardiac tissue from a patient with a history of myocardial infarction. The c-Kit$^+$ cells were isolated using magnetic beads bound to c-Kit antibodies and then expanded in culture before a bolus of the cells was reintroduced via intracoronary injection. Following the procedure, patients saw positive changes in heart structure and function, implying some of the lost myocardium had been recovered.[130] However, later studies showed that the injected cells did not survive to be engrafted into the myocardium, much less to differentiate into new cardiac myocytes.[132]

In order to find a mechanistic explanation of the clinical results, research has focused on exploring paracrine effects, potentially involving exosomes delivering miRNAs, which might be secreted by the c-Kit$^+$ cells to the benefit of existing cardiac myocytes.[133-135] Meanwhile, it has become increasingly clear that the heart may not have a native stem cell population capable of generating *de novo* cardiac myocytes. This has been shown via genetic lineage tracing experiments. In one study, an inducible knock-in approach was used to label c-Kit$^+$ cells and monitor their response to injury. Labeled cells proliferated in response to MI injury, but the overwhelming majority failed to become cardiac myocytes. Instead, the c-Kit$^+$ lineage was found in a variety of cardiac non-myocytes, including fibroblasts, smooth muscle cells, and especially endothelial and immune cells.[127] Furthermore, recent studies convincingly show that virtually no non-myocytes, c-Kit$^+$ or otherwise, differentiate into myocytes in the adult heart.[129] This finding is consistent with the long-known fact that cardiac muscle mass lost due to injury does not regenerate to a functionally relevant degree, if at all. However, it should be remembered that even though cardiac myocyte progenitor cells may not exist in the adult heart, that does not mean that the heart is devoid of cells that exhibit stemness and differentiative potential in response to injury or other stimuli, including c-Kit$^+$ cells. The fact that those stem cells differentiate into somatic cell types that are rarely mature cardiac myocytes does not mean these cells do not serve other biological roles critical to cardiac function.[127, 162]

ER stress response pathways have been found to be important during development and during differentiation of multiple cell types, especially those which secrete large amounts of cytokines or ECM proteins.[20, 167-169] In stimulated B-cells, which differentiate into antibody secreting plasma cells, activation of IRE1 and its downstream effector XBP1 is necessary to handle the required expansion of ER membrane and increased protein trafficking.[5] ATF6α relatives in the

OASIS family are associated with differentiation in chondrocytes[108, 113] and osteoblasts[113, 116] by upregulating necessary differentiation factors. Further, ATF6α itself was recently shown to drive iPSCs toward mesenchymal lineages, while suppressing endo- and ectodermal lineages.[6] Lastly, previous research in the Glembotski lab demonstrated that in CSCs, treatment with differentiation media induced ER stress downstream markers GRP78 and GRP94, while treatment with the ER stress-inducing chemical tunicamycin induced multilineage differentiation markers, demonstrating a link between ER stress and CSC differentiation (unpublished).

In order to understand the effect of ATF6α on proliferation and differentiation in the cardiac context, we chose to model ATF6α gain- and loss-of-function in cultured c-Kit$^+$ cardiac stem cells isolated from the adult murine heart.[147] These cells can be maintained in culture long term by supplementing their growth media with growth factors which preserve the multipotency of the cells, as described in the methods. These cells are amenable to transfection; thus cellular ATF6α levels can be manipulated using plasmids and RNAi, as well as small molecule activators and inhibitors. Multilineage differentiation was induced using differentiation media containing the synthetic GLucocorticoid dexamethasone. Dexamethasone is known to induce the differentiation of osteoblasts[170], mesenchymal stem cells[171], and embryonic stem cells[172], as well as c-Kit$^+$ cardiac stem cells[173], in culture.

2. Characterization of ER Stress in CSCs

The ER protein misfolding and the ER stress response are common to all mammalian cells and indeed, in some form, to all eukaryotic cells.[174] Nevertheless, neither have been studied before in c-Kit$^+$ cardiac stem cells. In order to study the role of ATF6α in these cells, we thus began by characterizing the degree of ER stress response, as measured by the induction of two ER stress chaperones, GRP94 and GRP78, which are frequently used as ER stress response markers and

both of which are ATF6α target genes.[21] We further examined these markers in response to four chemical stressors known to induce protein misfolding in the ER and thereby activate ATF6α. Thapsigargin (TG) is a sarco/endoplasmic reticulum Ca^{2+} ATPase (SERCA) inhibitor, which depletes the calcium concentration in the ER and inhibits the protein folding activity of several calcium-dependent ER chaperones.[175] Tunicamycin (TM) inhibits N-linked glycosylation of nascent proteins in the ER and prevents their proper folding.[176] Dithiothreitol (DTT) is a small molecule reducing agent capable of breaking protein disulfide bonds and otherwise disrupting the delicate redox environment necessary for proper protein folding in the ER.[177] Hydrogen peroxide (H_2O_2) is a reactive oxygen species and oxidizing agent which also disrupts the ER redox environment.[178] Initial experiments (not shown) quickly demonstrated that the CSCs were exquisitely sensitive to certain ER stressors, particularly TG and TM, and that mild doses in cardiac myocytes would result in rapid and complete cell death in CSCs. Conversely, CSCs were much less sensitive to H_2O_2. Because of this uncertainty we measured GRP94 and 78 levels in response to a range of concentrations for all these chemical stressors **(Figure 10)**. Even low nanomolar concentrations of TG could induce near maximal levels of the ER chaperones. Interestingly, but for unknown reasons, GRP94 was maximally induced by the low dose but then decreased with higher doses. This phenomenon was unique to GRP94 and TG treatment. TM also induced maximal levels of these markers, though the necessary concentration was closer to micromolar in range. DTT was still less effective and required millimolar concentrations to achieve induction. Lastly, H_2O_2 did not induce GRP94 or 78 and, in fact, higher doses decrease the levels of these proteins. This was not entirely unexpected and as we now know, while oxidative stress does activate ATF6α, its transcription program in response to this stress is primarily focused on antioxidants.[12] These data demonstrate that, like other mammalian cells, CSCs do respond to

certain ER stressors by upregulating common ER stress marker chaperones, though their sensitivities to various stressors differ.

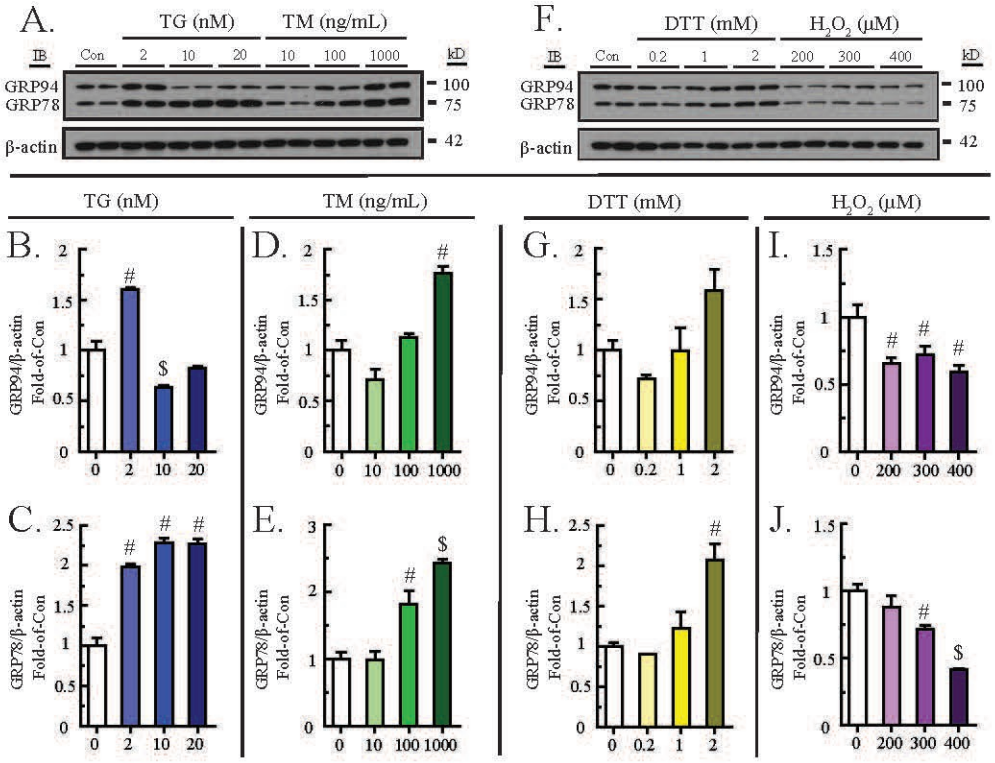

Figure 10. Effects of varying concentrations of chemical stressors on levels of ER stress markers GRP94 and GRP78 in cultured CSCs.

CSCs were treated with the indicated concentrations of thapsigargin (TG), tunicamycin (TM), or dithiothreitol (DTT) or 24 hours or hydrogen peroxide (H_2O_2) for 5 hours. TG concentrations are in nM, TM concentrations are in ng/mL, DTT concentrations are in mM, and H_2O_2 concentrations are in μM. **(A)** GRP94, GRP78, and β-actin were measured by immunoblot following TG and TM treatment. **(B-E)** Densitometry of the blots shown in **A** normalized to DMSO treated Con. **(F)** GRP94, GRP78, and β-actin were measured by immunoblot following DTT and H_2O_2 treatment. **(G-J)** Densitometry of the blots shown in **F** normalized to DMSO treated Con. *# and $ indicate distinct groups $p \leq 0.05$ different from Con (or zero dose) and all other groups, as determined by one-way ANOVA.*

In order to further explore this sensitivity and its effect on overall cell viability, we conducted MTT assays on CSCs subjected to similar ranges of all four stressors. MTT (3-(4,5-dimethylthiazol-2-yl)-2,5-diphenyltetrazolium) assays specifically measure the activity of NAD(P)H-dependent oxidoreductase enzymes to convert the yellow tetrazole into purple formazan crystals.[179] However, since this only occurs in living, metabolically active cells, we were able to use this assay as a measure of viability under these conditions, with the added consideration that greater cell proliferation also increases MTT signal. We further examined these same stressors in another common cardiac cell used as a model in the lab, neonatal rat ventricular myocytes (NRVM) **(Figure 11)**. Though we sought to use the same ranges of these chemical whenever possible, there was frequently little overlap in the sensitive ranges between cell types. As previously noted, the CSCs were, relative to the NRVM, much more sensitive for all the stressors which, in **Figure 10**, produced an induction of the ER chaperones. The opposite observation was made with H_2O_2, which NRVM are very sensitive to, but which was unable to produce more than 50% cell death in the CSCs until the highest dose.

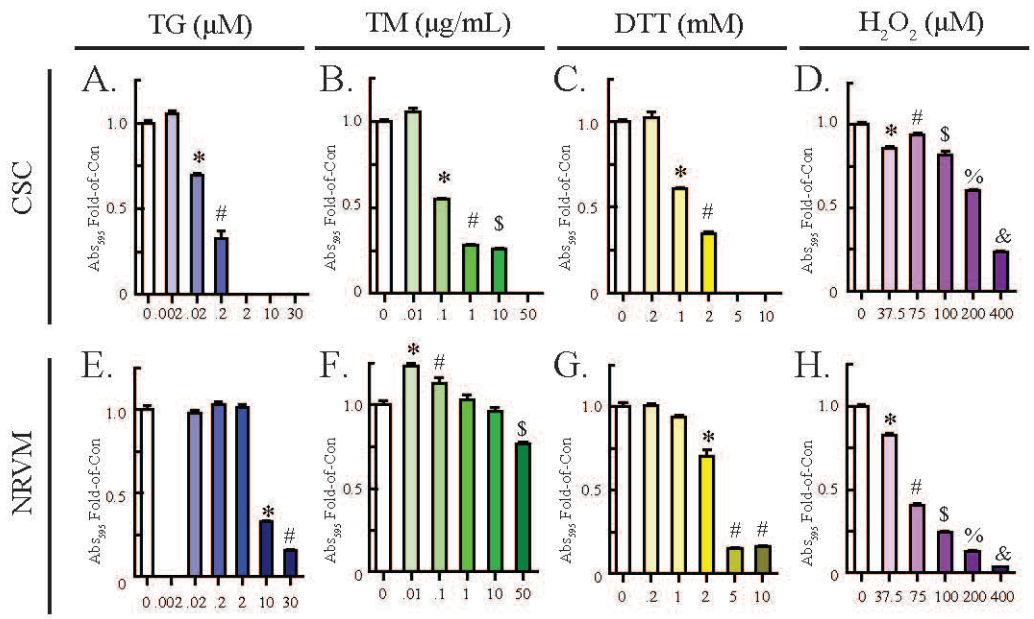

Figure 11. Effects of varying concentrations of chemical stressors on cell viability as measured by MTT assay, comparing cultured CSCs to NRVM.

CSCs and NRVM were treated with the indicated concentrations of thapsigargin (TG), tunicamycin (TM), or dithiothreitol (DTT) for 24 hours or hydrogen peroxide (H_2O_2) for 5 hours. TG concentrations are in μM, TM concentrations are in μg/mL, DTT concentrations are in mM, and H_2O_2 concentrations are in μM. **(A-D)** Viability of CSCs was measured by MTT assay following treatment with the indicated compounds. Blank columns represent concentrations not tested on those cells. **(E-H)** Viability of NRVM was measured by MTT assay following treatment with the indicated compounds. Blank columns represent concentrations not tested on those cells. **, #, $, %, and & indicate distinct groups $p \leq 0.05$ different from zero concentration (control) and all other groups, as determined by one-way ANOVA.*

3. ATF6α Loss of Function Effect on CSC Proliferation

To focus in on the role of ATF6α, HiPerfect transfection reagent was used to transfect 64 nM of siRNA, targeted to ATF6α, into the CSCs to achieve ATF6α knockdown. In order to guard against off-target effects, two siRNAs were designed. One targets the 3' untranslated region of the ATF6α transcript and was used in all subsequent experiments because it resulted in slightly greater knockdown of ATF6α protein. The second was designed against the 5' end of the open reading frame in order to target a region far from that of the first siRNA. Both siRNAs were similarly effective and only achieved about 40% knockdown, as measured by protein and RNA levels compared to the control siRNA (siCon) **(Figure 12A-C)**. However, as became quickly apparent, even with this minimal knockdown, there was a significantly reduced number of cells in the cultures with either ATF6α siRNA compared to control **(Figure 12D)**.

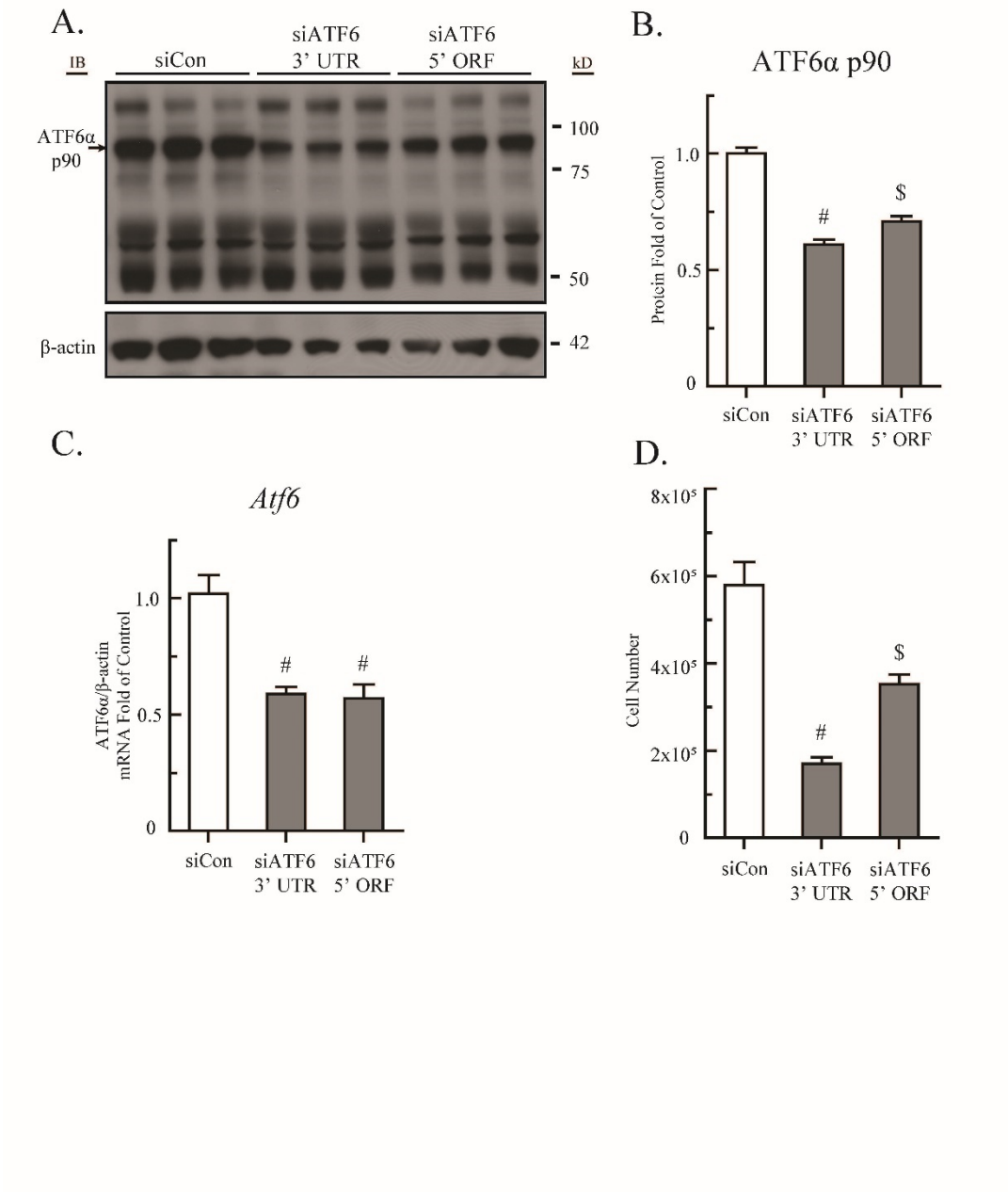

Figure 12. Knockdown of ATF6α in cultured CSCs via RNAi and its effect on cell number after four days. CSCs were transfected with 30 µL of 20 µM siRNA (64 nM final concentration) targeting ATF6α mRNA at either the 3' untranslated region (UTR) or the 5' end of the open reading frame (ORF) and then cultured for four days. The cells were then counted, and samples were taken for protein and RNA analysis. **(A)** Full length (p90) ATF6α and β-actin protein was measured by immunoblot. **(B)** Densitometry of the blots shown in A normalized to siCon treated CSC samples. **(C)** ATF6α and β-actin mRNA was measured by qPCR and relativized to siCon treated samples. **(D)** Cell counts of CSCs transfected and cultured in parallel to those from **A-C**. Counts were made via hemocytometer. **, #, and $ indicate distinct groups $p \leq 0.05$ different from siCon and all other groups, as determined by one-way ANOVA.*

This difference is further apparent in subsequent experiments examining the proliferation over six days of CSCs transfected with siCon or siATF6. ATF6α knockdown decreased both total cell number and the rate of cell proliferation over time and was visually apparent upon examination of the cultures under the microscope **(Figure 13A-B)**. To delineate whether the presence of ATF6α protein was required for this effect or whether ATF6α signaling was also necessary, CSCs were treated with different small molecule ATF6α inhibitors for 48 hours before the cells were counted. Because the effect of these inhibitors in this cell type was unknown, a range of doses were used. 4-(2-aminoethyl)benzenesulfonyl fluoride (AEBSF) is a general, irreversible serine protease inhibitor.[57] PF429242 dihydrochloride (PF) is a reversible inhibitor of SREBP site-1 protease (S1P).[58] S1P is one of the two Golgi proteases responsible for ATF6α processing and activation.[51] Because it is a serine protease, it is inhibited by both AEBSF and PF, and thus both can inhibit the activation of ATF6α without affecting the immediate amount of ATF6α present in the ER or activity of the other ER stress response effectors. However, AEBSF has potentially many possible off-target effects by globally affecting serine proteases; PF is more specific but still affects other signaling pathways, like SREBP, that are processed by the same S1P Golgi protease. Nevertheless, both inhibitors reduced CSC cell number in a dose dependent manner, which, together with the more specific RNAi-based ATF6α knockdown, confirms the critical role of ATF6α signaling in maintaining the viability and proliferation of CSCs. It should be noted that ATF6α inhibition was sufficient to reduce CSC proliferation in otherwise naïve conditions, without overlying ER stress.

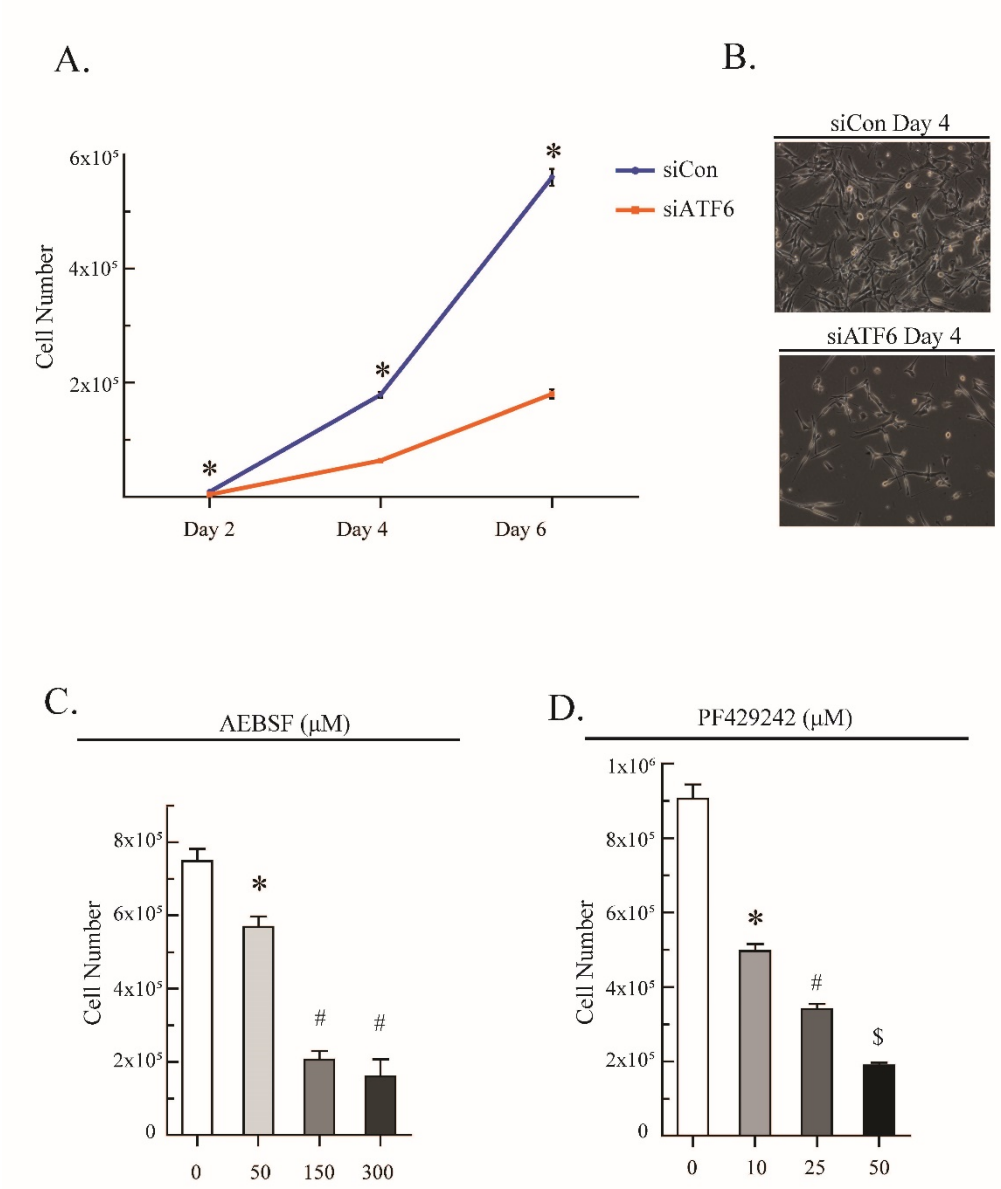

Figure 13. Effects of ATF6α knockdown or chemical inhibition on proliferation in cultured CSCs. **(A)** Cell counts of CSC cultures which were transfected with either siCon or siATF6 using HiPerfect transfection reagent and counted with a hemocytometer at the indicated times. * *indicates p ≤ 0.05 different from corresponding Con value, as determined by a Student's t-test.* **(B)** Representative phase contrast microscope images (40X) of CPC cultures from **A**. **(C)** Cell counts of CPCs treated and cultured with the indicated concentrations of 4-(2-aminoethyl) benzenesulfonyl fluoride (AEBSF). Counts were made via hemocytometer. **(D)** Cell counts of CPCs treated and cultured with the indicated concentrations of PF429242. Counts were made via hemocytometer. AEBSF and PF429242 concentrations are in μM. *, #, and $ indicate p ≤ 0.05 different from Con and all other values, as determined by one-way ANOVA.*

In order to gain insight into genes related to cell proliferation which might be perturbed by ATF6α loss of function, a PCR array of cell cycle regulators was run on cDNA from CSCs treated with siATF6 for two days **(Figure 14)**. Consistent with a role for ATF6α in cell cycle regulation, multiple genes known to promote entry into the cell cycle were decreased. Several more associated with preventing cell cycle progression and/or cell death were greatly increased. These notable genes are summarized in **Figure 14B**. Most notably, *Gadd45a*, a nuclear factor which promotes growth arrest and apoptosis in response to DNA damage[180], was increased more than 13-fold. None of these genes were previously known to be influenced by ATF6α. However, it remains to be seen whether their transcription is directly altered by ATF6α or whether there is an indirect mechanism.

A.

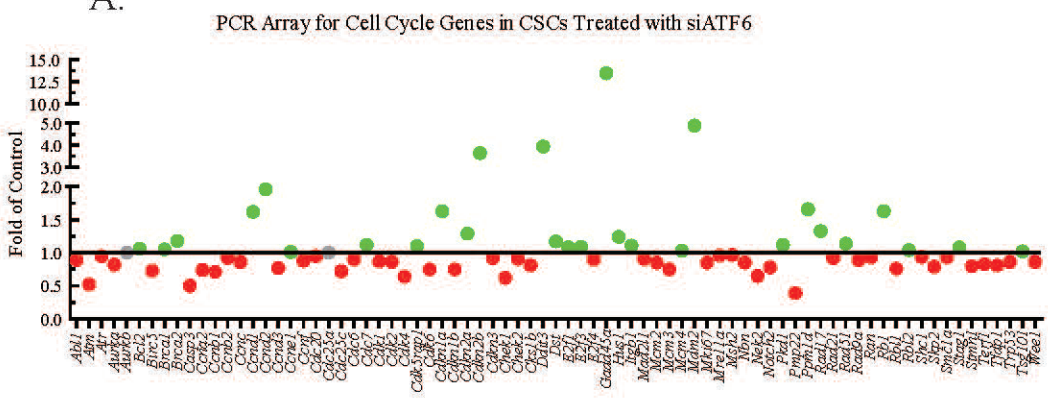

B.

Gene	Fold of Control	Cell Cycle Regulation
Atm	0.52	Positive
Cdkn2b	3.64	Negative
Ddit3	3.94	Negative
Gadd45a	13.47	Negative
Pmp22	0.39	Positive

Figure 14. PCR array for cell cycle genes in CSCs.
CSCs were treated with ±siRNA to ATF6α; all cultures were treated for 48 hours, then analyzed by a qRT-PCR array as described in the Methods (Section 4). In **(A)** green and red dots represent up- and downregulated genes, respectively. **(B)** A subset of notable altered genes from panel A; green and red numbers represent the fold up- or downregulation, respectively. Whether the gene is a positive or negative cell cycle regulator is listed in the third column.

4. Examining ATF6α and Paracrine Secretion in CSCs

As previously noted, one of the proposed mechanisms for the observed positive effects of autologous CSC therapy in heart failure patients is the potential secretion by the CSCs of factors beneficial to existing myocytes. Most secreted proteins, exosomes, miRNAs, and other factors are synthesized and secreted on the classical ER-Golgi pathway.[181] It is therefore reasonable to expect that these beneficial factors and their secretion are dependent on the maintenance of ER proteostasis and therefore ATF6α signaling. Rather than attempt to identify beneficial factors secreted by CSCs, we sought to assess the overall importance and functionality of the ER-Golgi secretory pathway in these cells. First, to assess whether beneficial factors are secreted by these cells in a paracrine or autocrine manner, we cultured the same number of naïve CSCs differing volumes of growth media (**Figure 15)**. Low-volume (1X) growth media concentrates the factors secreted by the cells; high-volume (10X) growth media dilutes the secreted factors but maintains the concentration of all other media components. Measuring the viability of the cultures by MTT demonstrated that low-volume, high-secreted factor concentration CSC cultures were significantly more viable than high-volume, dilute cultures. Though the total difference in media depth between the two conditions was approximately 2 cm, this is enough to affect the rate of oxygen diffusion to the cells. It is formally possible that this is responsible for the observed difference. To overcome this issue, additional CSC cultures were cultured in high (10X) volumes of conditioned media (CM). One well of CM had been generated over the course of the previous two days by culturing ten wells of other naïve CSCs in low volume growth media. Thus, high-volume CM has the same rate of oxygen diffusion as high-volume growth media and similar secreted factor concentration as low-volume growth media after two days of culture. Culturing CSCs in high-volume CM was

sufficient to restore CSC viability to higher than that observed in the low volume cultures. This demonstrates that CSCs secrete factors beneficial to themselves in culture.

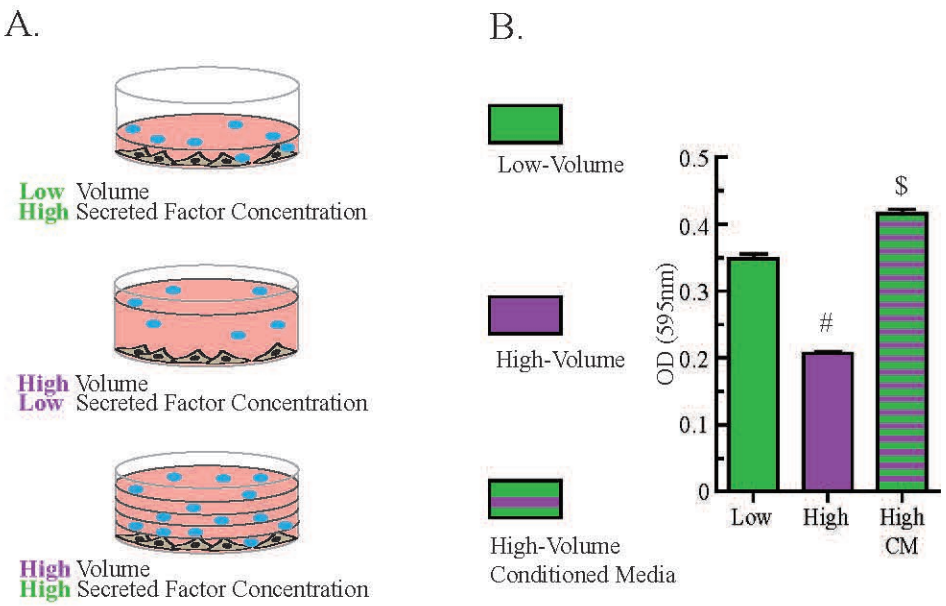

Figure 15. Effects of secreted factors on the viability of cultured CSCs.
(A) Diagram of experimental design. CSCs were cultured in a low (1X) volume of media, to concentrate any factors secreted by the cells, or a high (10X) volume of media to dilute any said factors. Lastly, CSCs were cultured in a high volume of media conditioned previously by other low volume CSC cultures. **(B)** CSCs cultured as above for 48 hours were subjected to MTT assay to assess viability. *#, and $ indicate $p \leq 0.05$ different from Low Volume condition and all other values, as determined by one-way ANOVA.*

If CSCs require factors synthesized and secreted on the ER-Golgi pathway for their viability, it may be that ATF6α is necessary for the function of this pathway and this may be a mechanism for why lack of ATF6α drastically reduces CSC viability. To assess the functionality of the ER-Golgi secretory pathway we utilized a *Gaussia* luciferase (GLuc) reporter, which is constitutively secreted in all eukaryotic cells.[182] 100 ng GFP (control) or GLuc plasmid construct was transfected into CSCs using Fugene transfection reagent. The next day, after a media change, 50 μL of media was removed from the wells at the indicated timepoints. Luminescence in the media, in the presence of luciferin substrate, was measured by a luminometer **(Figure 16A)**. Luciferin is oxidized in a luminescent reaction by luciferase. Thus, the amount of luminescence is a measure of the presence of GLuc in the media and therefore a measure of how much GLuc has been secreted by the ER-Golgi pathway. The luminescence in the media steadily increased over the course of 24 hours in the GLuc cultures, but not the GFP control cultures, as expected. To confirm that the GLuc in the media was from ER-Golgi secreted GLuc, and not from another source like non-canonical secretion or cell lysis, GLuc transfected CSC cultures were treated with 500 ng/mL brefeldin A, which inhibits ER-Golgi transport via COPI vesicles. BFA treatment completely blunted GLuc activity in the media. To further confirm that BFA was really keeping the GLuc inside the cells rather than inhibiting its translation or activity, the cells were lysed at the final timepoint, after media was collected, and GLuc activity was assayed from the lysate **(Figure 16B)**. GLuc activity was significantly increased in the BFA-treated cell lysates but not in the other conditions, indicating that GLuc was being synthesized and was functional but was not being secreted, thus validating the assay as a measure of the functionality of the ER-Golgi secretory pathway in CSCs. Further GLuc transfected CSC cultures were treated with DMSO (control), BFA, 2 nM TG, or 10 μM PF to determine if ER stress or ATF6α inhibition might decrease GLuc

secretion to a similar degree as BFA **(Figure 16C)**. While TG and PF slightly reduced GLuc signal in the media, it was not a significant difference by one-way ANOVA. Similarly, there was no significant increase in intracellular GLuc signal with TG or PF treatment **(Figure 16D)**. This indicates that, while secretion may be important in these cells, ATF6α inhibition does not impact this process, at least not during the conditions and timeframes that were previously seen to impact viability.

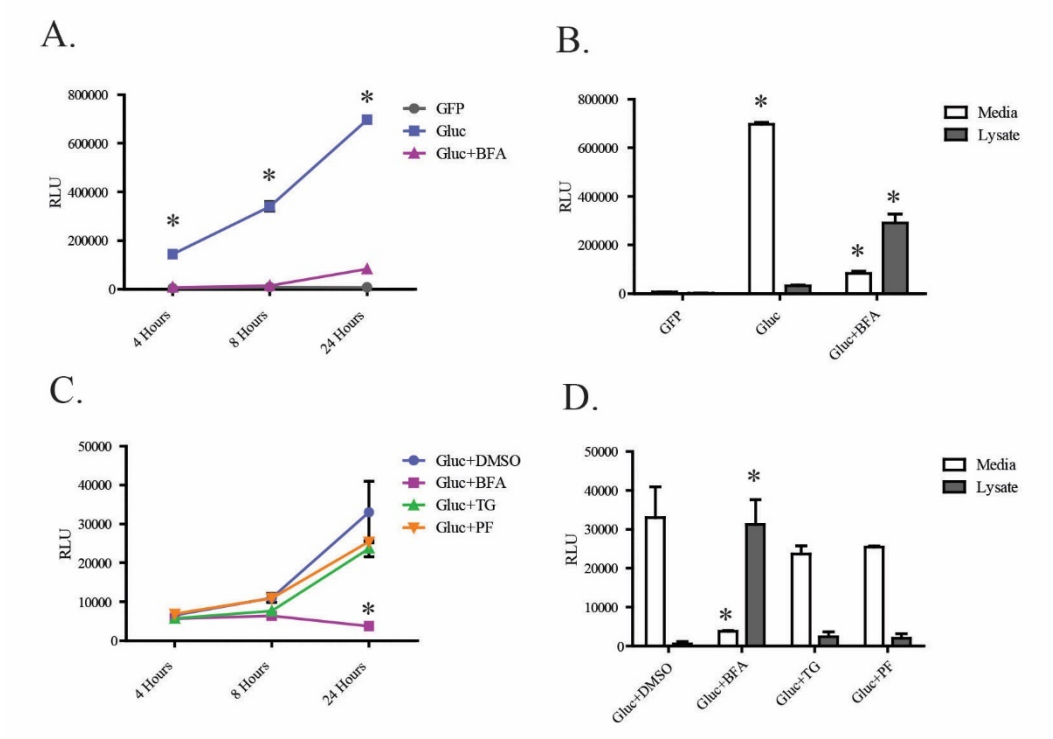

Figure 16. *Gaussia* luciferase (GLuc) as a measure of secretion in CSCs.
(A) CSCs were transfected with 100 ng GLuc plasmid or 100 ng GFP plasmid as a control and then treated with and without 500 ng/mL brefeldin A (BFA). Using a luminometer, fluorescence of excited luciferin substrate was measured as an indication of the presence of secreted luciferase in the media at the indicated timepoints. * *indicates $p \leq 0.05$ as determined by student's t-test.* **(B)** Cells from the final timepoint were lysed and the intracellular GLuc was compared to that found in the media. * *indicates $p \leq 0.05$ different from GFP control as determined by one-way ANOVA.* **(C)** CSCs were transfected with 100 ng GLuc as above and treated with DMSO (control), 500 ng/mL of BFA, 10 ng/mL TG, or 50 μM PF429242. Fluorescence was measured at the indicated timepoints. * *indicates $p \leq 0.05$ different from all other conditions as determined by one-way ANOVA.* **(D)** Again, cells from the final timepoint were lysed and the intracellular GLuc was compared to that found in the media. * *indicates $p \leq 0.05$ different from DMSO control, as determined by one-way ANOVA.*

5. ATF6α Gain- or Loss-of-Function in CSC Differentiation

Because c-Kit$^+$ cardiac cells have been found to respond to MI injury by differentiating into multiple different somatic cell types, differentiation is presumably an important part of their function. In culture, multiple somatic cell lineage markers can be induced in CSCs by treatment with the GLucocorticoid dexamethasone (Dex).[173] GLucocorticoids are also known to induce differentiation in multiple progenitor cell types.[170-172] Treating CSCs with Dex induced the smooth muscle marker αSMA (*Acta2*) and the cardiac muscle marker GATA4 (*Gata4*) at every timepoint tested **(Figure 17A)**. Dex also induced other lineage markers to lesser degrees. Surprisingly, ATF6α inhibition with PF also induced these markers, including αSMA, GATA4, and the endothelial marker VWF (*Vwf*). In the case of αSMA, this induction was synergistically increased when the two treatments were used in combination **(Figure 17B-C)**. This effect on the αSMA marker was also found when CSCs were treated with Dex after ATF6α was knocked down via RNAi. Conversely, treatment with the ATF6α activator compound 147 decreased αSMA transcript and completely blunted induction by Dex. 147 specifically activates ATF6α by promoting its transition from the ER membrane to the Golgi, without causing ER stress or the activation of the other ER stress branches. Though ATF6α has been associated with differentiation pathways in other cell types, this effect in CSCs was unexpected.

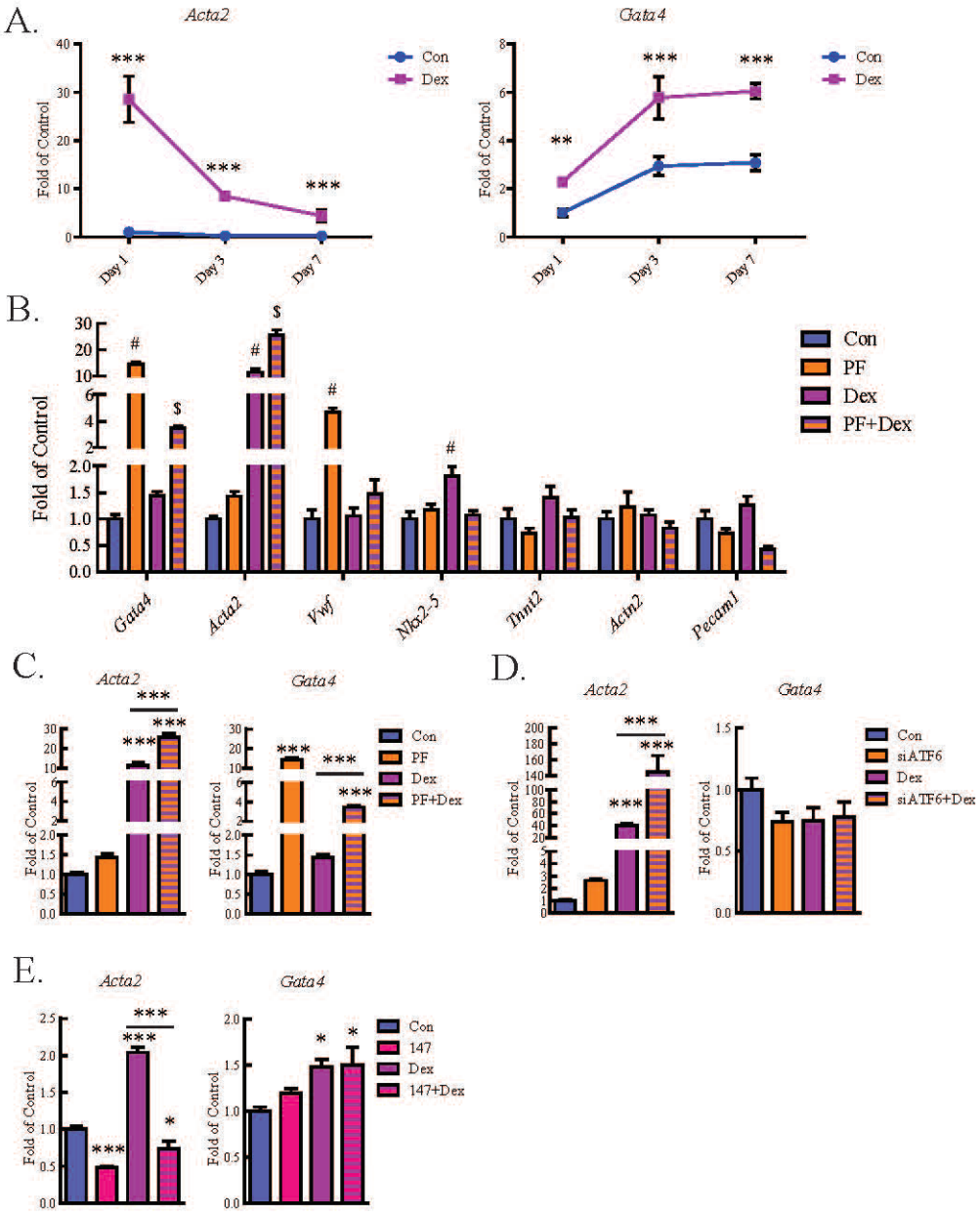

Figure 17. Effect of ATF6α gain- and loss-of-function on CSC differentiation.
(A) Time-course of 10 μM dexamethasone (Dex) treatment in CSCs, effect on *Acta2* and *Gata4* transcripts as measured by qRT-PCR. **** indicates p ≤ 0.001 difference by student's t-test.* **(B)** CSCs were treated with +/- 10 μM Dex and +/- 50 μM PF42942. qPCR showed changes in various lineage marker transcripts. *#, and $ indicate p ≤ 0.05 different from Con and all other values, as determined by one-way ANOVA.* **(C)** qPCR results from **B**. for *Acta2* and *Gata4* lineage markers. **(D)** CSCs were transfected with siCon or siATF6 +/- 10 μM Dex. qPCR for *Acta2* and *Gata4* lineage markers. **(E)** CSCs were treated with +/- Dex and +/- 10 μM 147. qPCR for *Acta2* and *Gata4* lineage markers. *, *** *indicates p ≤ 0.05 and p ≤ 0.001 difference, respectively from control or between compared groups, as determined by one-way ANOVA.*

6. Compensating for ATF6α Loss-of-Function with the Antioxidant NAC

The differentiation of certain stem cells, such as iPSCs, is known to be associated with the generation of ROS.[138] Treatment with antioxidants can improve the survival and proliferation of these cell types and can help maintain their pluripotency. This paradigm has been found to apply in the cardiovascular system as well. In cardiomyoblasts, a cardiac myocyte progenitor with differentiative potential, antioxidant treatment has been shown to increase cell survival after engraftment in transplantation experiments.[183] Furthermore, the chemical antioxidant N-acetyl cysteine (NAC) inhibits the differentiation of human preadipocytes into mature fat cells, by scavenging the ROS levels which increase with differentiation.[184] NAC has also been found to inhibit differentiation of ESCs toward cardiomyocyte lineages.[185] ATF6α is necessary for the viability and proliferation of CSCs and it acts to inhibit their differentiation toward certain somatic cell lineages. ATF6α is also known to induce antioxidant genes among its wider gene program in order to combat the generation of damaging ROS.

We thus assessed whether treatment with the antioxidant NAC would compensate for the effects of ATF6α loss-of-function in CSCs. MTT assays in CSCs transfected with siATF6 showed a decrease in viability at baseline but slight but significant increases with Dex treatment **(Figure 18A)**. While NAC slightly enhanced expression of the αSMA lineage marker, qPCR revealed NAC blunted induction by Dex. This decrease was especially significant when NAC treatment was applied to the previously observed synergistic induction of αSMA by simultaneous ATF6α knockdown and Dex treatment **(Figure 18B)**. NAC treatment may play more of a role in scavenging ROS generated by Dex-induced differentiation, though the drastic increase in the αSMA lineage marker with simultaneous knockdown of ATF6α may mean ROS normally suppressed as the result of ATF6α signaling plays a significant role in Dex induced differentiation.

NAC treatment likely results in a near complete scavenging of intracellular ROS and some of the effects of more subtle changes in ROS levels, such as those that might be expected from Dex treatment or alterations in ATF6α signaling might be lost. Nevertheless, NAC treatment did reduce αSMA levels with Dex and siATF6 to close to those seen with Dex alone, suggesting that NAC ROS scavenging can compensate for the loss of ATF6α. More research is needed to determine the role ROS levels play in ATF6α-suppression induced differentiation.

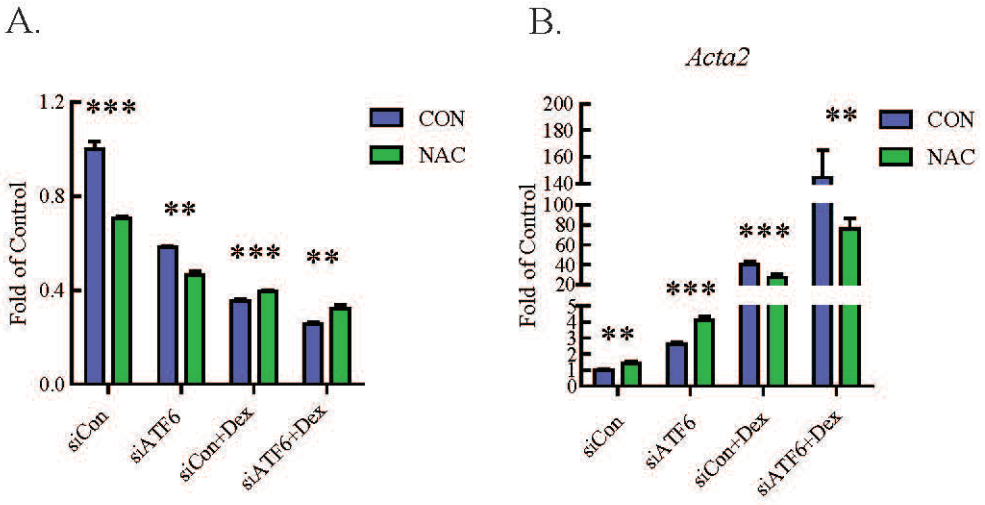

Figure 18. Effect of NAC antioxidant on ATF6α loss-of-function and differentiation in CSCs.
(A) MTT assay of CSCs transfected with siCon or siATF6 +/- 10 μM Dex and +/- 10 μM NAC. **(B)** RNA isolated from identically treated cells as in A. were probed for *Acta2* transcript via qPCR. ***, *** indicates $p \leq 0.01$ and $p \leq 0.001$ difference by student's t-test.*

To gain understanding of alterations in oxidative stress gene regulation in CSCs with ATF6α loss of function, we ran a PCR array of oxidative stress genes on cDNA from CSCs treated with siATF6 **(Figure 19)**. As expected, catalase (*Cat*) transcript, a known ATF6α target gene, and an important antioxidant[11], was reduced with siATF6. However, numerous other perturbed genes were also found which counteract or respond to oxidative stress. Some noted antioxidant transcripts like Cytoglobin (*Cygb*)[186], Peroxiredoxin 2 (*Prdx2*)[187], and isocitrate dehydrogenase 1 (*Idh1*)[188] were decreased to an even greater degree. The most increased gene transcript, *Ccl5*, is a cytokine known to be induced by increased ROS[189], an indication that CSCs with siATF6 are indeed undergoing oxidative stress.

A.

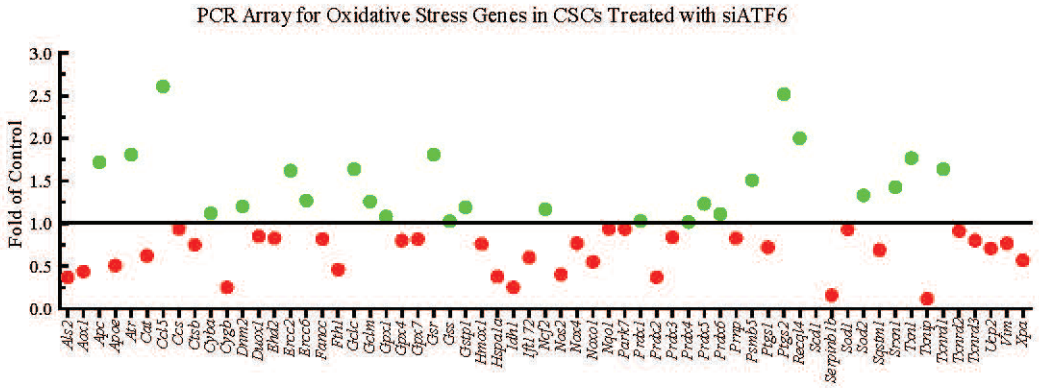

B.

Gene	Fold of Control	Oxidative Stress Response
Als2	**0.37**	Antioxidant
Cat	**0.62**	Antioxidant
Ccl5	**2.61**	Induced
Cygb	**0.25**	Antioxidant
Fth1	**0.46**	Antioxidant
Hspa1	**0.38**	Antioxidant
Idh1	**0.25**	Antioxidant
Prdx2	**0.37**	Antioxidant
Scd1	**0.43**	Inhibited
Serpinb1b	**0.16**	Antioxidant

Figure 19. PCR array for oxidative stress genes in CSCs.
CSCs were treated with ±siRNA to ATF6α; all cultures were treated for 48 hours, then analyzed by a qRT-PCR array as described in the Methods (Section 4). In **(A)** green and red dots represent up- and downregulated genes, respectively. **(B)** A subset of notable altered genes from panel A; green and red numbers represent the fold up- or downregulation, respectively. Whether the gene product acts as an antioxidant or is induced or inhibited by oxidative stress is listed in the third column.

7. Conclusions

CSCs are extremely sensitive to treatment with ER stressors that directly interrupt ER protein-folding, sensitivity that is more notable when compared to results from the same treatments performed on neonatal myocytes (NRVM). To a certain extent this difference might be expected when comparing neonatal cells to the adult CSCs. Adult myocytes are also very sensitive to ER stressors in culture, and aging is generally associated with a decline in ER stress response effectiveness.[190] However, resistance to ER stress is typically characteristic of highly proliferative cell types like stem cells[191] or cancer cells[192], because continual cell division requires constant protein translation, putting strain on protein folding machinery which is met by enhanced ER stress signaling. As was shown, CSCs are sensitive to ATF6α loss of function under even basal conditions, without additional ER stress. It should be remembered that even a 40% knockdown in ATF6α levels was enough to dramatically reduce CSC cell number and greatly alter levels of various cell cycle and oxidative stress genes. This suggests that CSC proliferation in culture requires a continual and precise level of ATF6α signaling. Whether this is also true *in vivo* remains to be seen. ATF6α global knockout mice develop normally and are healthy at baseline but this may be due to compensation by the less transcriptionally active ATF6β isoform. Double knockout of both ATF6 isoforms is embryonic lethal.[33] Additionally, isolating and culturing CSCs may cause a baseline level of stress that, conceivably, requires constant ATF6α signaling. However, given the proposed function of CSCs responding to stress conditions in the heart, the importance of ATF6α in culture is likely still relevant. Notably, a similar phenomenon has also been reported in isolated pancreatic β-cells where, under basal conditions, even partial ATF6α knockdown by RNAi caused significant increases in apoptosis.[193]

The necessity of secreted autocrine factors for CSC viability in culture is a novel finding which merits further exploration. ATF6α inhibition reduced secretion only slightly and not significantly. It is possible that ATF6α loss of function was compensated in this respect by hyperactivation of other ER stress branches that have been shown to influence secretion in other cell types. ATF6α knockdown in CSCs leads to increased IRE1 signaling as evidenced by increases in the spliced form of XBP1 **(Figure 20)**. More research is needed to determine whether IRE1 or PERK contribute to CSC secretion.

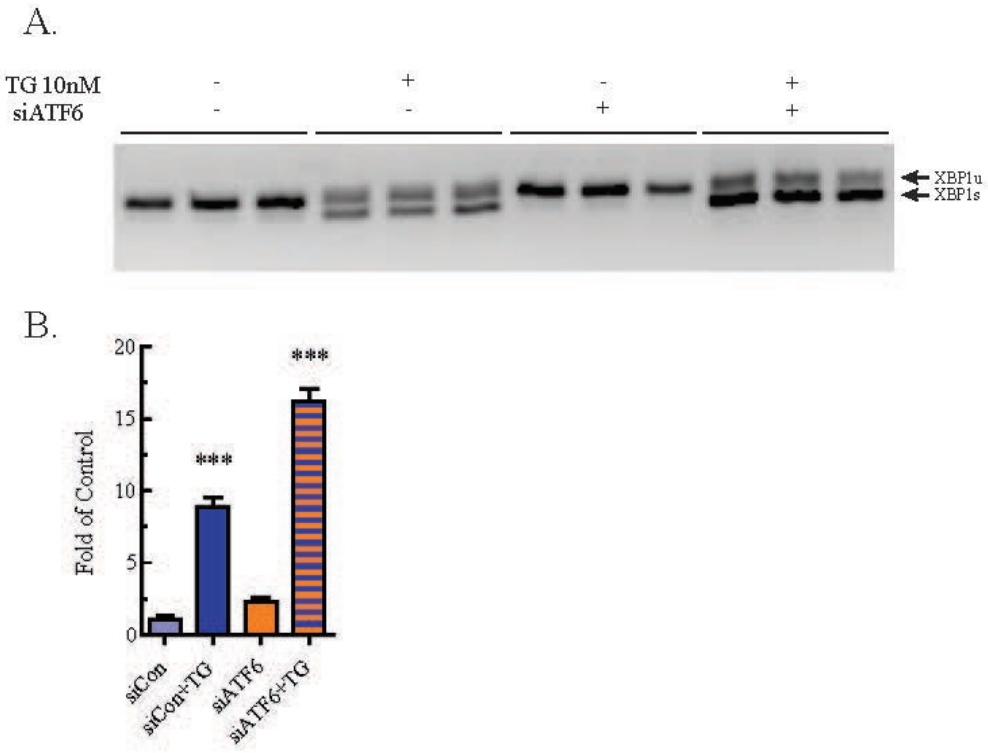

Figure 20. Effect of ATF6α knockdown and activation of IRE1 in CSCs.
(A) XBP1 splicing assay in CSCs transfected with siCon or siATF6 +/- 10 nM TG. Upon IRE1 activation, unspliced XBP1 transcript (XBP1u) is converted to a spliced transcript (XBP1s) that encodes the XBP1 transcription factor. Downward shift in XBP1 transcript bands reflects decreased sized following splicing. **(B)** Quantification of the ratio of spliced to unspliced XBP1 transcript in each condition. *** *indicates* $p \leq 0.001$ *difference from all other values by one-way ANOVA.*

The role of ATF6α in suppressing lineage markers, and presumably differentiation, in CSCs was a surprising finding. In other cell types, ATF6α has been associated with promoting differentiation towards certain lineages while suppressing others but this connection had not been made in this cell type. Given that so much research has gone in to exploring the differentiative potential of these cells, and whether this potential plays any role in cardiac disease, it is surprising that so little has been done to explore what pathways govern their differentiation. Of the lineage markers tested, αSMA was by far the most responsive to Dex treatment, and to Dex and ATF6α loss of function together. Further research will be needed to discover a mechanistic link between ATF6α and αSMA suppression in this cell type. In the next chapter, this association will be explored in a different cardiac cell type, the cardiac fibroblast.

C. ATF6α Decreases Activation of Cardiac Fibroblasts

1. Introduction

Generally, fibroblasts are cells which secrete fibrotic extracellular matrix (ECM) components, such as collagen or fibronectin, which contribute to many connective tissues in the body. This can include large, organized, fibrous structures like tendons and ligaments as well as the more irregular patterns of interstitial fibrosis and scarring.[20, 194, 195] In the heart, cardiac-resident fibroblasts are important during development as they are responsible for the deposition and later maintenance and homeostasis of the ECM scaffolding necessary for cardiac structure and function. Additionally, they contribute tissue to the valves of the heart and features of the heart's electrical conduction system. During pathology, they are a critical part of the heart's response to both acute and long-term injury.[7-9, 196] Following an MI which results in the death of an acute portion of the myocardium, fibroblasts infiltrate the affected area and become activated after undergoing a transdifferentiation process into a new type of cell.[24, 197] These newly activated cardiac fibroblasts, now designated myofibroblasts, have numerous differences from their quiescent predecessors. Two primary characteristics of myofibroblasts are their increased secretion of collagenous ECM proteins and their upregulation of smooth muscle contractile proteins like αSMA. Both components are consequently used as markers for fibroblast activation.[7, 197] The myofibroblasts contract like smooth muscle cells to hold the wound area closed, while newly deposited collagen forms a fibrotic scar over the wound area. Both the scar and wound contraction are necessary to prevent the heart from rupturing while the dead tissue is removed and replaced.[7, 195, 198, 199] This mode of fibrotic response is thus called replacement fibrosis. Fibrotic scarring in the heart is generally permanent, reflecting the non-regenerative nature of the myocardium. Additionally, cardiac fibroblasts contribute to diffuse fibrotic remodeling in the heart, also known as reactive or

interstitial fibrosis. This can occur as a result of long-term injuries that cause tissue-wide myocyte dropout, such as pressure overload or fibrillation, but can also be a natural consequence of aging.[7-9, 24, 196, 200, 201] While fibrotic response to cardiac injury is necessary to maintain the structural integrity of the heart, it can become a detriment to cardiac function, particularly if the fibroblasts become chronically activated in the long-term. Indeed, overactive cardiac fibroblasts are a common feature of many forms of cardiac dysfunction, including both hypertrophic and dilated cardiomyopathy (HCM and DCM).[7-9] Fibrotic tissue is stiff and non-compliant, which poses mechanical difficulty for the rest of the heart during both contraction and relaxation. Additionally, extensive interstitial fibrosis interferes with the propagation of action potentials through the heart, impeding cardiac myocyte electrical coupling.[7, 202, 203] Out-of-control fibrosis is also a feature of valvular pathologies like aortic stenosis.[7, 204]

Understanding how, when, and to what degree cardiac fibroblasts are activated is thus of great importance when considering treatment of cardiac disease. Cardiac fibroblasts can be activated by increased mechanical stretch, as during prolonged pressure overload.[205, 206] Activation can also occur via multiple intercellular signaling cytokines.[7] These include, but are not limited to, endothelin[207], angiotensin II[208], and the transforming growth factor β family[209], of which TGFβ1 (hereafter referred to as TGFβ) is the one most commonly associated with cardiac pathology[199, 210]. TGFβ is secreted by multiple cardiac cell types, including cardiac fibroblasts themselves.[211] Prior to activation, it is held in an extracellular complex which interacts with ECM. Thus, dissolution of the ECM is one mechanism for the activation of TGFβ.[212] Once active, TGFβ binds to its receptors, TGFβR1 and TGFβR2, the latter being a serine/threonine kinase, which initiates a downstream signaling cascade.[213, 214] Though TGFβ signaling can involve multiple pathways, the best studied involves the receptor-Smad proteins which are phosphorylated at the receptor and

form a transcription factor complex which moves to the nucleus, initiating downstream transcription of fibrotic genes.[215, 216]

Due to the increased demand that transdifferentiation and secretion place on the ER protein-folding apparatus, we theorized that ER stress pathways, potentially including ATF6α, might influence the cardiac fibroblast activation process. The results of the previous chapter, in which ATF6α loss of function greatly enhanced the αSMA lineage marker during differentiation in CSCs, further piqued our interest, given that αSMA is a primary marker of fibroblast activation.[7] ER stress and ATF6α have not been studied in cardiac fibroblasts before. However, ER stress has been found to mediate the differentiation of skin fibroblasts[20], as well as osteoblasts[168] and myoblasts[217]. Additionally, ER-associated degradation pathways, which are a critical part of the ER stress response and are heavily promoted by ATF6α, were shown to inhibit TGFβ signaling in β cells.[218] Lastly, ATF/CREB family member ATF3 protects against pathological cardiac remodeling by suppressing cardiac fibroblast activation pathways upstream of TGFβ.[109]

We thus decided on multiple models by which to investigate the effect of ATF6α on cardiac fibrosis and cardiac fibroblast activation. We used a murine permanent-occlusion MI model[123] to examine cardiac fibroblast activation markers *in vivo* during replacement fibrosis following acute injury. We also examined mouse hearts subjected to a trans-aortic constriction (TAC) model of long-term pressure overload injury.[12] In both cases global ATF6α knockout mice were examined, which would feature ATF6α deletion in all the cardiac cell types, including fibroblasts.[100] To study cardiac fibroblasts specifically, we isolated them from the adult mouse ventricle. These adult murine ventricular fibroblasts (AMVF) could then be manipulated in primary culture. Lastly, we verified the specificity of the effects of ATF6α in AMVF by also examining a non-cardiac immortalized fibroblast cell line, NIH 3T3 fibroblasts. ATF6α loss of function was examined by

either isolating AMVF from ATF6α global knockout mice or by transfecting wild-type AMVF with siRNA targeted to ATF6α. ATF6α gain of function was modeled by treatment with the ATF6α small-molecule activator compound 147. In culture, activation was achieved by treatment with extracellular porcine TGFβ. These combined approaches were designed to provide a comprehensive insight into the role of ATF6α in cardiac fibroblast activation and response to cardiac injury.

2. Following Cardiac Injury, Mouse Hearts with ATF6α Deletion Increase Fibroblast Activation Markers with Cardiac Injury

The Glembotski lab previously showed that ATF6α is activated in mouse hearts subjected to a variety of insults, including ischemic and oxidative stress and in response to pressure overload.[11-13] In each of these instances, ATF6α was activated and shown to reduce infarct size in response to ischemia/reperfusion, as well as promoting compensatory hypertrophic cardiac growth during pressure overload, improving heart function. While these effects were partly due to the protective role of ATF6α in cardiac myocytes, the effects of ATF6α in non-myocytes in the heart were not known. Among the non-myocytes in the heart, fibroblasts play a major role during recovery from all these pathologies.

As noted above, ischemic injury stimulates fibroblast migration to the damaged area, after which they differentiate into myofibroblasts. This differentiation is characterized by induction of contractile proteins, such as αSMA (*Acta2*), and extracellular matrix proteins, such as collagen 1a1 (*Col1a1*). Similarly, fibrosis is increased during pathological cardiac remodelling following injury.[7-9, 24] Here, we found that, compared to control mouse hearts, *Acta2* and *Col1a1* transcripts were significantly elevated in the hearts of ATF6α knockout (KO) mice subjected to one week of

permanent-occlusion myocardial infarction **(Figure 21)**. However, mouse hearts with and without ATF6α deletion exhibited similar fibrosis as measured by picrosirius red staining **(Figure 22)**.

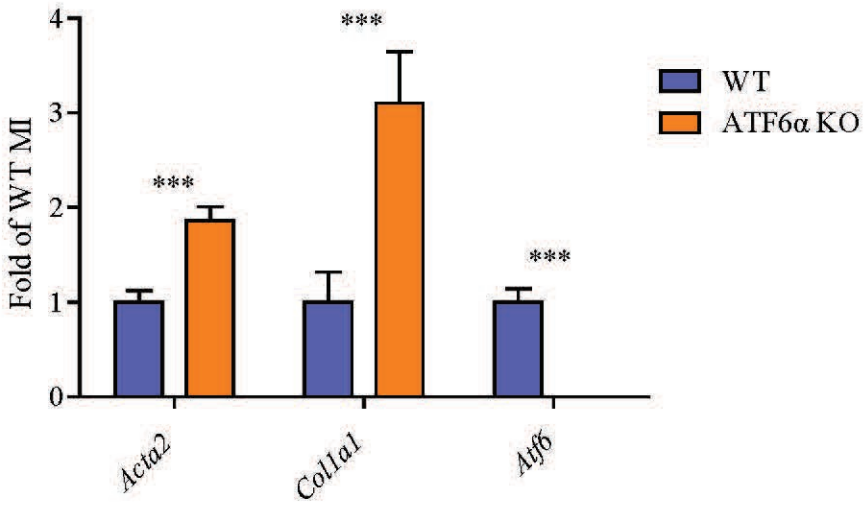

Figure 21. Markers of fibroblast activation in ATF6α KO hearts of mice subjected to MI surgery. Wild-type (WT) and ATF6α KO mice were subjected to permanent occlusion MI for one week. mRNA from infarcted regions in the hearts was then examined by qRT-PCR for genes indicative of cardiac fibroblast (CF) activation, α smooth muscle actin (αSMA) (*Acta2*) and collagen (*Col1a1*), as well as ATF6α (*Atf6*). **** $p \leq 0.001$ significant difference from WT by Student's t-test.*

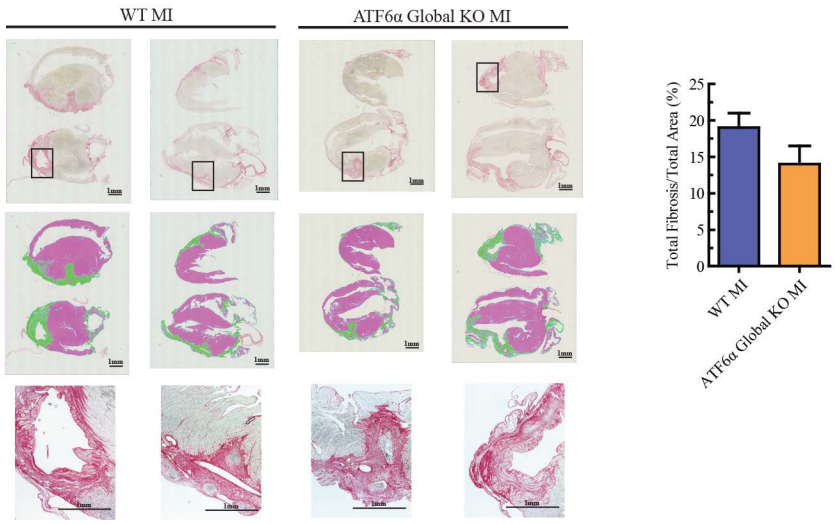

Figure 22. Fibrosis staining of hearts from WT or ATF6α KO mice subjected to MI surgery.
Picrosirius red staining of WT or global ATF6α KO mouse heart sections one week after being subjected to MI surgery. In the middle row, fibrotic areas were quantified using Keyence software (fibrotic areas are coded green) and shown in the graph at right. The bottom row is a 4x image detailing fibrosis staining in the black box from the top row.

The extent of fibrosis one week following MI is largely restricted to the infarcted area. The amount of fibrosis is thus presumed to be more a reflection of the infarct size, which, as observed in Results Section A, does not vary between WT and ATF6α KO mice in this model. Pressure overload stimulates fibroblast activation over a broader area of the heart in order to maintain cardiac structural integrity, especially in the face of myocyte apoptosis and dropout following hypertrophic growth. To examine the effect of ATF6α on fibrosis during pathological cardiac hypertrophy, ATF6α KO mice were subjected to one week of pressure overload via trans-aortic constriction (TAC). Upon TAC, the ATF6α KO heart exhibited greater fibrosis, as measured by picrosirius red staining, than the WT heart or hearts from mice undergoing sham surgeries **(Figure 23A)**. This difference was not observed between WT hearts and hearts with ATF6α deleted selectively in cardiac myocytes **(Figure 23B)**, consistent with a role for non-myocytes in the profibrotic response in ATF6α KO mouse hearts.

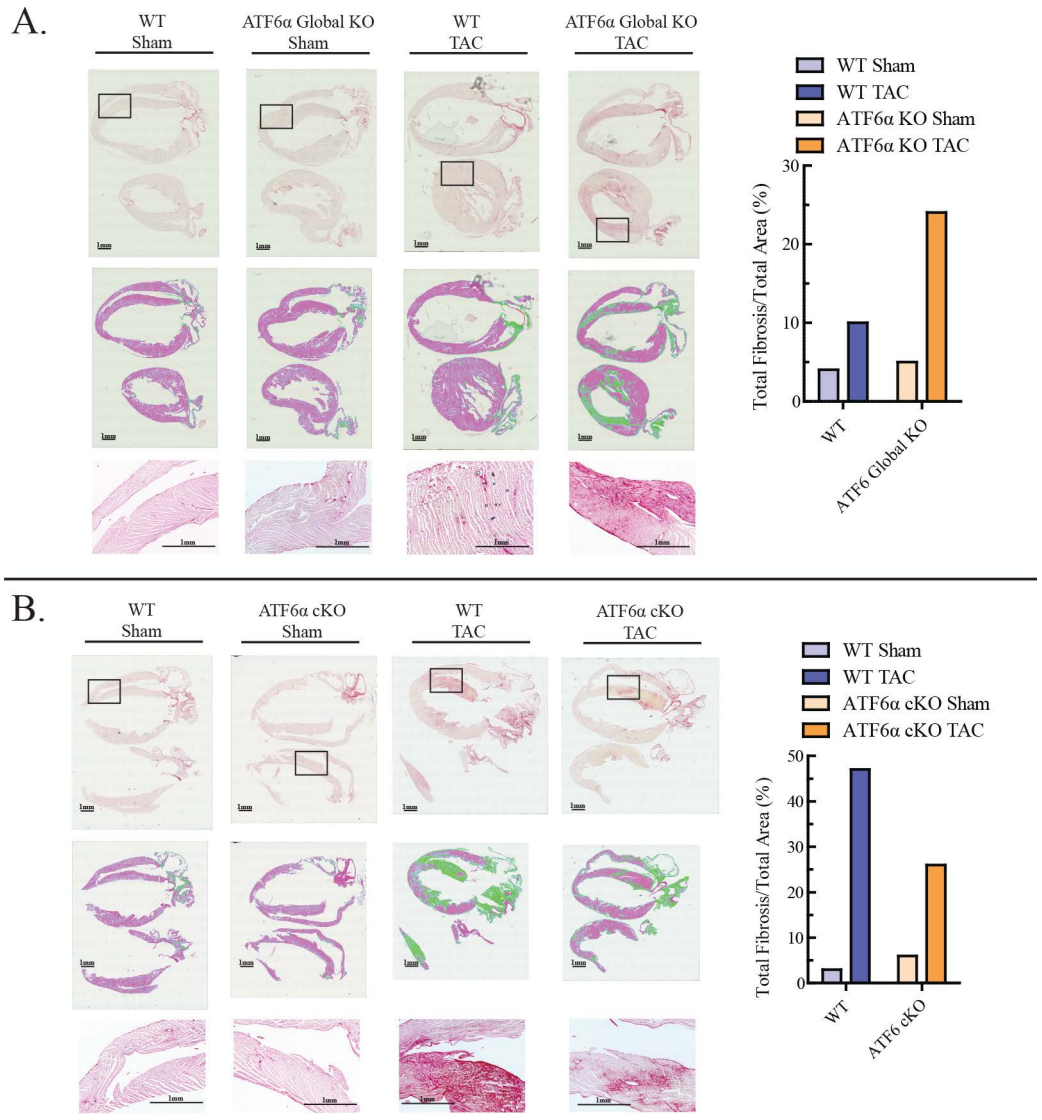

Figure 23. Fibrosis staining of hearts from WT and ATF6α KO mice subjected to sham or TAC surgery. **(A)** The top row shows picrosirius red staining of WT or global ATF6α KO mouse heart sections one week after being subjected to sham or TAC surgery. In the middle row, fibrotic areas were quantified using Keyence software (fibrotic areas are coded green) and shown in the graph at right. The bottom row is a 4x image detailing fibrosis staining in the black box from the top row. **(B)** Picrosirius red staining of WT or conditional, myocyte-specific ATF6α knockout (ATF6α cKO) heart sections one week after being subjected to sham or TAC surgery. As above, overall staining is shown in the top row, quantifications in the middle, and detailed images from the black box area on the bottom.

3. ATF6α Suppresses Genetic Markers of Fibroblast Activation in Isolated Adult Murine Ventricular Fibroblasts (AMVFs) in Response to TGFβ Treatment

Given the difference in fibrosis in the ATF6α KO mouse heart and the fact that fibroblasts are responsible for deposition of fibrotic material in the heart, we focused on investigating the role of ATF6α in cardiac fibroblasts. Accordingly, AMVFs were isolated **(Figure 6)** from WT and ATF6α KO mouse hearts, and then treated with 10 ng/mL TGFβ, to stimulate fibroblast activation, for 48 hours. As expected, TGFβ increased Acta2 and Col1a1 mRNA in fibroblasts from WT mouse hearts, an effect that was significantly increased in fibroblasts from ATF6α KO mouse hearts **(Figure 24A–C)**. Importantly, the effects of ATF6α deletion on TGFβ-mediated induction of fibroblast marker genes were recapitulated by siRNA-mediated knockdown of ATF6α in WT AMVFs **(Figure 24D–F)**. In contrast, when ATF6α was activated by treating WT AMVFs with 10 μM compound 147, a small-molecule activator of ATF6α, for 48 hours, there was a significant decrease of *Acta2* and *Col1a1* mRNA **(Figure 24G–I)**. Similar results were also shown in NIH 3T3 cultures **(Figure 25)**. Taken together, these results suggest ATF6α decreases expression of genetic markers of fibroblast activation.

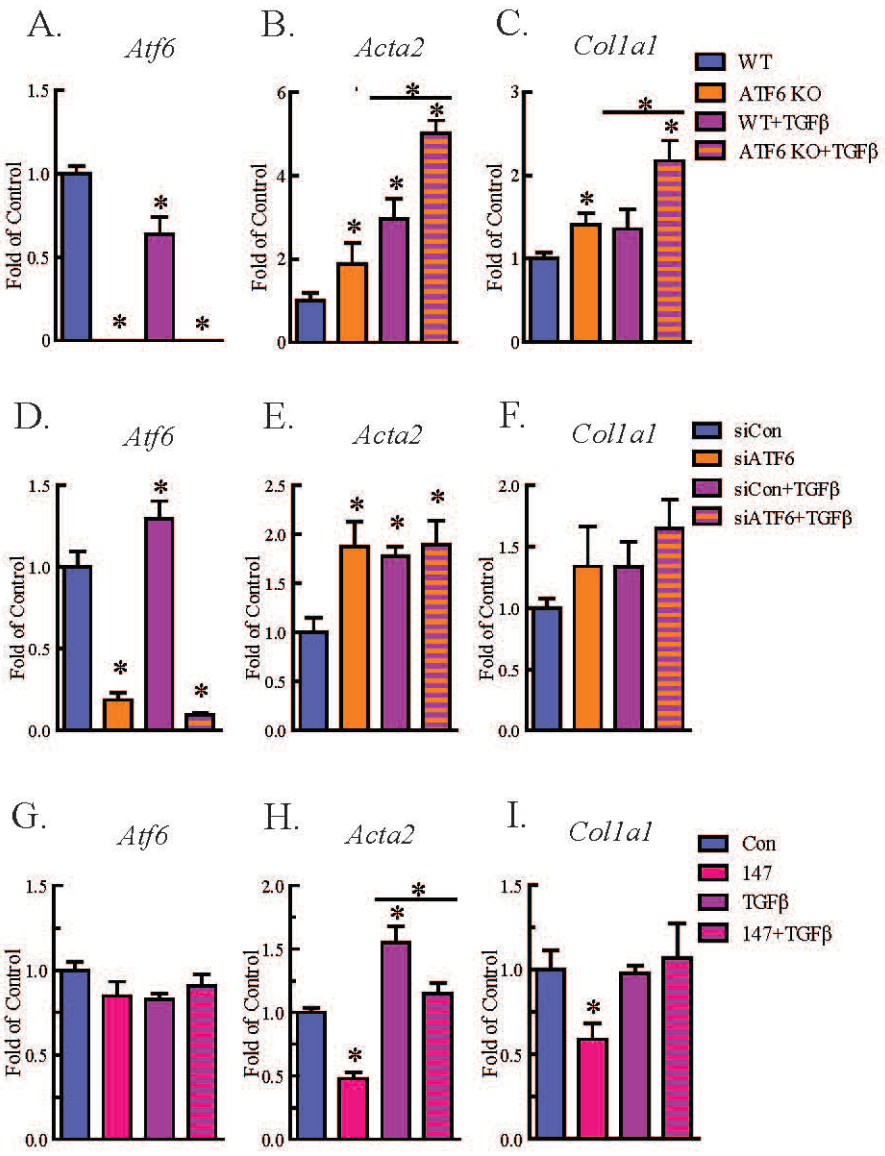

Figure 24. qRT-PCR of AMVFs with ATF6α gain- or loss-of-function.
(A–C) WT and ATF6α KO AMVFs were treated with ±10 ng/mL transforming growth factor β (TGFβ for 48 hours, then analyzed by qRT-PCR for *Atf6*, *Acta2*, and *Col1a1*. **(D–F)** AMVFs from WT mouse hearts were treated with ±siRNA targeted to murine ATF6α. Control (CON) and siRNA-treated cultures (ATF6α KD) were treated with ±10 ng/mL TGFβ, then analyzed by qRT-PCR for *Atf6*, *Acta2*, and *Col1a1*. **(G–I)** AMVFs from WT mouse hearts were treated with ±10 μM compound 147, a pharmacological activator of ATF6α. Control (CON) and 147-treated cultures (147) were co-treated with ±10 ng/mL TGFβfor 48 hours, then analyzed by qRT-PCR for *Atf6*, *Acta*, and *Col1a1*. * $p \leq 0.05$ *by one-way ANOVA.* * *Indicates significant difference between a condition and control according to Newman–Keuls post-test unless there is a line over two bars, which indicates those two bars are being compared as part of the same post-test.*

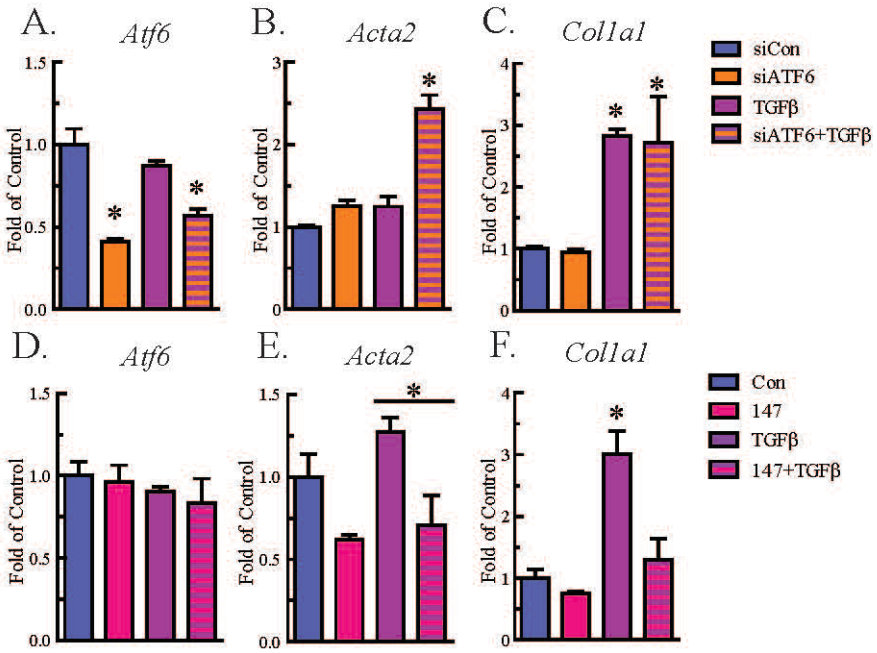

Figure 25. qRT-PCR of NIH 3T3s with ATF6α gain- or loss-of-function.
(A-C) NIH 3T3s were treated ± siRNA targeted to murine ATF6. Control (CON) and siRNA-treated cultures (ATF6α KD) were treated ± 10 ng/mL TGFβ for 48 hours, then analyzed by qRT-PCR for *Atf6*, *Acta2*, and *Col1a1*. **(D-F)** NIH 3T3s were treated ± 10 μM compound 147, a pharmacological activator of ATF6α. Control (CON) and 147-treated cultures (147) were co-treated ± 10 ng/mL TGFβ for 48 hours, then analyzed by qRT-PCR for *Atf6*, *Acta*, and *Col1a1*. *$p \leq 0.05$ by one-way ANOVA. * Indicates significant difference between a condition and control according to Newman–Keuls post-test unless there is a line over two bars, which indicates those two bars are being compared as part of the same post-test.*

4. ATF6α Activation Inhibits Fibroblast Contraction and Decreases αSMA Stress Fiber Formation in Response to TGFβ

As shown previously, when fibroblasts are activated, αSMA expression increases, and this leads to fibroblast contraction, a functional readout of fibroblast activation that is important in wound healing.[7] This contraction can be measured when fibroblasts are embedded in a disk of polymerized collagen gel and subjected to stimuli causing fibroblast activation, where increases in contraction reduce the disk diameter.[199] To examine the function of ATF6α on fibroblast activation, TGFβ-mediated contraction of NIH 3T3 fibroblasts was assessed in the setting of ATF6α pharmacological activation. Strikingly, TGFβ-mediated contraction was decreased upon ATF6α activation with compound 147 **(Figure 26A, B)**.

The inhibition of TGFβ-mediated fibroblast contraction by ATF6α activation implies that ATF6α exerts its effects at the level of αSMA contractile protein expression or structure. A major feature of fully activated myofibroblasts is the assembly of αSMA into contractile fibers, known as stress fibers, which are responsible for the contractile activity of the cell.[7] These fibers can be stained by fluorescent antibodies to αSMA and imaged as a final sign of complete myofibroblast activation. To study the effect of ATF6α activation on stress fiber formation, isolated AMVFs were treated with TGFβ with and without cotreatment with compound 147. As expected, compared to control, AMVFs treated with only TGFβ exhibited a significantly greater number of cells that had strongly expressed and fully assembled αSMA stress fibers. Intriguingly, cells treated with both TGFβ and 147 had far fewer stress-fiber-positive cells and were generally similar in appearance to control **(Figure 26C, D)**, reflecting previously observed results on the mRNA level. These results were also shown in NIH 3T3 cultures **(Figure 27)**. This demonstrates that the

inhibition of TGFβ-mediated fibroblast contraction by ATF6α is at least in part due to the decreased formation of αSMA stress fibers in fibroblasts.

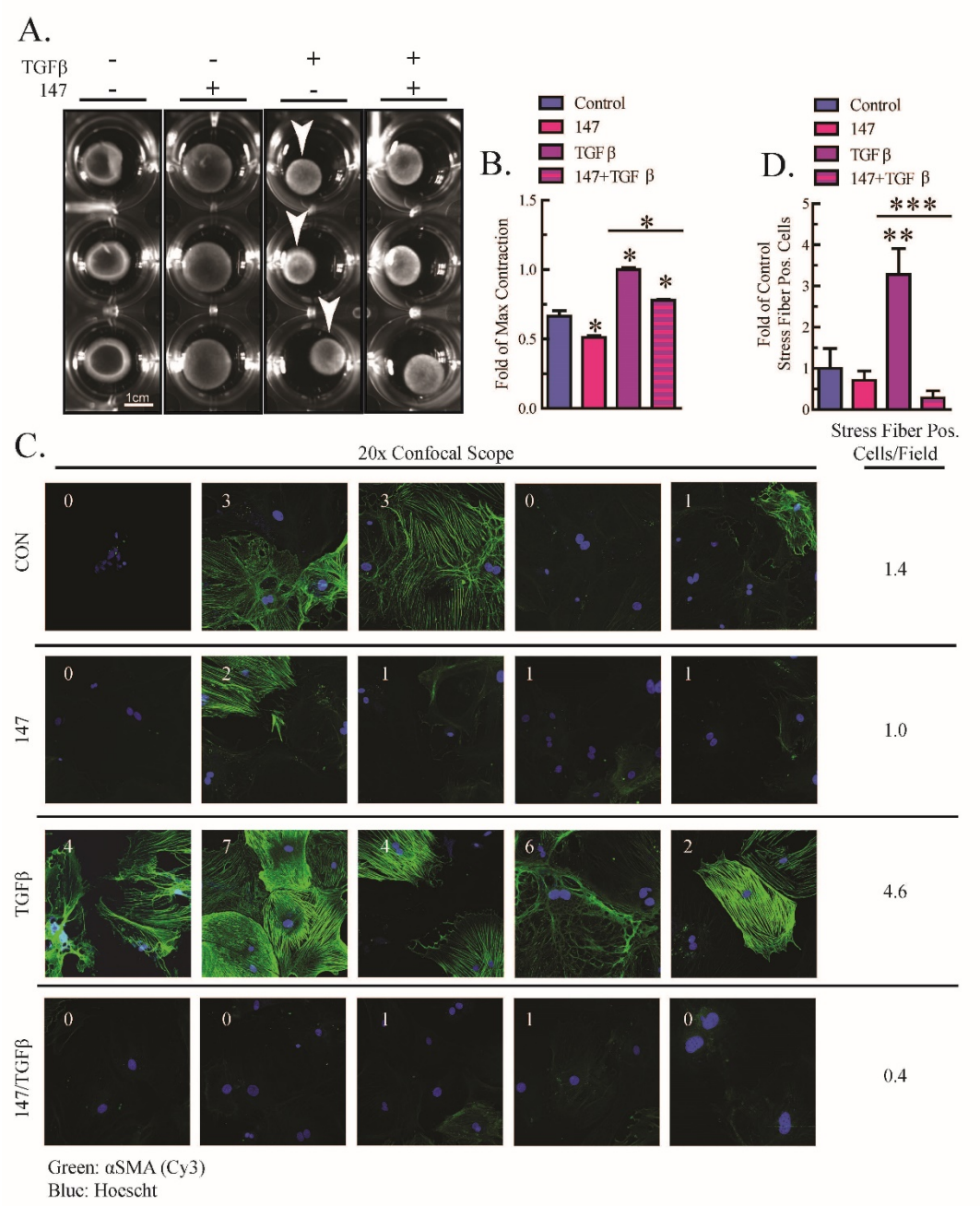

Figure 26. Effects of activating ATF6α on fibroblast contraction and stress fiber formation.
(A) NIH 3T3 fibroblasts embedded in collagen gel disks were treated with ±10 μM compound 147, and then analyzed for contraction with ±10 ng/mL TGFβ after 48 hours. Contraction is quantified in **(B),** n = 3 cultures of each type, normalized to those with maximum contraction (white arrows). **(C, D)** AMVFs from WT mice were treated with ±10 μM compound 147 and ±10 ng/mL TGFβ for 48 hours, then analyzed by actin staining for stress fiber formation. All images in **(C)** were taken with a 20× objective on a confocal microscope. In **(C)** the number in each field is the number of stress-fiber positive cells in that field. The number of stress-positive cells per field is averaged to the right and quantified in **(D)**, across n = 5 fields. * *p ≤ 0.05, ** p ≤ 0.01, and *** p≤0.001 by one-way ANOVA. A line over two bars indicates those two bars are being compared as part of the same post-test.*

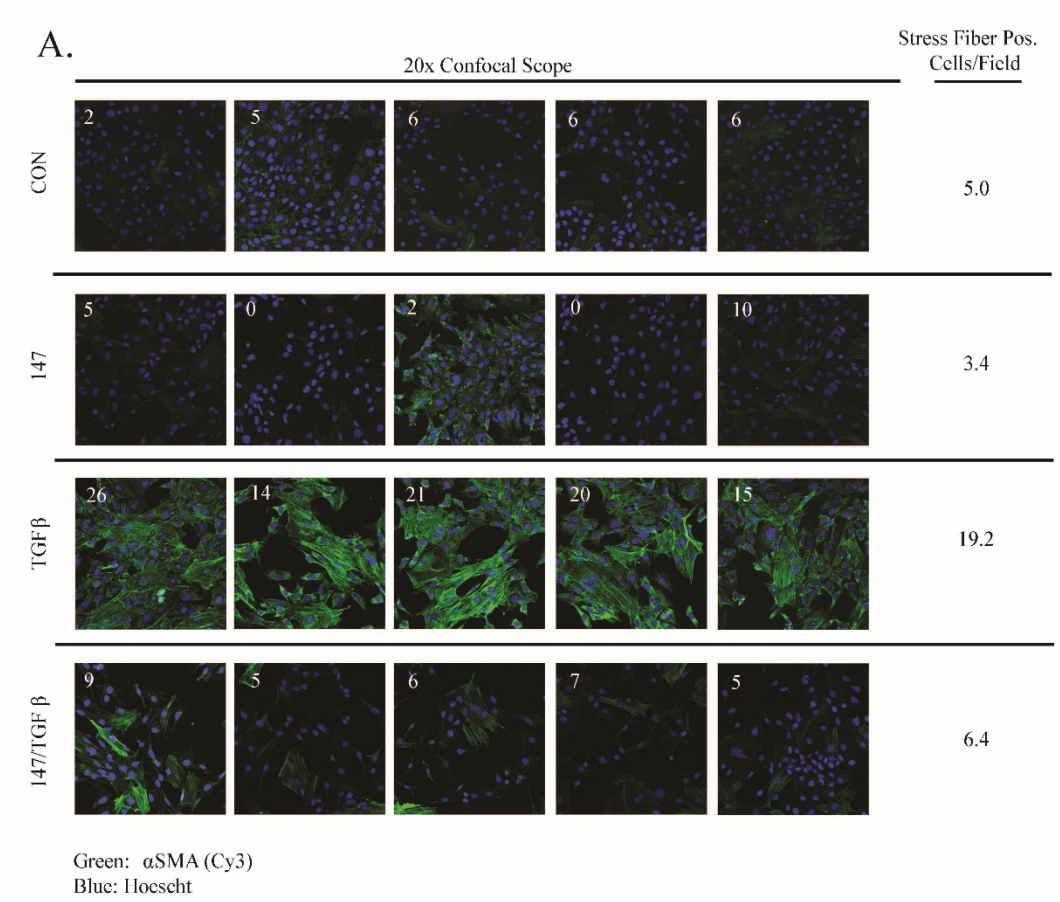

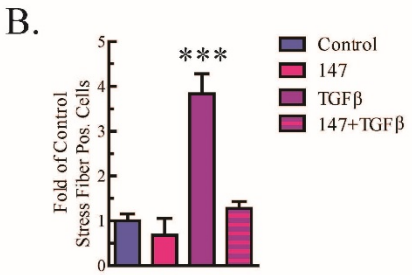

Figure 27. Effects of activating ATF6α on stress fiber formation in NIH 3T3s.
(A) NIH 3T3s were treated with ± 10 μM compound 147 and ±10 ng/mL TGFβ for 48 hours, then analyzed by actin staining for stress fiber formation, which is quantified in **(B)**. All images in **(A)** were taken with a 20x objective on a confocal scope. In **(A)** the number in each field represents the number of cells that were stress fiber-positive in that field. The number to the right is the average number of stress-positive cell per field, quantified in **(B)**. *** *p≤0.001 by one-way ANOVA.*

5. ATF6α Suppresses Smad2 Phosphorylation, a Measure of TGFβ-Mediated Fibroblast Activation, in Isolated AMVFs

To begin to dissect the level at which ATF6α affects TGFβ-mediated fibroblast activation, downstream events in the canonical TGFβ signaling pathway were interrogated. When TGFβ binds TGFβ receptors, the phosphorylation of receptor-Smad proteins 2 and 3 is increased, which leads to increased transcription of genes responsible for fibroblast activation.[200] Here, immunoblotting showed that, as expected, TGFβ increased the phosphorylation of Smad2 in WT AMVFs. Intriguingly, ATF6α knockdown **(Figure 28A)** slightly but significantly increased basal and TGFβ-mediated phosphorylation of Smad2 **(Figure 28B)**, while activation of ATF6α with 147 **(Figure 28C)** reduced Smad2 phosphorylation **(Figure 28D)**. These findings suggest that the inhibitory effect of ATF6α on fibroblast activation may be due to its ability to reduce TGFβ-mediated Smad2 signaling, though the potential for ATF6α to also act on other players in the TGFβ/Smad signaling pathway cannot be ruled out. To further confirm the involvement of ATF6α in the TGFβ/Smad signaling pathway in fibroblasts, AMVFs were treated with the TGFβ receptor inhibitor, SB431542 **(Figure 29)**. SB431542 reduced basal and TGFβ-mediated increases in αSMA and Col1a1, as well as completely blocking αSMA and Col1a1 induction by ATF6α knockdown. This further demonstrates that the fibroblast activation that takes place upon ATF6α loss-of-function is occurring because of a hyperactivation of the TGFβ/Smad pathway.

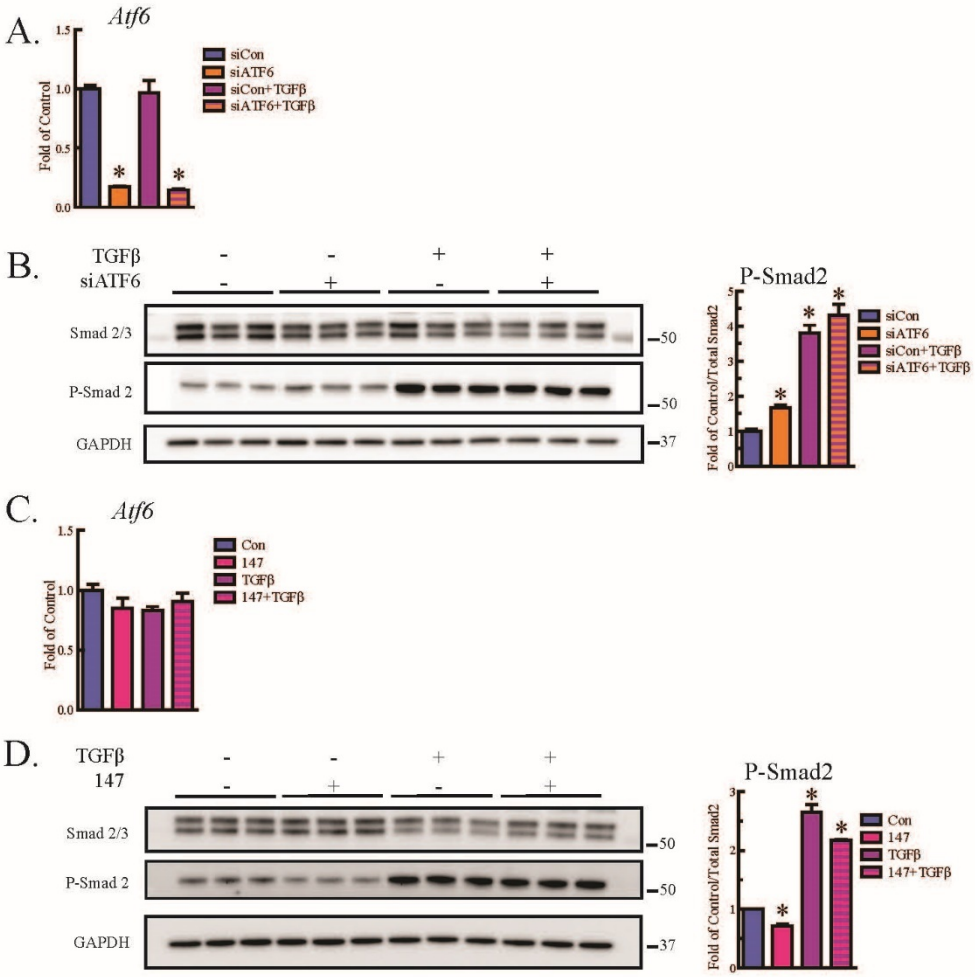

Figure 28. Immunoblots investigating activation of canonical TGFβ signaling pathways.
(A) AMVFs were treated with ±siRNA to ATF6α, ±10 ng/mL TGFβ for 48 hours. *Atf6* knockdown is quantified via qPCR. **(B)** Immunoblotting for total Smad 2/3, P-Smad 2, or glyceraldehyde 3-phosphate dehydrogenase (GAPDH), with quantification of P-Smad 2 shown at right. Quantification is a ratio of P-Smad 2 to total Smad 2 (the uppermost band), relative to control. **(C)** AMVFs were treated with ±10 μM compound 147, ±10 ng/mL TGFβ for 48 hours. *Atf6* levels were quantified via qPCR. **(D)** Immunoblotting for total Smad 2/3, P-Smad 2, or GAPDH, with quantification of P-Smad 2 shown at right. Quantification is a ratio of P-Smad 2 to total Smad 2 (the uppermost band), relative to control. * $p \leq 0.05$ *by ANOVA.* * *Indicates significant difference between a condition and control according to Newman–Keuls post-test.*

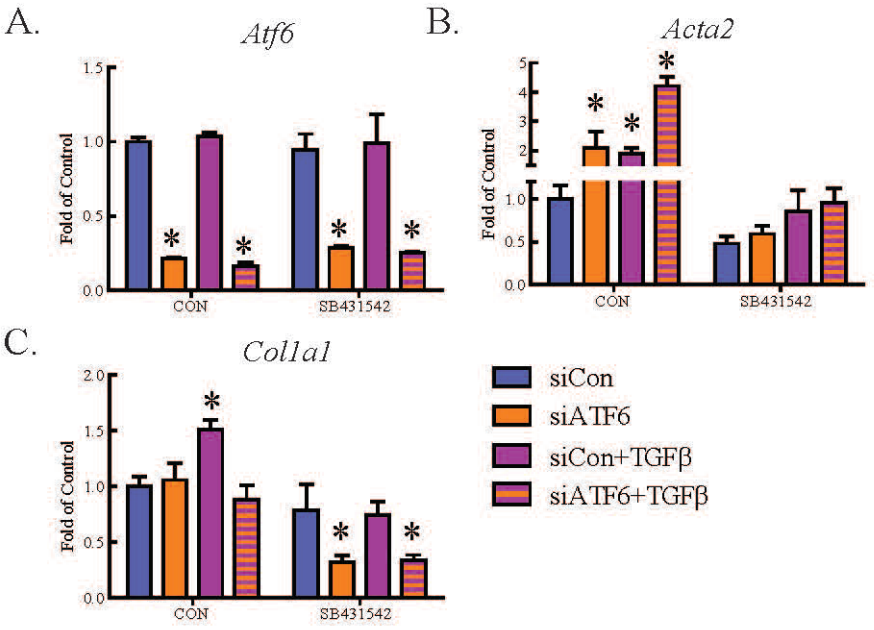

Figure 29. Effect of inhibiting the TGFβR1 on ATF6α and TGFβ-mediated increases in myofibroblast markers.

AMVFs were treated with ±siRNA to ATF6α, ±10 ng/mL TGFβ, ±10 μM of the TGFβRI inhibitor SB431542, and then analyzed by qRT-PCR for **(A)** *Atf6*, **(B)** *Acta2*, and **(C)** *Col1a1*. All treatments were for 48 hours. ** $p \leq 0.05$ by one-way ANOVA. * Indicates significant difference between a condition and control according to Newman–Keuls post-test.*

6. ATF6α Induces TGFβ/Smad Pathway Inhibitors and Suppresses Expression of TGFβ Receptors and Fibrosis-Related Genes

While the mechanisms by which ATF6α inhibits gene expression have not been explored, we considered it possible that, in fibroblasts, ATF6α might inhibit the expression of positive regulators of TGFβ/Smad signaling. Alternatively, ATF6α might increase the expression of negative regulators of the pathway. Accordingly, we examined the levels of several of these regulators in RNA isolated from AMVFs treated with 147. Among them, *Smurf1*[143], *Smurf2*[144], and *Pmepa1*[145, 146], all negative regulators of TGFβ/Smad signaling, were the most significantly induced **(Figure 30A)**. Smurf1 and 2 proteins ubiquitylate R-Smads and target them for degradation. PMEPA1 protein inhibits the TGFβ/Smad pathway by sequestering the R-Smads before they can be phosphorylated or interact with Smad4. *Pmepa1* is also heavily induced by TGFβ as a negative feedback loop. Importantly, *Smurf1* and *Pmepa1* transcript levels were significantly decreased when ATF6α was knocked down in AMVFs **(Figure 30B)**.

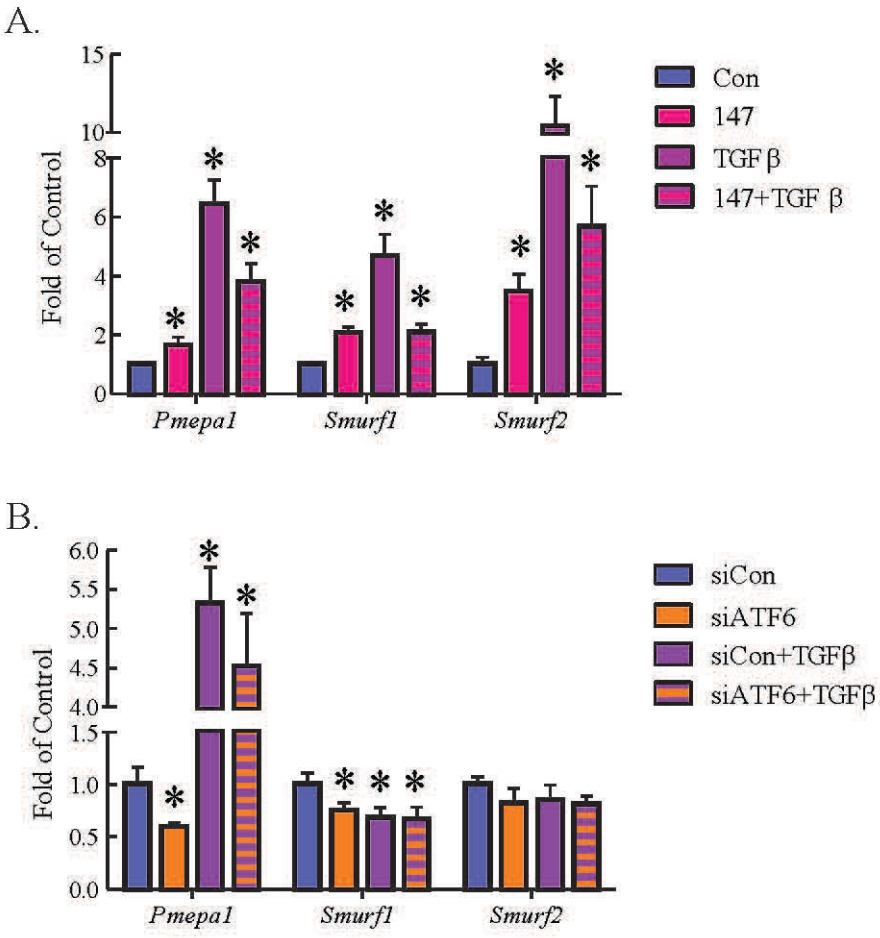

Figure 30. qRT-PCR of AMVFs treated with ATF6α knockdown and/or TGFβ for genes associated with TGFβ-Smad pathway inhibition.

AMVFs were treated with **(A)** ±10 μM compound 147, ±10 ng/mL TGFβ, or **(B)** ±siRNA to ATF6α, ±10 ng/mL TGFβ, then analyzed by qRT-PCR for *Pmepa1, Smurf1,* and *Smurf2*, as shown. All treatments were for 48 hours. ** $p \leq 0.05$ by one-way ANOVA within each gene group. * Indicates significant difference between a condition and control according to Newman–Keuls post-test.*

To more broadly investigate the effect of ATF6α on fibrosis gene expressions, we performed PCR arrays interrogating the effects of ATF6α activation or knockdown in AMVFs. Consistent with the results above, we found that numerous pro-fibrosis genes were downregulated upon ATF6α activation with compound 147 **(Figure 31A)**, and most of the same genes were upregulated upon ATF6α knockdown with siRNA **(Figure 31B)**. Notable differentially regulated genes are summarized in **Figure 31C**. Several of the affected genes are directly involved in the TGFβ/Smad signaling pathway; when we perused the arrays for genes that were common to both treatments, we found that multiple isoforms of TGFβ itself were downregulated upon ATF6α activation and upregulated upon ATF6α knockdown, as were TGFβ receptors 1[143] and 2[219]. RT-qPCR was used to validate these results, indicating that ATF6α may affect fibroblast activation by decreasing TGFβ and TGFβ receptor expression.

A.

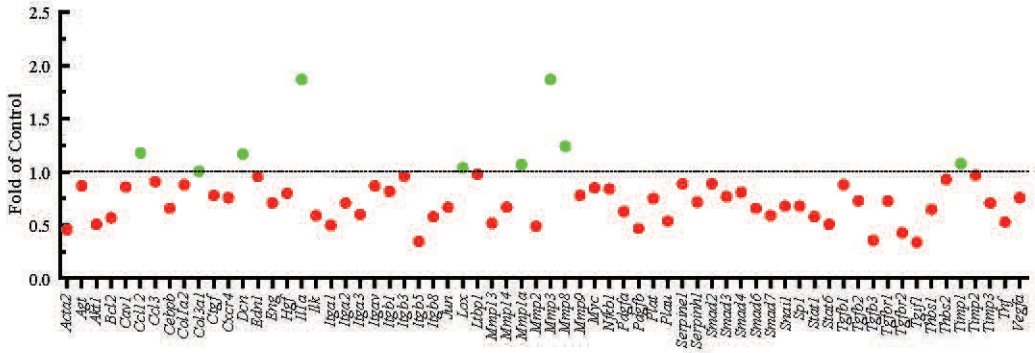

B.

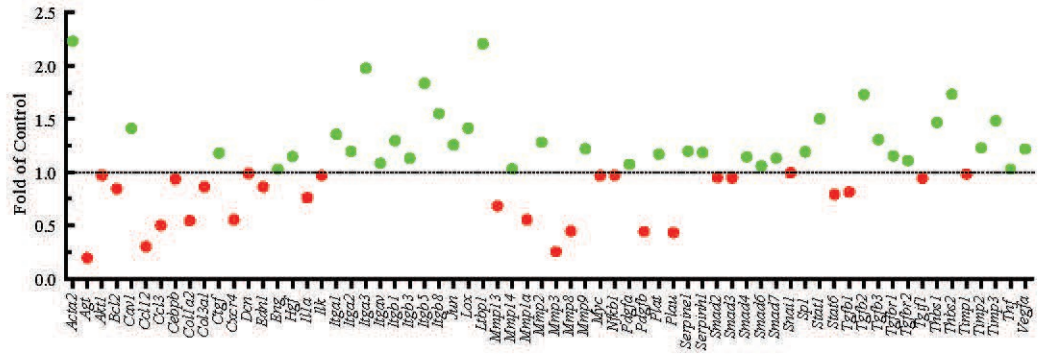

C.

Gene	AMVF Treated with 147	AMVF Treated with siATF6
Il1a	1.87	0.76
Mmp3	1.87	0.25
Mmp8	1.24	0.45
Tgfb2	0.73	1.73
Tgfb3	0.36	1.31
Tgfbr1	0.73	1.16
Tgfbr2	0.43	1.11

Figure 31. PCR array for fibrosis genes in AMVFs.
AMVFs were treated with **(A)** ±10 µM compound 147 or **(B)** ±siRNA to ATF6α; all cultures were treated for 48 hours, then analyzed by a qRT-PCR array as described in the Methods (Section 4). In **(A and B)** green and red dots represent up- and downregulated genes, respectively. **(C)** A subset of differentially regulated genes from panels A and B; green and red numbers represent the fold up- or downregulation, respectively.

7. Conclusions

This chapter shows that the ATF6α branch of the ER stress response has a role in regulating the activation of fibroblasts, including adult cardiac fibroblasts. This includes suppression of TGFβ–Smad2 signaling, part of the canonical pathway for fibroblast activation, which is summarized in **Figure 32**.[7, 142, 146, 200, 216] The process of fibroblast-to-myofibroblast differentiation naturally involves the induction of numerous genes, including many whose protein products are translated on ER resident ribosomes and subsequently pass through all or part of the ER–Golgi secretory pathway. This is especially true of the secretion of extracellular matrix proteins such as collagen, which are characteristic of the myofibroblast phenotype. As in the differentiation of other professional secretory cells such as plasma cells[5], the increased flux of newly translated proteins represents a challenge to ER proteostasis and can lead to activation of ER stress response pathways, including ATF6α[106]. Accordingly, TGFβ treatment has been reported to induce ER stress and to activate downstream ER UPR signaling.[220] Furthermore, amelioration of ER stress, through treatment with chemical chaperones 4-PBA or TUDCA, has been shown to reduce fibrosis and TGFβ signaling.[221-224]

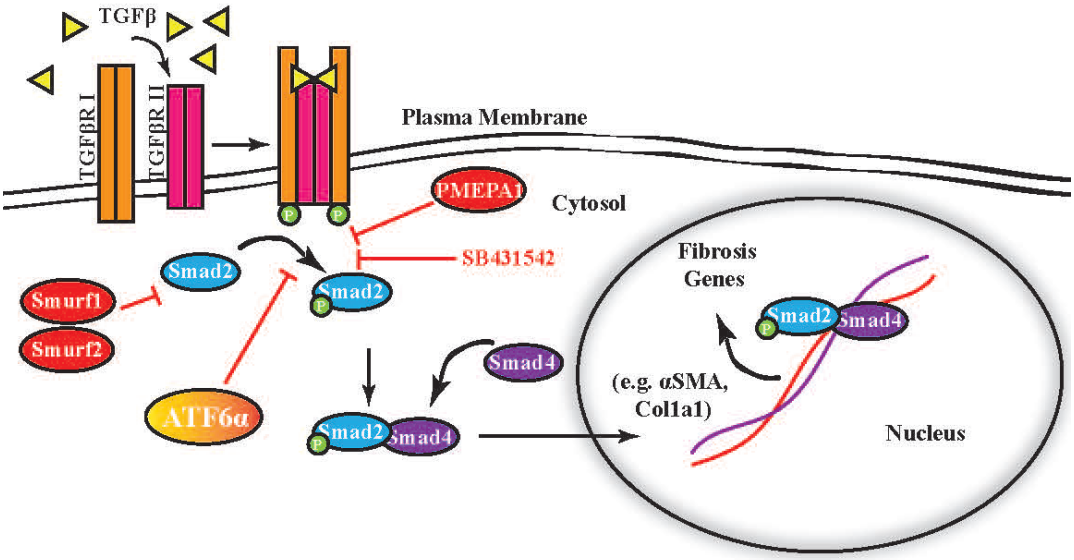

Figure 32. Proposed mechanism of ATF6α acting on the TGFβ–Smad pathway for induction of fibrosis genes. TGFβ is a ligand for TGFβ receptor II, which upon binding forms a receptor complex with TGFβ receptor I, activating their kinase function. The TGFβ receptor complex phosphorylates receptor-Smads 2 and 3, which then complex with co-Smad 4 and move to the nucleus where they activate fibrosis genes (black arrows). These data suggest ATF6α activity inhibits the phosphorylation of the receptor-Smads at or before the level of the TGFβ chemical inhibitor SB431542 (red "T" arrows).

Several potential mechanisms are possible for how ATF6α activation regulates fibroblast activation. For example, one or more negative regulators of TGFβ–Smad2 could be non-canonical targets of ATF6α. While ATF6α is primarily known for its role as a master regulator of the ER stress response and specifically of ER proteins involved in protein quality control, it is clear from recent publications that it is involved in many non-canonical pathways.[6, 11, 12, 61, 88, 225] Jin et. al. discovered that ATF6α governed an oxidative stress pathway by directly upregulating catalase, a well-known antioxidant targeted to the peroxisome.[11] More recently, Blackwood et. al. found that ATF6α directly upregulates Ras homolog enriched in brain (Rheb), a cytosolic small GTPase that regulates mammalian target of rapamycin complex 1 (mTORC1) to induce cell growth.[12] Furthermore, it was observed that the specific gene set upregulated by ATF6α varied in a stimulus-dependent manner. Thus, general ER stressors such as tunicamycin (TM) activated ATF6α to induce the typical ER protein folding and degradation machinery, while oxidative stressors caused ATF6α to upregulate catalase and cell growth signals caused an ATF6α-mediated induction principally of Rheb. Another study by Tam et. al. found that ATF6α was activated by sphingolipids, specifically dihydrosphingosine and dihydroceramide, which caused the upregulation of a previously unknown ATF6α gene set involved in the lipid biosynthesis pathway.[61] Thus, ATF6α induction of regulators of other non-ER stress pathways would not be unprecedented.

Though ATF6α is an activating transcription factor, it is also possible that it directly downregulates a necessary component of TGFβ–Smad, such as TGFβ receptors or TGFβ itself. It was shown that numerous genes are perturbed in hearts with an activated form of ATF6α and that many of those are downregulated.[88] Moreover, Belmont et. al. reported ATF6α is involved in the downregulation of many miRNAs, many of which did not target ER proteins and all of which

lacked the consensus ATF6α binding site in their promoters, termed the ER stress response element (ERSE).[225] Other studies found that ATF6α inhibits pathways by forming heterodimers with other transcription factors such as cAMP response element binding (CREB)[226] or sterol regulatory element binding protein 2 (SREBP2)[227] and altering their transcriptional activity. Thus, though its name implies otherwise, ATF6α can clearly participate in the inactivation of many genes, including some involved in fibroblast activation, as seen in **Figure 29**. Further study is needed to determine which of these genes, or a combination thereof, is necessary for ATF6α to confer this effect.

Section III. C. is, in part, a reprint of the research article "The ER Unfolded Protein Response Effector, ATF6, Reduces Cardiac Fibrosis and Decreases Activation of Cardiac Fibroblasts" as it appears in the International Journal of Molecular Sciences, 2020. Stauffer, Winston T.; Blackwood, Erik A.; Azizi, Khalid; Kaufman, Randal J.; Glembotski, Christopher C., *Int J Mol Sci*, 2020. The dissertation author was the primary author of this paper.

IV. Discussion

This work highlights the importance of ATF6α in a variety of heretofore unknown aspects of cardiac physiology and pathology. Previous cell-specific studies of ATF6α in the heart have focused exclusively on cardiac ventricular myocytes. This is understandable because, more than other cell types, the survival and performance of cardiac myocytes is more directly related to heart function.[228] This overlooks, however, that the heart is a complex organ with numerous tissues and cell types, all with critical roles.[1] Because of the highly specialized nature of cardiac myocytes, their function, structure, and response to stresses can vary greatly from other cardiac cells. It is thus necessary to fully explore pathways essential to cardiac function in less well studied paradigms.

While much of the protective effect of ATF6α has previously been shown to relate directly to its canonical role as one of the three main sensors of the ER stress response[21], this work, and other recent publications[6, 11, 12, 61, 88, 225], suggest ATF6α has an influence on a far wider range of cellular processes. The ubiquity and importance of ER proteostasis makes it plausible that merely controlling this master switch alone might influence far-flung functions of the cell. The data presented here concern ATF6α regulation of further processes important for cell function, such as proliferation, oxidative stress, and transdifferentation, that are at best indirectly related to ER proteostasis. Likewise, these pathways also include proteins not localized to the ER and fit the wider pattern of noncanonical ATF6α regulatory targets found to have importance to a variety of cellular functions.

This work investigates the role of ATF6α in an unexamined cardiac disease model, long-term permanent-occlusion MI-induced heart failure, as well as two cardiac non-myocyte cell types

known to be important during cardiac pathology. All three chapters reveal potential avenues of research likely to be of further interest to the field and worthy of future study.

The disadvantage of using of global knockout mice to study any disease model is the uncertainty as to the tissues and cell types in which loss of the gene of interest is having the greatest effect, because the gene has been deleted in all cells. Also of concern is the fact that the gene is missing throughout development, possibly leading to differences in the baseline phenotype of the adult animals. These concerns are partially abrogated in the context of global ATF6α knockout mice for the investigation of MI-induced heart failure because, while ATF6α is important in development, lack of the α isoform appears to be compensated in this context by the continued presence of the β isoform.[119] Adult ATF6α knockout mice thus, at baseline, appear physiologically normal.[100] Furthermore, ATF6α is mostly characterized as a stress response gene, ubiquitously expressed but only activated under certain stress conditions, such as ischemia.[13] Thus, in an acute injury model in the heart, the effect of loss of ATF6α might reasonably be expected to be felt directly only in the heart. Formally, though, the effect of the lack of ATF6α elsewhere in the body cannot be ruled out. Additionally, as previously stated, it is unknown in which cell types in the heart ATF6α is most critical. Future studies can be designed to address these issues, which might involve cell type-specific promoters for targeted ATF6α deletion or overexpression. The expression of Cre recombinase in transgenic mice behind a *Tnnt2* promoter achieves cardiomyocyte specific ATF6α deletion when crossed with ATF6α-floxed transgenic mice. This can also be achieved by expression of the *Tnnt2-Cre* introduced by a viral vector in ATF6α-floxed mice, as seen in **Figure 23**, with the added benefit that deletion does not occur until administration of the virus in adulthood, immediately prior to commencement of the study.[12] Conditional knockout can also be achieved in other cell types for which a sufficiently specific promoter can be

identified. Examples used in other contexts in the literature include *Tcf21* for quiescent cardiac fibroblasts[24], *Postn* for activated myofibroblasts[229], *Kit* for CSCs[127], or *Tek* for endothelial cells[230]. A logical follow up to a global knockout model would be to repeat the study using any of these more specific knockout models to take advantage of cell specificity, temporal specificity, or both.

Similar techniques could also be used to achieve cell specificity for overexpression of either full-length or N-terminal (active) ATF6α. In such cases conditional activation would be even more desirable, as long-term ER stress signaling, potentially including ATF6α, can lead to cell death.[231] Thus, a chemically activated fusion-protein might be used, as in Martindale et.al., such that the expressed active portion of ATF6α would only be free to move to the nucleus upon treatment with a chemical such as tamoxifen.[21] Pharmacological activation of endogenous ATF6α as with compound 147 would also be useful in this paradigm, though with the drawback of not being cardiac specific.[105]

In isolated CSCs, further research is needed to determine the mechanistic link between ATF6α and promotion of proliferation and suppression of differentiation. The cell cycle PCR array revealed multiple notable genes that are altered with ATF6α knockdown. By far the most induced was *Gadd45a*, which halts cell cycle progression and promotes cell death pathways.[180] It is possible ATF6α promotes a repressor of GADD45α, regulation which is lost with ATF6α knockdown. *Gadd45a* is also induced by DNA damage, as evidenced by its role as a tumor suppressor gene. Future experiments should determine whether ATF6α knockdown alone causes genotoxicity in CSCs and other cell types, perhaps by probing for histones phosphorylated in the presence of DNA double-stranded breaks.

Likewise, the role of oxidative stress potentially caused by the lack of ATF6α in these cells should be further explored. If ROS scavenging by NAC can reverse Dex-induced differentiation,

perhaps ATF6α in its role as a regulator of antioxidant genes acts in a similar manner. The most obvious ATF6α antioxidant target is catalase, localized to the peroxisome, which was shown to blunt ROS-induced damage following ischemia/reperfusion injury.[11] Future experiments should determine to what degree ATF6α loss promotes ROS production in cultured CSCs and whether catalase alone is responsible for the effects of ATF6α in this context. It is possible that other known ATF6α antioxidant targets not included in the array, like *Vimp*, may also contribute.[11]

It is tempting to suggest that induced activation of ATF6α might improve outcomes in patients in clinical trials undergoing autologous CSC therapy. Conceivably pharmacological ATF6α activation, either while the CSCs are being expanded in culture or during reinsertion, might preserve stemness, proliferative potential, or even secretory capacity. Thus, the ATF6α-stimulated CSCs hypothetically might be more beneficial following reimplantation. It is important however, to understand how exactly CSCs are beneficial in this therapy, if indeed they are, and whether other cell types might be more effective. This understanding would aid in deciding whether further exploring the role of ATF6α in this treatment is worthwhile. If CSCs do not differentiate into mature cardiac myocytes, as the data suggest[127, 129], further research should determine how this treatment aids patient outcomes, before further clinical trials continue.

In cultured cardiac fibroblasts, next steps should further dissect where in the TGFβ pathway ATF6α acts to suppress signaling. There are multiple avenues worth exploring. It is possible ATF6α acts directly to suppress transcription of TGFβ. ATF6α itself has been shown to act as a transcriptional repressor of miRNAs, thus increasing translation of their target transcripts.[96] Other bZip transcription factors also sometimes function as transcriptional repressors, potentially by suppressing or altering the activity of other DNA binding partners.[76] As before, ATF6α may also act indirectly by upregulating a TGFβ repressor. One potential target not included in the fibrosis

array is miR-130b, an miRNA which is predicted to suppress expression of both TGFβ receptors and various Smad family members, including Smad2 and Smad4.[232] A microRNA array from mouse hearts with activated ATF6α showed that miR-130b was overexpressed 2-fold compared to control.[88]

Recent publications suggest further possible mechanisms. In β-cells, the maintenance of maturation markers is dependent on the Sel1L-Hrd1 complex, a critical component of ERAD.[218] ERAD effectors, especially Hrd1, are heavily upregulated by ATF6α signaling in response to ER stress.[95] Loss of ERAD in β-cells causes their dedifferentiation, which coincides with elevated TGFβ signaling via Smad secondary messengers. Importantly for the future directions of this study, TGFβ receptor 1 was found to be a substrate of Hrd1, resulting in the observed effects on β-cell maturation.[218] Subsequent studies should establish whether TGFβR1, or any other TGFβ-Smad component, is also an ERAD substrate in cardiac fibroblasts and whether ATF6α activity results in their increased ubiquitylation and degradation.

ATF/CREB family member and stress response transcription factor ATF3 has been repeatedly shown to regulate cardiac fibrosis. Intriguingly, whether it is a positive or negative regulator of fibrosis seems to depend on which cell type it is active in.[109, 233, 234] In cardiac fibroblast specific knockout models, ATF3 acts to inhibit fibroblast activation by inhibiting MAPK transcription and downstream p38 signaling.[109] This inhibition requires binding to HDAC1 in the nucleus. ATF6α has been shown to recruit HDAC1 to attenuate transcription of SREBP2-target lipogenic genes.[227] Though we did not detect changes in p38 phosphorylation with modulation of ATF6α levels in AMVF, future studies should establish whether HDAC1 interaction is involved in ATF6α suppression of other fibroblast activation pathways.

Lastly, the above studies further highlight the need for cell-specific knockout models. Future directions for all the chapters in this work should include efforts to manipulate ATF6α signaling with as much specificity as possible, in recognition of the complex cellular makeup of the heart.

V. References

1. Pinto, A.R., A. Ilinykh, M.J. Ivey, J.T. Kuwabara, M.L. D'Antoni, R. Debuque, A. Chandran, L. Wang, K. Arora, N.A. Rosenthal, and M.D. Tallquist, "Revisiting Cardiac Cellular Composition". *Circ Res*, 2016. **118**(3): p. 400-9.

2. Moore, K.A. and J. Hollien, "The unfolded protein response in secretory cell function". *Annu Rev Genet*, 2012. **46**: p. 165-83.

3. Kaufman, R.J., D. Scheuner, M. Schroder, X. Shen, K. Lee, C.Y. Liu, and S.M. Arnold, "The unfolded protein response in nutrient sensing and differentiation". *Nat Rev Mol Cell Biol*, 2002. **3**(6): p. 411-21.

4. Iwakoshi, N.N., A.H. Lee, P. Vallabhajosyula, K.L. Otipoby, K. Rajewsky, and L.H. Glimcher, "Plasma cell differentiation and the unfolded protein response intersect at the transcription factor XBP-1". *Nat Immunol*, 2003. **4**(4): p. 321-9.

5. Jurkin, J., T. Henkel, A.F. Nielsen, M. Minnich, J. Popow, T. Kaufmann, K. Heindl, T. Hoffmann, M. Busslinger, and J. Martinez, "The mammalian tRNA ligase complex mediates splicing of XBP1 mRNA and controls antibody secretion in plasma cells". *EMBO J*, 2014. **33**(24): p. 2922-36.

6. Kroeger, H., N. Grimsey, R. Paxman, W.C. Chiang, L. Plate, Y. Jones, P.X. Shaw, J. Trejo, S.H. Tsang, E. Powers, J.W. Kelly, R.L. Wiseman, and J.H. Lin, "The unfolded protein response regulator ATF6 promotes mesodermal differentiation". *Sci Signal*, 2018. **11**(517).

7. Travers, J.G., F.A. Kamal, J. Robbins, K.E. Yutzey, and B.C. Blaxall, "Cardiac Fibrosis: The Fibroblast Awakens". *Circ Res*, 2016. **118**(6): p. 1021-40.

8. Souders, C.A., S.L. Bowers, and T.A. Baudino, "Cardiac fibroblast: the renaissance cell". *Circ Res*, 2009. **105**(12): p. 1164-76.

9. Tallquist, M.D., "Cardiac fibroblasts: from origin to injury". *Curr Opin Physiol*, 2018. **1**: p. 75-79.

10. Glembotski, C.C., "Roles for the sarco-/endoplasmic reticulum in cardiac myocyte contraction, protein synthesis, and protein quality control". *Physiology (Bethesda)*, 2012. **27**(6): p. 343-50.

11. Jin, J.K., E.A. Blackwood, K. Azizi, D.J. Thuerauf, A.G. Fahem, C. Hofmann, R.J. Kaufman, S. Doroudgar, and C.C. Glembotski, "ATF6 Decreases Myocardial Ischemia/Reperfusion Damage and Links ER Stress and Oxidative Stress Signaling Pathways in the Heart". *Circ Res*, 2017. **120**(5): p. 862-875.

12. Blackwood, E.A., C. Hofmann, M. Santo Domingo, A.S. Bilal, A. Sarakki, W. Stauffer, A. Arrieta, D.J. Thuerauf, F.W. Kolkhorst, O.J. Muller, T. Jakobi, C. Dieterich, H.A. Katus,

S. Doroudgar, and C.C. Glembotski, "ATF6 Regulates Cardiac Hypertrophy by Transcriptional Induction of the mTORC1 Activator, Rheb". *Circ Res*, 2019. **124**(1): p. 79-93.

13. Doroudgar, S., D.J. Thuerauf, M.C. Marcinko, P.J. Belmont, and C.C. Glembotski, "Ischemia activates the ATF6 branch of the endoplasmic reticulum stress response". *J Biol Chem*, 2009. **284**(43): p. 29735-45.

14. Harding, H.P., Y. Zhang, and D. Ron, "Protein translation and folding are coupled by an endoplasmic-reticulum-resident kinase". *Nature*, 1999. **397**(6716): p. 271-4.

15. Lee, K., W. Tirasophon, X. Shen, M. Michalak, R. Prywes, T. Okada, H. Yoshida, K. Mori, and R.J. Kaufman, "IRE1-mediated unconventional mRNA splicing and S2P-mediated ATF6 cleavage merge to regulate XBP1 in signaling the unfolded protein response". *Genes Dev*, 2002. **16**(4): p. 452-66.

16. Shen, J. and R. Prywes, "ER stress signaling by regulated proteolysis of ATF6". *Methods*, 2005. **35**(4): p. 382-9.

17. Walter, P. and D. Ron, "The unfolded protein response: from stress pathway to homeostatic regulation". *Science*, 2011. **334**(6059): p. 1081-6.

18. Glembotski, C.C., "Endoplasmic reticulum stress in the heart". *Circ Res*, 2007. **101**(10): p. 975-84.

19. Kondo, S., A. Saito, R. Asada, S. Kanemoto, and K. Imaizumi, "Physiological unfolded protein response regulated by OASIS family members, transmembrane bZIP transcription factors". *IUBMB Life*, 2011. **63**(4): p. 233-9.

20. Matsuzaki, S., T. Hiratsuka, M. Taniguchi, K. Shingaki, T. Kubo, K. Kiya, T. Fujiwara, S. Kanazawa, R. Kanematsu, T. Maeda, H. Takamura, K. Yamada, K. Miyoshi, K. Hosokawa, M. Tohyama, and T. Katayama, "Physiological ER Stress Mediates the Differentiation of Fibroblasts". *PLoS One*, 2015. **10**(4): p. e0123578.

21. Martindale, J.J., R. Fernandez, D. Thuerauf, R. Whittaker, N. Gude, M.A. Sussman, and C.C. Glembotski, "Endoplasmic reticulum stress gene induction and protection from ischemia/reperfusion injury in the hearts of transgenic mice with a tamoxifen-regulated form of ATF6". *Circ Res*, 2006. **98**(9): p. 1186-93.

22. Murao, N. and H. Nishitoh, "Role of the unfolded protein response in the development of central nervous system". *J Biochem*, 2017. **162**(3): p. 155-162.

23. Mitra, S. and H.D. Ryoo, "The unfolded protein response in metazoan development". *J Cell Sci*, 2019. **132**(5).

24. Fu, X., H. Khalil, O. Kanisicak, J.G. Boyer, R.J. Vagnozzi, B.D. Maliken, M.A. Sargent, V. Prasad, I. Valiente-Alandi, B.C. Blaxall, and J.D. Molkentin, "Specialized fibroblast differentiated states underlie scar formation in the infarcted mouse heart". *J Clin Invest*, 2018. **128**(5): p. 2127-2143.

25. Adomavicius, T., M. Guaita, Y. Zhou, M.D. Jennings, Z. Latif, A.M. Roseman, and G.D. Pavitt, "The structural basis of translational control by eIF2 phosphorylation". *Nat Commun*, 2019. **10**(1): p. 2136.

26. Sonenberg, N. and A.G. Hinnebusch, "Regulation of translation initiation in eukaryotes: mechanisms and biological targets". *Cell*, 2009. **136**(4): p. 731-45.

27. Teske, B.F., S.A. Wek, P. Bunpo, J.K. Cundiff, J.N. McClintick, T.G. Anthony, and R.C. Wek, "The eIF2 kinase PERK and the integrated stress response facilitate activation of ATF6 during endoplasmic reticulum stress". *Mol Biol Cell*, 2011. **22**(22): p. 4390-405.

28. Vattem, K.M. and R.C. Wek, "Reinitiation involving upstream ORFs regulates ATF4 mRNA translation in mammalian cells". *Proc Natl Acad Sci U S A*, 2004. **101**(31): p. 11269-74.

29. Marciniak, S.J., C.Y. Yun, S. Oyadomari, I. Novoa, Y. Zhang, R. Jungreis, K. Nagata, H.P. Harding, and D. Ron, "CHOP induces death by promoting protein synthesis and oxidation in the stressed endoplasmic reticulum". *Genes Dev*, 2004. **18**(24): p. 3066-77.

30. Oyadomari, S. and M. Mori, "Roles of CHOP/GADD153 in endoplasmic reticulum stress". *Cell Death Differ*, 2004. **11**(4): p. 381-9.

31. Puthalakath, H., L.A. O'Reilly, P. Gunn, L. Lee, P.N. Kelly, N.D. Huntington, P.D. Hughes, E.M. Michalak, J. McKimm-Breschkin, N. Motoyama, T. Gotoh, S. Akira, P. Bouillet, and A. Strasser, "ER stress triggers apoptosis by activating BH3-only protein Bim". *Cell*, 2007. **129**(7): p. 1337-49.

32. Ghosh, A.P., B.J. Klocke, M.E. Ballestas, and K.A. Roth, "CHOP potentially co-operates with FOXO3a in neuronal cells to regulate PUMA and BIM expression in response to ER stress". *PLoS One*, 2012. **7**(6): p. e39586.

33. Yamamoto, K., T. Sato, T. Matsui, M. Sato, T. Okada, H. Yoshida, A. Harada, and K. Mori, "Transcriptional induction of mammalian ER quality control proteins is mediated by single or combined action of ATF6alpha and XBP1". *Dev Cell*, 2007. **13**(3): p. 365-76.

34. Tirosh, B., N.N. Iwakoshi, L.H. Glimcher, and H.L. Ploegh, "Rapid turnover of unspliced Xbp-1 as a factor that modulates the unfolded protein response". *J Biol Chem*, 2006. **281**(9): p. 5852-60.

35. Tirasophon, W., A.A. Welihinda, and R.J. Kaufman, "A stress response pathway from the endoplasmic reticulum to the nucleus requires a novel bifunctional protein

kinase/endoribonuclease (Ire1p) in mammalian cells". *Genes Dev*, 1998. **12**(12): p. 1812-24.

36. Uemura, A., M. Oku, K. Mori, and H. Yoshida, "Unconventional splicing of XBP1 mRNA occurs in the cytoplasm during the mammalian unfolded protein response". *J Cell Sci*, 2009. **122**(Pt 16): p. 2877-86.

37. Cox, J.S. and P. Walter, "A novel mechanism for regulating activity of a transcription factor that controls the unfolded protein response". *Cell*, 1996. **87**(3): p. 391-404.

38. Urano, F., X. Wang, A. Bertolotti, Y. Zhang, P. Chung, H.P. Harding, and D. Ron, "Coupling of stress in the ER to activation of JNK protein kinases by transmembrane protein kinase IRE1". *Science*, 2000. **287**(5453): p. 664-6.

39. Maurel, M., E. Chevet, J. Tavernier, and S. Gerlo, "Getting RIDD of RNA: IRE1 in cell fate regulation". *Trends Biochem Sci*, 2014. **39**(5): p. 245-54.

40. Hollien, J., J.H. Lin, H. Li, N. Stevens, P. Walter, and J.S. Weissman, "Regulated Ire1-dependent decay of messenger RNAs in mammalian cells". *J Cell Biol*, 2009. **186**(3): p. 323-31.

41. Hai, T. and M.G. Hartman, "The molecular biology and nomenclature of the activating transcription factor/cAMP responsive element binding family of transcription factors: activating transcription factor proteins and homeostasis". *Gene*, 2001. **273**(1): p. 1-11.

42. Amoutzias, G.D., A.S. Veron, J. Weiner, 3rd, M. Robinson-Rechavi, E. Bornberg-Bauer, S.G. Oliver, and D.L. Robertson, "One billion years of bZIP transcription factor evolution: conservation and change in dimerization and DNA-binding site specificity". *Mol Biol Evol*, 2007. **24**(3): p. 827-35.

43. Thuerauf, D.J., M. Marcinko, P.J. Belmont, and C.C. Glembotski, "Effects of the isoform-specific characteristics of ATF6 alpha and ATF6 beta on endoplasmic reticulum stress response gene expression and cell viability". *J Biol Chem*, 2007. **282**(31): p. 22865-78.

44. Haze, K., T. Okada, H. Yoshida, H. Yanagi, T. Yura, M. Negishi, and K. Mori, "Identification of the G13 (cAMP-response-element-binding protein-related protein) gene product related to activating transcription factor 6 as a transcriptional activator of the mammalian unfolded protein response". *Biochem J*, 2001. **355**(Pt 1): p. 19-28.

45. Shen, J., X. Chen, L. Hendershot, and R. Prywes, "ER stress regulation of ATF6 localization by dissociation of BiP/GRP78 binding and unmasking of Golgi localization signals". *Dev Cell*, 2002. **3**(1): p. 99-111.

46. Nadanaka, S., H. Yoshida, and K. Mori, "Reduction of disulfide bridges in the lumenal domain of ATF6 in response to glucose starvation". *Cell Struct Funct*, 2006. **31**(2): p. 127-34.

47. Nadanaka, S., T. Okada, H. Yoshida, and K. Mori, "Role of disulfide bridges formed in the luminal domain of ATF6 in sensing endoplasmic reticulum stress". *Mol Cell Biol*, 2007. **27**(3): p. 1027-43.

48. Shen, J., E.L. Snapp, J. Lippincott-Schwartz, and R. Prywes, "Stable binding of ATF6 to BiP in the endoplasmic reticulum stress response". *Mol Cell Biol*, 2005. **25**(3): p. 921-32.

49. Bertolotti, A., Y. Zhang, L.M. Hendershot, H.P. Harding, and D. Ron, "Dynamic interaction of BiP and ER stress transducers in the unfolded-protein response". *Nat Cell Biol*, 2000. **2**(6): p. 326-32.

50. Ma, K., K.M. Vattem, and R.C. Wek, "Dimerization and release of molecular chaperone inhibition facilitate activation of eukaryotic initiation factor-2 kinase in response to endoplasmic reticulum stress". *J Biol Chem*, 2002. **277**(21): p. 18728-35.

51. Ye, J., R.B. Rawson, R. Komuro, X. Chen, U.P. Dave, R. Prywes, M.S. Brown, and J.L. Goldstein, "ER stress induces cleavage of membrane-bound ATF6 by the same proteases that process SREBPs". *Mol Cell*, 2000. **6**(6): p. 1355-64.

52. Lynch, J.M., M. Maillet, D. Vanhoutte, A. Schloemer, M.A. Sargent, N.S. Blair, K.A. Lynch, T. Okada, B.J. Aronow, H. Osinska, R. Prywes, J.N. Lorenz, K. Mori, J. Lawler, J. Robbins, and J.D. Molkentin, "A thrombospondin-dependent pathway for a protective ER stress response". *Cell*, 2012. **149**(6): p. 1257-68.

53. Higa, A., S. Taouji, S. Lhomond, D. Jensen, M.E. Fernandez-Zapico, J.C. Simpson, J.M. Pasquet, R. Schekman, and E. Chevet, "Endoplasmic reticulum stress-activated transcription factor ATF6alpha requires the disulfide isomerase PDIA5 to modulate chemoresistance". *Mol Cell Biol*, 2014. **34**(10): p. 1839-49.

54. Oka, O.B., M. van Lith, J. Rudolf, W. Tungkum, M.A. Pringle, and N.J. Bulleid, "ERp18 regulates activation of ATF6alpha during unfolded protein response". *EMBO J*, 2019. **38**(15): p. e100990.

55. Gallagher, C.M., C. Garri, E.L. Cain, K.K. Ang, C.G. Wilson, S. Chen, B.R. Hearn, P. Jaishankar, A. Aranda-Diaz, M.R. Arkin, A.R. Renslo, and P. Walter, "Ceapins are a new class of unfolded protein response inhibitors, selectively targeting the ATF6alpha branch". *Elife*, 2016. **5**.

56. Gallagher, C.M. and P. Walter, "Ceapins inhibit ATF6alpha signaling by selectively preventing transport of ATF6alpha to the Golgi apparatus during ER stress". *Elife*, 2016. **5**.

57. Okada, T., K. Haze, S. Nadanaka, H. Yoshida, N.G. Seidah, Y. Hirano, R. Sato, M. Negishi, and K. Mori, "A serine protease inhibitor prevents endoplasmic reticulum stress-

induced cleavage but not transport of the membrane-bound transcription factor ATF6". *J Biol Chem*, 2003. **278**(33): p. 31024-32.

58. Pasquato, A., C. Rochat, D.J. Burri, G. Pasqual, J.C. de la Torre, and S. Kunz, "Evaluation of the anti-arenaviral activity of the subtilisin kexin isozyme-1/site-1 protease inhibitor PF-429242". *Virology*, 2012. **423**(1): p. 14-22.

59. Plate, L., C.B. Cooley, J.J. Chen, R.J. Paxman, C.M. Gallagher, F. Madoux, J.C. Genereux, W. Dobbs, D. Garza, T.P. Spicer, L. Scampavia, S.J. Brown, H. Rosen, E.T. Powers, P. Walter, P. Hodder, R.L. Wiseman, and J.W. Kelly, "Small molecule proteostasis regulators that reprogram the ER to reduce extracellular protein aggregation". *Elife*, 2016. **5**.

60. Paxman, R., L. Plate, E.A. Blackwood, C. Glembotski, E.T. Powers, R.L. Wiseman, and J.W. Kelly, "Pharmacologic ATF6 activating compounds are metabolically activated to selectively modify endoplasmic reticulum proteins". *Elife*, 2018. **7**.

61. Tam, A.B., L.S. Roberts, V. Chandra, I.G. Rivera, D.K. Nomura, D.J. Forbes, and M. Niwa, "The UPR Activator ATF6 Responds to Proteotoxic and Lipotoxic Stress by Distinct Mechanisms". *Dev Cell*, 2018. **46**(3): p. 327-343 e7.

62. Hai, T.W., F. Liu, W.J. Coukos, and M.R. Green, "Transcription factor ATF cDNA clones: an extensive family of leucine zipper proteins able to selectively form DNA-binding heterodimers". *Genes Dev*, 1989. **3**(12B): p. 2083-90.

63. Thuerauf, D.J., L.E. Morrison, H. Hoover, and C.C. Glembotski, "Coordination of ATF6-mediated transcription and ATF6 degradation by a domain that is shared with the viral transcription factor, VP16". *J Biol Chem*, 2002. **277**(23): p. 20734-9.

64. Desterro, J.M., M.S. Rodriguez, and R.T. Hay, "Regulation of transcription factors by protein degradation". *Cell Mol Life Sci*, 2000. **57**(8-9): p. 1207-19.

65. Thuerauf, D.J., L. Morrison, and C.C. Glembotski, "Opposing roles for ATF6alpha and ATF6beta in endoplasmic reticulum stress response gene induction". *J Biol Chem*, 2004. **279**(20): p. 21078-84.

66. Fonseca, S.G., S. Ishigaki, C.M. Oslowski, S. Lu, K.L. Lipson, R. Ghosh, E. Hayashi, H. Ishihara, Y. Oka, M.A. Permutt, and F. Urano, "Wolfram syndrome 1 gene negatively regulates ER stress signaling in rodent and human cells". *J Clin Invest*, 2010. **120**(3): p. 744-55.

67. Kim, W., E.J. Bennett, E.L. Huttlin, A. Guo, J. Li, A. Possemato, M.E. Sowa, R. Rad, J. Rush, M.J. Comb, J.W. Harper, and S.P. Gygi, "Systematic and quantitative assessment of the ubiquitin-modified proteome". *Mol Cell*, 2011. **44**(2): p. 325-40.

68. Hong, M., M. Li, C. Mao, and A.S. Lee, "Endoplasmic reticulum stress triggers an acute proteasome-dependent degradation of ATF6". *J Cell Biochem*, 2004. **92**(4): p. 723-32.

69. Zhu, Q., J. Yao, G. Wani, J. Chen, Q.E. Wang, and A.A. Wani, "The ubiquitin-proteasome pathway is required for the function of the viral VP16 transcriptional activation domain". *FEBS Lett*, 2004. **556**(1-3): p. 19-25.

70. Hong, M., S. Luo, P. Baumeister, J.M. Huang, R.K. Gogia, M. Li, and A.S. Lee, "Underglycosylation of ATF6 as a novel sensing mechanism for activation of the unfolded protein response". *J Biol Chem*, 2004. **279**(12): p. 11354-63.

71. Hou, X., Z. Yang, K. Zhang, D. Fang, and F. Sun, "SUMOylation represses the transcriptional activity of the Unfolded Protein Response transducer ATF6". *Biochem Biophys Res Commun*, 2017. **494**(3-4): p. 446-451.

72. Geng, F., S. Wenzel, and W.P. Tansey, "Ubiquitin and proteasomes in transcription". *Annu Rev Biochem*, 2012. **81**: p. 177-201.

73. Freedman, D.A. and A.J. Levine, "Nuclear export is required for degradation of endogenous p53 by MDM2 and human papillomavirus E6". *Mol Cell Biol*, 1998. **18**(12): p. 7288-93.

74. Chen, L. and K. Madura, "Yeast importin-alpha (Srp1) performs distinct roles in the import of nuclear proteins and in targeting proteasomes to the nucleus". *J Biol Chem*, 2014. **289**(46): p. 32339-52.

75. Dang, F.W., L. Chen, and K. Madura, "Catalytically Active Proteasomes Function Predominantly in the Cytosol". *J Biol Chem*, 2016. **291**(36): p. 18765-77.

76. Rodriguez-Martinez, J.A., A.W. Reinke, D. Bhimsaria, A.E. Keating, and A.Z. Ansari, "Combinatorial bZIP dimers display complex DNA-binding specificity landscapes". *Elife*, 2017. **6**.

77. Huet, A., A. Parlakian, M.C. Arnaud, J.M. Glandieres, P. Valat, S. Fermandjian, D. Paulin, B. Alpert, and C. Zentz, "Mechanism of binding of serum response factor to serum response element". *FEBS J*, 2005. **272**(12): p. 3105-19.

78. Zhu, C., F.E. Johansen, and R. Prywes, "Interaction of ATF6 and serum response factor". *Mol Cell Biol*, 1997. **17**(9): p. 4957-66.

79. Yoshida, H., T. Okada, K. Haze, H. Yanagi, T. Yura, M. Negishi, and K. Mori, "ATF6 activated by proteolysis binds in the presence of NF-Y (CBF) directly to the cis-acting element responsible for the mammalian unfolded protein response". *Mol Cell Biol*, 2000. **20**(18): p. 6755-67.

80. Li, M., P. Baumeister, B. Roy, T. Phan, D. Foti, S. Luo, and A.S. Lee, "ATF6 as a transcription activator of the endoplasmic reticulum stress element: thapsigargin stress-induced changes and synergistic interactions with NF-Y and YY1". *Mol Cell Biol*, 2000. **20**(14): p. 5096-106.

81. Wu, J., J.L. Ruas, J.L. Estall, K.A. Rasbach, J.H. Choi, L. Ye, P. Bostrom, H.M. Tyra, R.W. Crawford, K.P. Campbell, D.T. Rutkowski, R.J. Kaufman, and B.M. Spiegelman, "The unfolded protein response mediates adaptation to exercise in skeletal muscle through a PGC-1alpha/ATF6alpha complex". *Cell Metab*, 2011. **13**(2): p. 160-9.

82. Misra, J., D.K. Kim, W. Choi, S.H. Koo, C.H. Lee, S.H. Back, R.J. Kaufman, and H.S. Choi, "Transcriptional cross talk between orphan nuclear receptor ERRgamma and transmembrane transcription factor ATF6alpha coordinates endoplasmic reticulum stress response". *Nucleic Acids Res*, 2013. **41**(14): p. 6960-74.

83. Zhang, K., X. Shen, J. Wu, K. Sakaki, T. Saunders, D.T. Rutkowski, S.H. Back, and R.J. Kaufman, "Endoplasmic reticulum stress activates cleavage of CREBH to induce a systemic inflammatory response". *Cell*, 2006. **124**(3): p. 587-99.

84. Chen, X., J. Shen, and R. Prywes, "The luminal domain of ATF6 senses endoplasmic reticulum (ER) stress and causes translocation of ATF6 from the ER to the Golgi". *J Biol Chem*, 2002. **277**(15): p. 13045-52.

85. Vinson, C., A. Acharya, and E.J. Taparowsky, "Deciphering B-ZIP transcription factor interactions in vitro and in vivo". *Biochim Biophys Acta*, 2006. **1759**(1-2): p. 4-12.

86. Yoshida, H., K. Haze, H. Yanagi, T. Yura, and K. Mori, "Identification of the cis-acting endoplasmic reticulum stress response element responsible for transcriptional induction of mammalian glucose-regulated proteins. Involvement of basic leucine zipper transcription factors". *J Biol Chem*, 1998. **273**(50): p. 33741-9.

87. Kokame, K., H. Kato, and T. Miyata, "Identification of ERSE-II, a new cis-acting element responsible for the ATF6-dependent mammalian unfolded protein response". *J Biol Chem*, 2001. **276**(12): p. 9199-205.

88. Belmont, P.J., A. Tadimalla, W.J. Chen, J.J. Martindale, D.J. Thuerauf, M. Marcinko, N. Gude, M.A. Sussman, and C.C. Glembotski, "Coordination of growth and endoplasmic reticulum stress signaling by regulator of calcineurin 1 (RCAN1), a novel ATF6-inducible gene". *J Biol Chem*, 2008. **283**(20): p. 14012-21.

89. Haze, K., H. Yoshida, H. Yanagi, T. Yura, and K. Mori, "Mammalian transcription factor ATF6 is synthesized as a transmembrane protein and activated by proteolysis in response to endoplasmic reticulum stress". *Mol Biol Cell*, 1999. **10**(11): p. 3787-99.

90. Vekich, J.A., P.J. Belmont, D.J. Thuerauf, and C.C. Glembotski, "Protein disulfide isomerase-associated 6 is an ATF6-inducible ER stress response protein that protects cardiac myocytes from ischemia/reperfusion-mediated cell death". *J Mol Cell Cardiol*, 2012. **53**(2): p. 259-67.

91. Werner, E.D., J.L. Brodsky, and A.A. McCracken, "Proteasome-dependent endoplasmic reticulum-associated protein degradation: an unconventional route to a familiar fate". *Proc Natl Acad Sci U S A*, 1996. **93**(24): p. 13797-801.

92. Hampton, R.Y., R.G. Gardner, and J. Rine, "Role of 26S proteasome and HRD genes in the degradation of 3-hydroxy-3-methylglutaryl-CoA reductase, an integral endoplasmic reticulum membrane protein". *Mol Biol Cell*, 1996. **7**(12): p. 2029-44.

93. Nadav, E., A. Shmueli, H. Barr, H. Gonen, A. Ciechanover, and Y. Reiss, "A novel mammalian endoplasmic reticulum ubiquitin ligase homologous to the yeast Hrd1". *Biochem Biophys Res Commun*, 2003. **303**(1): p. 91-7.

94. Kikkert, M., R. Doolman, M. Dai, R. Avner, G. Hassink, S. van Voorden, S. Thanedar, J. Roitelman, V. Chau, and E. Wiertz, "Human HRD1 is an E3 ubiquitin ligase involved in degradation of proteins from the endoplasmic reticulum". *J Biol Chem*, 2004. **279**(5): p. 3525-34.

95. Doroudgar, S., M. Volkers, D.J. Thuerauf, M. Khan, S. Mohsin, J.L. Respress, W. Wang, N. Gude, O.J. Muller, X.H. Wehrens, M.A. Sussman, and C.C. Glembotski, "Hrd1 and ER-Associated Protein Degradation, ERAD, are Critical Elements of the Adaptive ER Stress Response in Cardiac Myocytes". *Circ Res*, 2015. **117**(6): p. 536-46.

96. Belmont, P.J., W.J. Chen, M.N. San Pedro, D.J. Thuerauf, N. Gellings Lowe, N. Gude, B. Hilton, R. Wolkowicz, M.A. Sussman, and C.C. Glembotski, "Roles for endoplasmic reticulum-associated degradation and the novel endoplasmic reticulum stress response gene Derlin-3 in the ischemic heart". *Circ Res*, 2010. **106**(2): p. 307-16.

97. Oda, Y., T. Okada, H. Yoshida, R.J. Kaufman, K. Nagata, and K. Mori, "Derlin-2 and Derlin-3 are regulated by the mammalian unfolded protein response and are required for ER-associated degradation". *J Cell Biol*, 2006. **172**(3): p. 383-93.

98. Reeves, M.A. and P.R. Hoffmann, "The human selenoproteome: recent insights into functions and regulation". *Cell Mol Life Sci*, 2009. **66**(15): p. 2457-78.

99. Glembotski, C.C., "Roles for ATF6 and the sarco/endoplasmic reticulum protein quality control system in the heart". *J Mol Cell Cardiol*, 2014. **71**: p. 11-5.

100. Wu, J., D.T. Rutkowski, M. Dubois, J. Swathirajan, T. Saunders, J. Wang, B. Song, G.D. Yau, and R.J. Kaufman, "ATF6alpha optimizes long-term endoplasmic reticulum function to protect cells from chronic stress". *Dev Cell*, 2007. **13**(3): p. 351-64.

101. Kaufman, R.J., "Stress signaling from the lumen of the endoplasmic reticulum: coordination of gene transcriptional and translational controls". *Genes Dev*, 1999. **13**(10): p. 1211-33.

102. Ubeda, M. and J.F. Habener, "CHOP gene expression in response to endoplasmic-reticular stress requires NFY interaction with different domains of a conserved DNA-binding element". *Nucleic Acids Res*, 2000. **28**(24): p. 4987-97.

103. Gotoh, T., S. Oyadomari, K. Mori, and M. Mori, "Nitric oxide-induced apoptosis in RAW 264.7 macrophages is mediated by endoplasmic reticulum stress pathway involving ATF6 and CHOP". *J Biol Chem*, 2002. **277**(14): p. 12343-50.

104. Meex, S.J., D. Weissglas-Volkov, C.J. van der Kallen, D.J. Thuerauf, M.M. van Greevenbroek, C.G. Schalkwijk, C.D. Stehouwer, E.J. Feskens, L. Heldens, T.A. Ayoubi, M.H. Hofker, B.G. Wouters, R. Vlietinck, J.S. Sinsheimer, M.R. Taskinen, J. Kuusisto, M. Laakso, T.W. de Bruin, P. Pajukanta, and C.C. Glembotski, "The ATF6-Met[67]Val substitution is associated with increased plasma cholesterol levels". *Arterioscler Thromb Vasc Biol*, 2009. **29**(9): p. 1322-7.

105. Blackwood, E.A., K. Azizi, D.J. Thuerauf, R.J. Paxman, L. Plate, J.W. Kelly, R.L. Wiseman, and C.C. Glembotski, "Pharmacologic ATF6 activation confers global protection in widespread disease models by reprograming cellular proteostasis". *Nat Commun*, 2019. **10**(1): p. 187.

106. Sharma, R.B., A.C. O'Donnell, R.E. Stamateris, B. Ha, K.M. McCloskey, P.R. Reynolds, P. Arvan, and L.C. Alonso, "Insulin demand regulates beta cell number via the unfolded protein response". *J Clin Invest*, 2015. **125**(10): p. 3831-46.

107. Kohl, S., D. Zobor, W.C. Chiang, N. Weisschuh, J. Staller, I. Gonzalez Menendez, S. Chang, S.C. Beck, M. Garcia Garrido, V. Sothilingam, M.W. Seeliger, F. Stanzial, F. Benedicenti, F. Inzana, E. Heon, A. Vincent, J. Beis, T.M. Strom, G. Rudolph, S. Roosing, A.I. Hollander, F.P. Cremers, I. Lopez, H. Ren, A.T. Moore, A.R. Webster, M. Michaelides, R.K. Koenekoop, E. Zrenner, R.J. Kaufman, S.H. Tsang, B. Wissinger, and J.H. Lin, "Mutations in the unfolded protein response regulator ATF6 cause the cone dysfunction disorder achromatopsia". *Nat Genet*, 2015. **47**(7): p. 757-65.

108. Kondo, S., A. Saito, S. Hino, T. Murakami, M. Ogata, S. Kanemoto, S. Nara, A. Yamashita, K. Yoshinaga, H. Hara, and K. Imaizumi, "BBF2H7, a novel transmembrane bZIP transcription factor, is a new type of endoplasmic reticulum stress transducer". *Mol Cell Biol*, 2007. **27**(5): p. 1716-29.

109. Li, Y., Z. Li, C. Zhang, P. Li, Y. Wu, C. Wang, W. Bond Lau, X.L. Ma, and J. Du, "Cardiac Fibroblast-Specific Activating Transcription Factor 3 Protects Against Heart Failure by Suppressing MAP2K3-p38 Signaling". *Circulation*, 2017. **135**(21): p. 2041-2057.

110. Zhou, D., L.R. Palam, L. Jiang, J. Narasimhan, K.A. Staschke, and R.C. Wek, "Phosphorylation of eIF2 directs ATF5 translational control in response to diverse stress conditions". *J Biol Chem*, 2008. **283**(11): p. 7064-73.

111. Bailey, D. and P. O'Hare, "Transmembrane bZIP transcription factors in ER stress signaling and the unfolded protein response". *Antioxid Redox Signal*, 2007. **9**(12): p. 2305-21.

112. Asada, R., S. Kanemoto, S. Kondo, A. Saito, and K. Imaizumi, "The signalling from endoplasmic reticulum-resident bZIP transcription factors involved in diverse cellular physiology". *J Biochem*, 2011. **149**(5): p. 507-18.

113. Horiuchi, K., T. Tohmonda, and H. Morioka, "The unfolded protein response in skeletal development and homeostasis". *Cell Mol Life Sci*, 2016. **73**(15): p. 2851-69.

114. Chan, C.P., K.H. Kok, and D.Y. Jin, "CREB3 subfamily transcription factors are not created equal: Recent insights from global analyses and animal models". *Cell Biosci*, 2011. **1**(1): p. 6.

115. DenBoer, L.M., P.W. Hardy-Smith, M.R. Hogan, G.P. Cockram, T.E. Audas, and R. Lu, "Luman is capable of binding and activating transcription from the unfolded protein response element". *Biochem Biophys Res Commun*, 2005. **331**(1): p. 113-9.

116. Omori, Y., J. Imai, Y. Suzuki, S. Watanabe, A. Tanigami, and S. Sugano, "OASIS is a transcriptional activator of CREB/ATF family with a transmembrane domain". *Biochem Biophys Res Commun*, 2002. **293**(1): p. 470-7.

117. Stirling, J. and P. O'Hare, "CREB4, a transmembrane bZip transcription factor and potential new substrate for regulation and cleavage by S1P". *Mol Biol Cell*, 2006. **17**(1): p. 413-26.

118. Forouhan, M., K. Mori, and R.P. Boot-Handford, "Paradoxical roles of ATF6alpha and ATF6beta in modulating disease severity caused by mutations in collagen X". *Matrix Biol*, 2018. **70**: p. 50-71.

119. Correll, R.N., K.M. Grimes, V. Prasad, J.M. Lynch, H. Khalil, and J.D. Molkentin, "Overlapping and differential functions of ATF6alpha versus ATF6beta in the mouse heart". *Sci Rep*, 2019. **9**(1): p. 2059.

120. Sutton, M.G. and N. Sharpe, "Left ventricular remodeling after myocardial infarction: pathophysiology and therapy". *Circulation*, 2000. **101**(25): p. 2981-8.

121. Talman, V. and H. Ruskoaho, "Cardiac fibrosis in myocardial infarction-from repair and remodeling to regeneration". *Cell Tissue Res*, 2016. **365**(3): p. 563-81.

122. Bahit, M.C., A. Kochar, and C.B. Granger, "Post-Myocardial Infarction Heart Failure". *JACC Heart Fail*, 2018. **6**(3): p. 179-186.

123. Lugrin, J., R. Parapanov, T. Krueger, and L. Liaudet, "Murine Myocardial Infarction Model using Permanent Ligation of Left Anterior Descending Coronary Artery". *J Vis Exp*, 2019(150).

124. Beltrami, A.P., L. Barlucchi, D. Torella, M. Baker, F. Limana, S. Chimenti, H. Kasahara, M. Rota, E. Musso, K. Urbanek, A. Leri, J. Kajstura, B. Nadal-Ginard, and P. Anversa, "Adult cardiac stem cells are multipotent and support myocardial regeneration". *Cell*, 2003. **114**(6): p. 763-76.

125. Ellison, G.M., C. Vicinanza, A.J. Smith, I. Aquila, A. Leone, C.D. Waring, B.J. Henning, G.G. Stirparo, R. Papait, M. Scarfo, V. Agosti, G. Viglietto, G. Condorelli, C. Indolfi, S. Ottolenghi, D. Torella, and B. Nadal-Ginard, "Adult c-kit(pos) cardiac stem cells are necessary and sufficient for functional cardiac regeneration and repair". *Cell*, 2013. **154**(4): p. 827-42.

126. Nadal-Ginard, B., G.M. Ellison, and D. Torella, "The cardiac stem cell compartment is indispensable for myocardial cell homeostasis, repair and regeneration in the adult". *Stem Cell Res*, 2014. **13**(3 Pt B): p. 615-30.

127. van Berlo, J.H., O. Kanisicak, M. Maillet, R.J. Vagnozzi, J. Karch, S.C. Lin, R.C. Middleton, E. Marban, and J.D. Molkentin, "c-kit+ cells minimally contribute cardiomyocytes to the heart". *Nature*, 2014. **509**(7500): p. 337-41.

128. Sultana, N., L. Zhang, J. Yan, J. Chen, W. Cai, S. Razzaque, D. Jeong, W. Sheng, L. Bu, M. Xu, G.Y. Huang, R.J. Hajjar, B. Zhou, A. Moon, and C.L. Cai, "Resident c-kit(+) cells in the heart are not cardiac stem cells". *Nat Commun*, 2015. **6**: p. 8701.

129. Li, Y., L. He, X. Huang, S.I. Bhaloo, H. Zhao, S. Zhang, W. Pu, X. Tian, Y. Li, Q. Liu, W. Yu, L. Zhang, X. Liu, K. Liu, J. Tang, H. Zhang, D. Cai, A.H. Ralf, Q. Xu, K.O. Lui, and B. Zhou, "Genetic Lineage Tracing of Nonmyocyte Population by Dual Recombinases". *Circulation*, 2018. **138**(8): p. 793-805.

130. Bolli, R., A.R. Chugh, D. D'Amario, J.H. Loughran, M.F. Stoddard, S. Ikram, G.M. Beache, S.G. Wagner, A. Leri, T. Hosoda, F. Sanada, J.B. Elmore, P. Goichberg, D. Cappetta, N.K. Solankhi, I. Fahsah, D.G. Rokosh, M.S. Slaughter, J. Kajstura, and P. Anversa, "Cardiac stem cells in patients with ischaemic cardiomyopathy (SCIPIO): initial results of a randomised phase 1 trial". *Lancet*, 2011. **378**(9806): p. 1847-57.

131. Makkar, R.R., R.R. Smith, K. Cheng, K. Malliaras, L.E. Thomson, D. Berman, L.S. Czer, L. Marban, A. Mendizabal, P.V. Johnston, S.D. Russell, K.H. Schuleri, A.C. Lardo, G. Gerstenblith, and E. Marban, "Intracoronary cardiosphere-derived cells for heart regeneration after myocardial infarction (CADUCEUS): a prospective, randomised phase 1 trial". *Lancet*, 2012. **379**(9819): p. 895-904.

132. Hong, K.U., Y. Guo, Q.H. Li, P. Cao, T. Al-Maqtari, B.N. Vajravelu, J. Du, M.J. Book, X. Zhu, Y. Nong, A. Bhatnagar, and R. Bolli, "c-kit+ Cardiac stem cells alleviate post-myocardial infarction left ventricular dysfunction despite poor engraftment and negligible retention in the recipient heart". *PLoS One*, 2014. **9**(5): p. e96725.

133. Tang, X.L., Q. Li, G. Rokosh, S.K. Sanganalmath, N. Chen, Q. Ou, H. Stowers, G. Hunt, and R. Bolli, "Long-Term Outcome of Administration of c-kit(POS) Cardiac Progenitor Cells After Acute Myocardial Infarction: Transplanted Cells Do not Become Cardiomyocytes, but Structural and Functional Improvement and Proliferation of Endogenous Cells Persist for at Least One Year". *Circ Res*, 2016. **118**(7): p. 1091-105.
134. Gray, W.D., K.M. French, S. Ghosh-Choudhary, J.T. Maxwell, M.E. Brown, M.O. Platt, C.D. Searles, and M.E. Davis, "Identification of therapeutic covariant microRNA clusters in hypoxia-treated cardiac progenitor cell exosomes using systems biology". *Circ Res*, 2015. **116**(2): p. 255-63.

135. Barile, L., V. Lionetti, E. Cervio, M. Matteucci, M. Gherghiceanu, L.M. Popescu, T. Torre, F. Siclari, T. Moccetti, and G. Vassalli, "Extracellular vesicles from human cardiac progenitor cells inhibit cardiomyocyte apoptosis and improve cardiac function after myocardial infarction". *Cardiovasc Res*, 2014. **103**(4): p. 530-41.

136. Pashkovskaia, N., U. Gey, and G. Rodel, "Mitochondrial ROS direct the differentiation of murine pluripotent P19 cells". *Stem Cell Res*, 2018. **30**: p. 180-191.

137. Hom, J.R., R.A. Quintanilla, D.L. Hoffman, K.L. de Mesy Bentley, J.D. Molkentin, S.S. Sheu, and G.A. Porter, Jr., "The permeability transition pore controls cardiac mitochondrial maturation and myocyte differentiation". *Dev Cell*, 2011. **21**(3): p. 469-78.

138. Bigarella, C.L., R. Liang, and S. Ghaffari, "Stem cells and the impact of ROS signaling". *Development*, 2014. **141**(22): p. 4206-18.

139. Ezerina, D., Y. Takano, K. Hanaoka, Y. Urano, and T.P. Dick, "N-Acetyl Cysteine Functions as a Fast-Acting Antioxidant by Triggering Intracellular H2S and Sulfane Sulfur Production". *Cell Chem Biol*, 2018. **25**(4): p. 447-459 e4.

140. Hillary, R.F. and U. FitzGerald, "A lifetime of stress: ATF6 in development and homeostasis". *J Biomed Sci*, 2018. **25**(1): p. 48.

141. Guo, F., X. Han, Z. Wu, Z. Cheng, Q. Hu, Y. Zhao, Y. Wang, and C. Liu, "ATF6a, a Runx2-activable transcription factor, is a new regulator of chondrocyte hypertrophy". *J Cell Sci*, 2016. **129**(4): p. 717-28.

142. Moustakas, A., "Smad signalling network". *J Cell Sci*, 2002. **115**(Pt 17): p. 3355-6.

143. Ebisawa, T., M. Fukuchi, G. Murakami, T. Chiba, K. Tanaka, T. Imamura, and K. Miyazono, "Smurf1 interacts with transforming growth factor-beta type I receptor through Smad7 and induces receptor degradation". *J Biol Chem*, 2001. **276**(16): p. 12477-80.

144. Lin, X., M. Liang, and X.H. Feng, "Smurf2 is a ubiquitin E3 ligase mediating proteasome-dependent degradation of Smad2 in transforming growth factor-beta signaling". *J Biol Chem*, 2000. **275**(47): p. 36818-22.

145. Fournier, P.G., P. Juarez, G. Jiang, G.A. Clines, M. Niewolna, H.S. Kim, H.W. Walton, X.H. Peng, Y. Liu, K.S. Mohammad, C.D. Wells, J.M. Chirgwin, and T.A. Guise, "The TGF-beta Signaling Regulator PMEPA1 Suppresses Prostate Cancer Metastases to Bone". *Cancer Cell*, 2015. **27**(6): p. 809-21.

146. Watanabe, Y., S. Itoh, T. Goto, E. Ohnishi, M. Inamitsu, F. Itoh, K. Satoh, E. Wiercinska, W. Yang, L. Shi, A. Tanaka, N. Nakano, A.M. Mommaas, H. Shibuya, P. Ten Dijke, and M. Kato, "TMEPAI, a transmembrane TGF-beta-inducible protein, sequesters Smad proteins from active participation in TGF-beta signaling". *Mol Cell*, 2010. **37**(1): p. 123-34.

147. Fransioli, J., B. Bailey, N.A. Gude, C.T. Cottage, J.A. Muraski, G. Emmanuel, W. Wu, R. Alvarez, M. Rubio, S. Ottolenghi, E. Schaefer, and M.A. Sussman, "Evolution of the c-kit-positive cell response to pathological challenge in the myocardium". *Stem Cells*, 2008. **26**(5): p. 1315-24.

148. Engin, F., A. Yermalovich, T. Nguyen, S. Hummasti, W. Fu, D.L. Eizirik, D. Mathis, and G.S. Hotamisligil, "Restoration of the unfolded protein response in pancreatic beta cells protects mice against type 1 diabetes". *Sci Transl Med*, 2013. **5**(211): p. 211ra156.

149. Werfel, S., A. Jungmann, L. Lehmann, J. Ksienzyk, R. Bekeredjian, Z. Kaya, B. Leuchs, A. Nordheim, J. Backs, S. Engelhardt, H.A. Katus, and O.J. Muller, "Rapid and highly efficient inducible cardiac gene knockout in adult mice using AAV-mediated expression of Cre recombinase". *Cardiovasc Res*, 2014. **104**(1): p. 15-23.

150. VanderLaan, P.A., C.A. Reardon, and G.S. Getz, "Site specificity of atherosclerosis: site-selective responses to atherosclerotic modulators". *Arterioscler Thromb Vasc Biol*, 2004. **24**(1): p. 12-22.

151. Libby, P., P.M. Ridker, and G.K. Hansson, "Progress and challenges in translating the biology of atherosclerosis". *Nature*, 2011. **473**(7347): p. 317-25.

152. Crossman, D.C., "The pathophysiology of myocardial ischaemia". *Heart*, 2004. **90**(5): p. 576-80.

153. Neely, J.R. and D. Feuvray, "Metabolic products and myocardial ischemia". *Am J Pathol*, 1981. **102**(2): p. 282-91.

154. Reddy, K., A. Khaliq, and R.J. Henning, "Recent advances in the diagnosis and treatment of acute myocardial infarction". *World J Cardiol*, 2015. **7**(5): p. 243-76.

155. Turer, A.T. and J.A. Hill, "Pathogenesis of myocardial ischemia-reperfusion injury and rationale for therapy". *Am J Cardiol*, 2010. **106**(3): p. 360-8.

156. Cowled, P. and R. Fitridge, *Pathophysiology of Reperfusion Injury*, in *Mechanisms of Vascular Disease: A Reference Book for Vascular Specialists*, R. Fitridge and M. Thompson, Editors. 2011: Adelaide (AU).

157. Valensi, P., L. Lorgis, and Y. Cottin, "Prevalence, incidence, predictive factors and prognosis of silent myocardial infarction: a review of the literature". *Arch Cardiovasc Dis*, 2011. **104**(3): p. 178-88.

158. Yutzey, K.E., "Cardiomyocyte Proliferation: Teaching an Old Dogma New Tricks". *Circ Res*, 2017. **120**(4): p. 627-629.

159. Fraccarollo, D., S. Berger, P. Galuppo, S. Kneitz, L. Hein, G. Schutz, S. Frantz, G. Ertl, and J. Bauersachs, "Deletion of cardiomyocyte mineralocorticoid receptor ameliorates adverse remodeling after myocardial infarction". *Circulation*, 2011. **123**(4): p. 400-8.

160. Riehle, C. and J. Bauersachs, "Small animal models of heart failure". *Cardiovasc Res*, 2019. **115**(13): p. 1838-1849.

161. Taegtmeyer, H., S. Sen, and D. Vela, "Return to the fetal gene program: a suggested metabolic link to gene expression in the heart". *Ann N Y Acad Sci*, 2010. **1188**: p. 191-8.

162. Gude, N.A. and M.A. Sussman, "Chasing c-Kit through the heart: Taking a broader view". *Pharmacol Res*, 2018. **127**: p. 110-115.

163. Fraser, L., A.H. Taylor, and L.M. Forrester, "SCF/KIT inhibition has a cumulative but reversible effect on the self-renewal of embryonic stem cells and on the survival of differentiating cells". *Cell Reprogram*, 2013. **15**(4): p. 259-68.

164. Ikuta, K. and I.L. Weissman, "Evidence that hematopoietic stem cells express mouse c-kit but do not depend on steel factor for their generation". *Proc Natl Acad Sci U S A*, 1992. **89**(4): p. 1502-6.

165. Czarna, A., F. Sanada, A. Matsuda, J. Kim, S. Signore, J.D. Pereira, A. Sorrentino, R. Kannappan, A. Cannata, T. Hosoda, M. Rota, F. Crea, P. Anversa, and A. Leri, "Single-cell analysis of the fate of c-kit-positive bone marrow cells". *NPJ Regen Med*, 2017. **2**: p. 27.

166. Lennartsson, J. and L. Ronnstrand, "Stem cell factor receptor/c-Kit: from basic science to clinical implications". *Physiol Rev*, 2012. **92**(4): p. 1619-49.

167. Tsang, K.Y., D. Chan, D. Cheslett, W.C. Chan, C.L. So, I.G. Melhado, T.W. Chan, K.M. Kwan, E.B. Hunziker, Y. Yamada, J.F. Bateman, K.M. Cheung, and K.S. Cheah, "Surviving endoplasmic reticulum stress is coupled to altered chondrocyte differentiation and function". *PLoS Biol*, 2007. **5**(3): p. e44.

168. Saito, A., K. Ochiai, S. Kondo, K. Tsumagari, T. Murakami, D.R. Cavener, and K. Imaizumi, "Endoplasmic reticulum stress response mediated by the PERK-eIF2(alpha)-ATF4 pathway is involved in osteoblast differentiation induced by BMP2". *J Biol Chem*, 2011. **286**(6): p. 4809-18.

169. Baek, H.A., D.S. Kim, H.S. Park, K.Y. Jang, M.J. Kang, D.G. Lee, W.S. Moon, H.J. Chae, and M.J. Chung, "Involvement of endoplasmic reticulum stress in myofibroblastic differentiation of lung fibroblasts". *Am J Respir Cell Mol Biol*, 2012. **46**(6): p. 731-9.

170. Ghali, O., O. Broux, G. Falgayrac, N. Haren, J.P. van Leeuwen, G. Penel, P. Hardouin, and C. Chauveau, "Dexamethasone in osteogenic medium strongly induces adipocyte differentiation of mouse bone marrow stromal cells and increases osteoblast differentiation". *BMC Cell Biol*, 2015. **16**: p. 9.

171. Xiao, Y., V. Peperzak, L. van Rijn, J. Borst, and J.D. de Bruijn, "Dexamethasone treatment during the expansion phase maintains stemness of bone marrow mesenchymal stem cells". *J Tissue Eng Regen Med*, 2010. **4**(5): p. 374-86.

172. Tanaka, H., C.L. Murphy, C. Murphy, M. Kimura, S. Kawai, and J.M. Polak, "Chondrogenic differentiation of murine embryonic stem cells: effects of culture conditions and dexamethasone". *J Cell Biochem*, 2004. **93**(3): p. 454-62.

173. Vajravelu, B.N., K.U. Hong, T. Al-Maqtari, P. Cao, M.C. Keith, M. Wysoczynski, J. Zhao, J.B.t. Moore, and R. Bolli, "C-Kit Promotes Growth and Migration of Human Cardiac Progenitor Cells via the PI3K-AKT and MEK-ERK Pathways". *PLoS One*, 2015. **10**(10): p. e0140798.

174. Lin, J.H., P. Walter, and T.S. Yen, "Endoplasmic reticulum stress in disease pathogenesis". *Annu Rev Pathol*, 2008. **3**: p. 399-425.

175. Lytton, J., M. Westlin, and M.R. Hanley, "Thapsigargin inhibits the sarcoplasmic or endoplasmic reticulum Ca-ATPase family of calcium pumps". *J Biol Chem*, 1991. **266**(26): p. 17067-71.

176. Duksin, D. and P. Bornstein, "Impaired conversion of procollagen to collagen by fibroblasts and bone treated with tunicamycin, an inhibitor of protein glycosylation". *J Biol Chem*, 1977. **252**(3): p. 955-62.

177. Cleland, W.W., "Dithiothreitol, a New Protective Reagent for Sh Groups". *Biochemistry*, 1964. **3**: p. 480-2.

178. Rashdan, N.A. and C.B. Pattillo, "Hydrogen peroxide in the ER: A tale of triage". *Redox Biol*, 2020. **28**: p. 101358.

179. Riss, T.L., R.A. Moravec, A.L. Niles, S. Duellman, H.A. Benink, T.J. Worzella, and L. Minor, *Cell Viability Assays*, in *Assay Guidance Manual*, G.S. Sittampalam, et al., Editors. 2004: Bethesda (MD).

180. Salvador, J.M., J.D. Brown-Clay, and A.J. Fornace, Jr., "Gadd45 in stress signaling, cell cycle control, and apoptosis". *Adv Exp Med Biol*, 2013. **793**: p. 1-19.

181. Blackwood, E.A., D.J. Thuerauf, M. Stastna, H. Stephens, Z. Sand, A. Pentoney, K. Azizi, T. Jakobi, J.E. Van Eyk, H.A. Katus, C.C. Glembotski, and S. Doroudgar, "Proteomic analysis of the cardiac myocyte secretome reveals extracellular protective functions for the ER stress response". *J Mol Cell Cardiol*, 2020. **143**: p. 132-144.

182. Tannous, B.A., "Gaussia luciferase reporter assay for monitoring biological processes in culture and in vivo". *Nat Protoc*, 2009. **4**(4): p. 582-91.

183. Rodriguez-Porcel, M., O. Gheysens, R. Paulmurugan, I.Y. Chen, K.M. Peterson, J.K. Willmann, J.C. Wu, X. Zhu, L.O. Lerman, and S.S. Gambhir, "Antioxidants improve early survival of cardiomyoblasts after transplantation to the myocardium". *Mol Imaging Biol*, 2010. **12**(3): p. 325-34.

184. Calzadilla, P., D. Sapochnik, S. Cosentino, V. Diz, L. Dicelio, J.C. Calvo, and L.N. Guerra, "N-acetylcysteine reduces markers of differentiation in 3T3-L1 adipocytes". *Int J Mol Sci*, 2011. **12**(10): p. 6936-51.

185. Sauer, H., G. Rahimi, J. Hescheler, and M. Wartenberg, "Role of reactive oxygen species and phosphatidylinositol 3-kinase in cardiomyocyte differentiation of embryonic stem cells". *FEBS Lett*, 2000. **476**(3): p. 218-23.

186. Kawada, N., D.B. Kristensen, K. Asahina, K. Nakatani, Y. Minamiyama, S. Seki, and K. Yoshizato, "Characterization of a stellate cell activation-associated protein (STAP) with peroxidase activity found in rat hepatic stellate cells". *J Biol Chem*, 2001. **276**(27): p. 25318-23.

187. Low, F.M., M.B. Hampton, A.V. Peskin, and C.C. Winterbourn, "Peroxiredoxin 2 functions as a noncatalytic scavenger of low-level hydrogen peroxide in the erythrocyte". *Blood*, 2007. **109**(6): p. 2611-7.

188. Shi, J., H. Zuo, L. Ni, L. Xia, L. Zhao, M. Gong, D. Nie, P. Gong, D. Cui, W. Shi, and J. Chen, "An IDH1 mutation inhibits growth of glioma cells via GSH depletion and ROS generation". *Neurol Sci*, 2014. **35**(6): p. 839-45.

189. Braunersreuther, V., C. Pellieux, G. Pelli, F. Burger, S. Steffens, C. Montessuit, C. Weber, A. Proudfoot, F. Mach, and C. Arnaud, "Chemokine CCL5/RANTES inhibition reduces myocardial reperfusion injury in atherosclerotic mice". *J Mol Cell Cardiol*, 2010. **48**(4): p. 789-98.

190. Naidoo, N., "The endoplasmic reticulum stress response and aging". *Rev Neurosci*, 2009. **20**(1): p. 23-37.

191. Yang, Y., H.H. Cheung, J. Tu, K.K. Miu, and W.Y. Chan, "New insights into the unfolded protein response in stem cells". *Oncotarget*, 2016. **7**(33): p. 54010-54027.

192. Madden, E., S.E. Logue, S.J. Healy, S. Manie, and A. Samali, "The role of the unfolded protein response in cancer progression: From oncogenesis to chemoresistance". *Biol Cell*, 2019. **111**(1): p. 1-17.

193. Teodoro, T., T. Odisho, E. Sidorova, and A. Volchuk, "Pancreatic beta-cells depend on basal expression of active ATF6alpha-p50 for cell survival even under nonstress conditions". *Am J Physiol Cell Physiol*, 2012. **302**(7): p. C992-1003.

194. Lynch, M.D. and F.M. Watt, "Fibroblast heterogeneity: implications for human disease". *J Clin Invest*, 2018. **128**(1): p. 26-35.

195. Grinnell, F., "Fibroblasts, myofibroblasts, and wound contraction". *J Cell Biol*, 1994. **124**(4): p. 401-4.

196. Ivey, M.J. and M.D. Tallquist, "Defining the Cardiac Fibroblast". *Circ J*, 2016. **80**(11): p. 2269-2276.

197. Baum, J. and H.S. Duffy, "Fibroblasts and myofibroblasts: what are we talking about?". *J Cardiovasc Pharmacol*, 2011. **57**(4): p. 376-9.

198. Bell, E., B. Ivarsson, and C. Merrill, "Production of a tissue-like structure by contraction of collagen lattices by human fibroblasts of different proliferative potential in vitro". *Proc Natl Acad Sci U S A*, 1979. **76**(3): p. 1274-8.

199. Lijnen, P., V. Petrov, K. Rumilla, and R. Fagard, "Transforming growth factor-beta 1 promotes contraction of collagen gel by cardiac fibroblasts through their differentiation into myofibroblasts". *Methods Find Exp Clin Pharmacol*, 2003. **25**(2): p. 79-86.

200. Khalil, H., O. Kanisicak, V. Prasad, R.N. Correll, X. Fu, T. Schips, R.J. Vagnozzi, R. Liu, T. Huynh, S.J. Lee, J. Karch, and J.D. Molkentin, "Fibroblast-specific TGF-beta-Smad2/3 signaling underlies cardiac fibrosis". *J Clin Invest*, 2017. **127**(10): p. 3770-3783.

201. Biernacka, A. and N.G. Frangogiannis, "Aging and Cardiac Fibrosis". *Aging Dis*, 2011. **2**(2): p. 158-173.

202. Dzeshka, M.S., G.Y. Lip, V. Snezhitskiy, and E. Shantsila, "Cardiac Fibrosis in Patients With Atrial Fibrillation: Mechanisms and Clinical Implications". *J Am Coll Cardiol*, 2015. **66**(8): p. 943-59.

203. Smaill, B.H., "Fibrosis, myofibroblasts, and atrial fibrillation". *Circ Arrhythm Electrophysiol*, 2015. **8**(2): p. 256-7.

204. Bing, R., J.L. Cavalcante, R.J. Everett, M.A. Clavel, D.E. Newby, and M.R. Dweck, "Imaging and Impact of Myocardial Fibrosis in Aortic Stenosis". *JACC Cardiovasc Imaging*, 2019. **12**(2): p. 283-296.

205. Herum, K.M., J. Choppe, A. Kumar, A.J. Engler, and A.D. McCulloch, "Mechanical regulation of cardiac fibroblast profibrotic phenotypes". *Mol Biol Cell*, 2017. **28**(14): p. 1871-1882.

206. van Putten, S., Y. Shafieyan, and B. Hinz, "Mechanical control of cardiac myofibroblasts". *J Mol Cell Cardiol*, 2016. **93**: p. 133-42.

207. Piacentini, L., M. Gray, N.Y. Honbo, J. Chentoufi, M. Bergman, and J.S. Karliner, "Endothelin-1 stimulates cardiac fibroblast proliferation through activation of protein kinase C". *J Mol Cell Cardiol*, 2000. **32**(4): p. 565-76.

208. Diez, J., R. Querejeta, B. Lopez, A. Gonzalez, M. Larman, and J.L. Martinez Ubago, "Losartan-dependent regression of myocardial fibrosis is associated with reduction of left ventricular chamber stiffness in hypertensive patients". *Circulation*, 2002. **105**(21): p. 2512-7.

209. Leask, A., "TGFbeta, cardiac fibroblasts, and the fibrotic response". *Cardiovasc Res*, 2007. **74**(2): p. 207-12.

210. Petrov, V.V., R.H. Fagard, and P.J. Lijnen, "Stimulation of collagen production by transforming growth factor-beta1 during differentiation of cardiac fibroblasts to myofibroblasts". *Hypertension*, 2002. **39**(2): p. 258-63.

211. Nuchel, J., S. Ghatak, A.V. Zuk, A. Illerhaus, M. Morgelin, K. Schonborn, K. Blumbach, S.A. Wickstrom, T. Krieg, G. Sengle, M. Plomann, and B. Eckes, "TGFB1 is secreted through an unconventional pathway dependent on the autophagic machinery and cytoskeletal regulators". *Autophagy*, 2018. **14**(3): p. 465-486.

212. Shi, M., J. Zhu, R. Wang, X. Chen, L. Mi, T. Walz, and T.A. Springer, "Latent TGF-beta structure and activation". *Nature*, 2011. **474**(7351): p. 343-9.

213. Dore, J.J., Jr., M. Edens, N. Garamszegi, and E.B. Leof, "Heteromeric and homomeric transforming growth factor-beta receptors show distinct signaling and endocytic responses in epithelial cells". *J Biol Chem*, 1998. **273**(48): p. 31770-7.

214. Wrana, J.L., L. Attisano, J. Carcamo, A. Zentella, J. Doody, M. Laiho, X.F. Wang, and J. Massague, "TGF beta signals through a heteromeric protein kinase receptor complex". *Cell*, 1992. **71**(6): p. 1003-14.

215. Runyan, C.E., H.W. Schnaper, and A.C. Poncelet, "The role of internalization in transforming growth factor beta1-induced Smad2 association with Smad anchor for receptor activation (SARA) and Smad2-dependent signaling in human mesangial cells". *J Biol Chem*, 2005. **280**(9): p. 8300-8.

216. Hu, H.H., D.Q. Chen, Y.N. Wang, Y.L. Feng, G. Cao, N.D. Vaziri, and Y.Y. Zhao, "New insights into TGF-beta/Smad signaling in tissue fibrosis". *Chem Biol Interact*, 2018. **292**: p. 76-83.

217. Nakanishi, K., N. Dohmae, and N. Morishima, "Endoplasmic reticulum stress increases myofiber formation in vitro". *FASEB J*, 2007. **21**(11): p. 2994-3003.

218. Shrestha, N., T. Liu, Y. Ji, R.B. Reinert, M. Torres, X. Li, M. Zhang, C.A. Tang, C.A. Hu, C. Liu, A. Naji, M. Liu, J.D. Lin, S. Kersten, P. Arvan, and L. Qi, "Sel1L-Hrd1 ER-associated degradation maintains beta cell identity via TGF-beta signaling". *J Clin Invest*, 2020.

219. Meng, Q., B. Bhandary, M.S. Bhuiyan, J. James, H. Osinska, I. Valiente-Alandi, K. Shay-Winkler, J. Gulick, J.D. Molkentin, B.C. Blaxall, and J. Robbins, "Myofibroblast-Specific TGFbeta Receptor II Signaling in the Fibrotic Response to Cardiac Myosin Binding Protein C-Induced Cardiomyopathy". *Circ Res*, 2018. **123**(12): p. 1285-1297.

220. Okumura, N., K. Hashimoto, M. Kitahara, H. Okuda, E. Ueda, K. Watanabe, M. Nakahara, T. Sato, S. Kinoshita, T. Tourtas, U. Schlotzer-Schrehardt, F. Kruse, and N. Koizumi, "Activation of TGF-beta signaling induces cell death via the unfolded protein response in Fuchs endothelial corneal dystrophy". *Sci Rep*, 2017. **7**(1): p. 6801.

221. Kassan, M., M. Galan, M. Partyka, Z. Saifudeen, D. Henrion, M. Trebak, and K. Matrougui, "Endoplasmic reticulum stress is involved in cardiac damage and vascular endothelial dysfunction in hypertensive mice". *Arterioscler Thromb Vasc Biol*, 2012. **32**(7): p. 1652-61.

222. Lenna, S. and M. Trojanowska, "The role of endoplasmic reticulum stress and the unfolded protein response in fibrosis". *Curr Opin Rheumatol*, 2012. **24**(6): p. 663-8.

223. Groenendyk, J., D. Lee, J. Jung, J.R. Dyck, G.D. Lopaschuk, L.B. Agellon, and M. Michalak, "Inhibition of the Unfolded Protein Response Mechanism Prevents Cardiac Fibrosis". *PLoS One*, 2016. **11**(7): p. e0159682.

224. Hsu, H.S., C.C. Liu, J.H. Lin, T.W. Hsu, J.W. Hsu, K. Su, and S.C. Hung, "Involvement of ER stress, PI3K/AKT activation, and lung fibroblast proliferation in bleomycin-induced pulmonary fibrosis". *Sci Rep*, 2017. **7**(1): p. 14272.

225. Belmont, P.J., W.J. Chen, D.J. Thuerauf, and C.C. Glembotski, "Regulation of microRNA expression in the heart by the ATF6 branch of the ER stress response". *J Mol Cell Cardiol*, 2012. **52**(5): p. 1176-82.

226. Seo, H.Y., M.K. Kim, A.K. Min, H.S. Kim, S.Y. Ryu, N.K. Kim, K.M. Lee, H.J. Kim, H.S. Choi, K.U. Lee, K.G. Park, and I.K. Lee, "Endoplasmic reticulum stress-induced activation of activating transcription factor 6 decreases cAMP-stimulated hepatic gluconeogenesis via inhibition of CREB". *Endocrinology*, 2010. **151**(2): p. 561-8.

227. Zeng, L., M. Lu, K. Mori, S. Luo, A.S. Lee, Y. Zhu, and J.Y. Shyy, "ATF6 modulates SREBP2-mediated lipogenesis". *EMBO J*, 2004. **23**(4): p. 950-8.

228. Peter, A.K., M.A. Bjerke, and L.A. Leinwand, "Biology of the cardiac myocyte in heart disease". *Mol Biol Cell*, 2016. **27**(14): p. 2149-60.

229. Kanisicak, O., H. Khalil, M.J. Ivey, J. Karch, B.D. Maliken, R.N. Correll, M.J. Brody, J.L. SC, B.J. Aronow, M.D. Tallquist, and J.D. Molkentin, "Genetic lineage tracing defines myofibroblast origin and function in the injured heart". *Nat Commun*, 2016. **7**: p. 12260.

230. Zhu, M., S.C. Goetsch, Z. Wang, R. Luo, J.A. Hill, J. Schneider, S.M. Morris, Jr., and Z.P. Liu, "FoxO4 promotes early inflammatory response upon myocardial infarction via endothelial Arg1". *Circ Res*, 2015. **117**(11): p. 967-77.

231. Glembotski, C.C., A. Arrieta, E.A. Blackwood, and W.T. Stauffer, "ATF6 as a Nodal Regulator of Proteostasis in the Heart". *Front Physiol*, 2020. **11**: p. 267.

232. Castro, N.E., M. Kato, J.T. Park, and R. Natarajan, "Transforming growth factor beta1 (TGF-beta1) enhances expression of profibrotic genes through a novel signaling cascade and microRNAs in renal mesangial cells". *J Biol Chem*, 2014. **289**(42): p. 29001-13.

233. Mallano, T., K. Palumbo-Zerr, P. Zerr, A. Ramming, B. Zeller, C. Beyer, C. Dees, J. Huang, T. Hai, O. Distler, G. Schett, and J.H. Distler, "Activating transcription factor 3 regulates canonical TGFbeta signalling in systemic sclerosis". *Ann Rheum Dis*, 2016. **75**(3): p. 586-92.

234. Kalfon, R., L. Koren, S. Aviram, O. Schwartz, T. Hai, and A. Aronheim, "ATF3 expression in cardiomyocytes preserves homeostasis in the heart and controls peripheral glucose tolerance". *Cardiovasc Res*, 2017. **113**(2): p. 134-146.